Closing capacity of bone defects

Scaffolds, porosity and growth factors updated.

Colofon:
Thesis Radboud University Nijmegen Medical Centre, with summary in Dutch.
Closing capacity of bone defects. Scaffolds, porosity and growth factors updated.

Henriette Christine Kroese-Deutman

H.C. Kroese-Deutman, Nijmegen 2009
ISBN: 978-90-9024203-3

Lay-out interior: Jochem Verschure
Cover design: Mirjam Lems
Printing: Wöhrmann Print Service, Zutphen

The research in this thesis was partly supported by the NWO-AGIKO foundation.

Closing capacity of bone defects

Scaffolds, porosity and growth factors updated.

Een wetenschappelijke proeve op het gebied van de Medische Wetenschappen.

Proefschrift

**Ter verkrijging van de graad van doctor aan de Radboud Universiteit Nijmegen
op gezag van de Rector Magnificus, prof. mr. S.C.J.J. Kortmann,
volgens besluit van het College van Decanen in het openbaar te verdedigen
op woensdag 20 mei 2009, om 10.30 uur precies**

door

Henriette Christine Kroese-Deutman

Geboren op 2 juni 1969 te Rotterdam

Promotores:
Prof. dr. P.H.M. Spauwen
Prof. dr. J.A. Jansen

Manuscriptcommissie:
Prof. dr. P. Buma, voorzitter
Prof. dr. R.P. Bleichrodt
Prof. dr. P.M.N. Werker (Universiteit Groningen)

Paranimfen:
A.F. Deutman jr.
Drs. A.B.C. Deutman

Contents

1

GENERAL INTRODUCTION

CLOSING CAPACITY OF BONE DEFECTS: SCAFFOLDS, POROSITY AND GROWTH FACTORS UPDATED

GENERAL INTRODUCTION

CLOSING CAPACITY OF BONE DEFECTS: SCAFFOLDS, POROSITY AND GROWTH FACTORS UPDATED

1.1 BACKGROUND

Bone tissue is one of the tissues needed for transplantation. In clinical practice, many patients are treated for skeletal problems in the fields of plastic surgery, orthopaedic surgery, maxillofacial surgery and neurosurgery. There is demand for bone due to various reasons, for example to fill bone defects caused by trauma or tumour resection, as well as to reconstruct congenital malformations and age related osteoarthritis. The use of autologous bone grafts is still considered to be the standard method, but there are several major disadvantages of this technique, for example: (1) low availability of transplantable tissue, (2) postoperative morbidity and (3) lack of functional shape of the transplant. Therefore, several alternatives to autologous bone have been investigated. In this respect, basic knowledge of the mechanism of bone growth is important because this understanding may lead to improve clinical methods of bone repair. Analysing and updating scaffolds and growth factor molecules may solve a small portion of this complex puzzle of bone generation.

1.2 BONE

'The hard, largely calcified connective tissue of which the adult skeleton of most vertebrates is chiefly composed' (Webster's New World Dictionary)

1.2.1 Bone structure

Bone provides structural support for the human body, has a protective function and is the support system of the internal organs. Mature lammelar bone is composed of approximately 93% solid material and 7% water.[1]
Bone consists of an organic and an inorganic component. The organic component, consists of bone cells and extracellular matrix and is composed for 95% of type I collagen. Proteoglycans and numerous non-collagenous proteins are present in the remaining 5%.
The inorganic part constitutes most of the total bone volume by weight (approximately 70%) and is formed by the crystalline salt which is composed by calcium phosphate in the form of hydroxyapatite (HA) ($Ca_{10}(PO_4)_6(OH)_2$).

Furthermore, there are two bone types, trabecular/ cancellous bone and compact cortical bone. They have different embryologic functions, distributions and biologic behavior. Irregular bars, or trabeculae, form organized layers and a mesh filled with bone marrow, which finally will be trabecular/ cancellous bone. Compact cortical bone has mechanical and protective functions.
Two embryologically distinct bone types are known: direct intramembranous bone and indirect (endochondral) bone. Direct intramembranous ossification occurs in flat bones for example the skull, parts of mandible and clavicula. The intramembranous bone is derived from direct ossification of mesenchymal precursors. The mesenchymal tissue is strongly vascularised and mesenchymal cells are able to differentiate directly into osteoblasts. Mineralization takes place in the extracellular organelles (matrix vesicles) in which

proteinase, peptidases and alkaline phosphatase (APL) are present.[2,3]
Endochondral ossification typically occurs in tubular long bones of the skeleton. The bone is formed by ossification of a cartilaginous intermediate.[4]
Basically, three principal bone cells types, osteoblasts, osteoclasts and osteocytes are identified during bone formation and remodeling. Mesenchymal cells first differentiate into chondroblasts forming a cartilaginous matrix developing into the direction of the bone, which is subsequently mineralized. Osteoclasts then remove part of this mineralized cartilage and create space for vascularisation and new bone production by osteoblasts, while the remnants of calcified cartilage form a supporting framework.[4,5]

1.3 BONE CELLS

1.3.1 Mesenchymal stem cells

Stem cells can be of mesenchymal origin and are non-hematopoetic cells that are capable of both self-renewal and differentiation into, muscle, fat, cartilage, fibrous and soft connective tissue and bone cells.[5-7] They reside in the bone marrow and can be induced to differentiate into various components of the marrow microenvironment.

1.3.2 Osteoprogenitor cells

Mesenchymal stem cells may differentiate into cells that are referred to as committed osteoblastic or osteoprogenitor cells. In the later stage of bone formation preosteoblasts and transitory osteoblasts are formed. These are both capable of division. Preosteoblasts are flat and induce osteoblast cell proliferation and are present in the periosteum and in the marrow stroma.[8] Recent in vitro studies suggest that under certain conditions, these cells may be converted to adipocytes and that this might be a reason for impaired bone formation.[9,10]

1.3.3 Osteoblasts

Osteoblasts are bone-forming and remodeling cells and are made out of mesenchymal stem cells through induction by osteoprogenitor cells. The function of these metabolically active mesenchymal cells is to produce new bone matrix, ostoid and to mineralize it. Osteoblasts produce osteocalcin during the mineralization phase, a major non-collagenous protein in bone, containing gamma carboxylated glutamic acid.[11]
Approximately 10-20% of the osteoblasts will become either osteocytes, covered by their own matrix or form a layer of resting cells on the bone surface (flattened bone-lining cell). Further, the rest of the osteoblasts die through programmed cell death (apoptosis).[12]
Osteoblasts have receptors for factors that influence bone remodelling and they produce many regulators of bone growth.

1.3.4 Osteocytes

Thus, osteocytes descend from osteoblast. When osteoblasts are embedded in the bone matrix, the cells are called osteocytes. Osteocytes develop in mesenchyme and are networked to each other via long cytoplasmic extensions. They are responsible for the routine turnover of bone matrix and the maintenance of the bone. They constitute a functional syncytium, which communicates through dentritic processes and gap junction.[13,14] This syncytium of interconnected cells is probably critical for sensing mechanical forces.

During differentiation from osteoblasts to mature osteocytes, the cells lose a large part of their cell organelles.[14] The production of nitric oxide and prostaglandins can be stimulated by shear stress, which may mediate the response of bone to mechanical loading.[15] The occurrence of osteocyte apoptosis is consistent with the description of apoptosis as an essential homeostatic mechanism for the healthy maintenance of tissues.[16]

1.3.5 Osteoclasts

The osteoclasts are bone resorbing cells that remove bone tissue by removing its mineral matrix. Thus, they are responsible for the degradation of bone tissue. Osteoclasts are formed by the fusion of mononuclear precursors derived from haemopoetic stem cells in the bone marrow.[17]
Bone degradation occurs in the extracellular space between the bone matrix and the cell border in which the mineral and organic components of the bone matrix are degraded by osteoclasts.

1.4 BONE HEALING / BONE FRACTURE REPAIR

Bone healing takes place in three stages: inflammation, the repair stage and the late remodelling stage. It is a complex series of biologic events designed to repair and regenerate damaged bone. Two types of bone repair are known, i.e. primary bone repair (non displaced bone fragments heal without cartilaginous intermediate) and secondary bone/callus (unstable bone segments heal with cartilaginous intermediate) repair. Mechanical stabilisation enables new vessel ingrowth, mineralization and osteoid deposition. However, absolute immobilisation may cause disturbance in bone healing by promoting bone resorption due to stress protection and inhibition of callus formation. Controlled axial loading and micromotion have been shown to accelerate fracture repair.[18] Although the histologic and ultrastructural characteristics of fracture repair have been well studied, the exact sequence of molecular events responsible for these events remains unknown.

When defects are too large and fracture healing is not possible in a spontaneous way, the defect is called a Critical Size Defect (CSD). The definition is that the CSD is the smallest size of a defect, which does not heal spontaneously, when left untreated for a certain period of time.[19] In this case, bone grafts or substitutes are necessary.
Different bone graft materials can be autografts, allografts and xenografts. An autograft is bone harvested from the same individual. The major disadvantages in this technique are donor site morbidity, low availability of transplantable tissue and lack of functional shape of the transplant. An allograft is tissue from one individual implanted into another individual of the same species. The disadvantages of allografts include risk of transmission of diseases and immunogenicity. Allografts also have less vascularisation, a poor degree of cellularity and a higher resorption rate.[20,21] A xenograft is tissue harvested from one species and implanted into another different species. Xenografts have similarly disadvantages as allografts.[22]

Biomaterials have the potential to replace these natural grafts in the future. Several materials have been developed as bone substitutes: natural coral, calcium sulphate, hydroxyapatite, tricalcium phosphate, calcium phosphate, bio-active glasses, titanium and

polymers. When improving the osteoconductivity of these materials, the defect can be closed more easily. By preference, a biomaterial should be biodegradable, immunologically inert and mechanical stable. Furthermore, when looking at the economical demands, they should be mouldable, user friendly, easy to manufacture and cost-effective.[23]
Biomaterials are also used as scaffold/carrier material in bone tissue engineering.

1.5 BONE TISSUE ENGINEERING

Meijer et all concluded in their review article about cell based bone tissue engineering that for successful bone engineering four prerequisites are needed. A sufficient number of cells, an appropriate scaffold to seed the cells, factors to stimulate osteogenic differentiation in vivo and sufficient vascular supply.[24]
Therefore, from the point of bone tissue engineering, the principal aim of generating new bone is to restore structural support, as losses are typically limited and the other functions of the skeleton can be adequately served by remaining bone.
In 1965 Urist discovered that bone tissue contains specific growth factors that can induce bone formation in ectopic places in rabbits.[25] This means that stimulation of the body to make new bone independent from the surrounding bone tissue is possible, both in a non-bone environment (ectopical) and in a bone environment (orthotopical). Currently, BMPs (Bone Morphogenetic Proteins) are known to be responsible for ectopical bone formation.[26-30]
With improved purification methods for native BMPs and modern gene technology unlimited amounts of recombinant BMPs can be provided, which allow a lot of research to the bone inducing potentials of BMPs. Still, the search is continued for the bone graft material that is an ideal carrier for BMPs. Also a lot of questions have to be answered concerning the release kinetics of BMPs and the optimum dosage for inducing bone generation at a defect site. Until recently, no convincing successes were achieved in humans.[24]

1.6 BONE GRAFTS SUBSTITUTES / SCAFFOLDS

A lot of prerequisites have been postulated for the ideal scaffold material with regard to mechanical properties, biocompatibility and biodegradability, absence of allergic reactions, disease transmission, gross architecture, shaping, clinical handling, and regulatory issues. It has to be emphasized that none of the currently available scaffold materials meet all of the formulated demands.
A bone graft material is any implanted material that alone or in combination with other materials promotes a bone healing response by presenting bioactive, osteoconductive or osteoinductive activity. Bioactivity is a property of the ceramic surface which induces biological integration of living soft and hard tissues.[1] An osteoconductive material promotes bone apposition to its surface, which means that the surface characteristics can optimize bone ingrowth and in this way enhance bone formation.[31] Thus, the bone graft substitute supports the growth of bone over its surface. An osteoinductive material needs a rich surface charge and affinity for cells to attach and provides a biologic stimulus that induces local or transplanted cells to enter a pathway of differentiation, leading to mature osteoblasts.[32]

1.6.1 Calcium Phosphate (Ca-P)

Calcium Phosphate based bone substitutes posses excellent biocompatibitity. Studies in the past decade demonstrated that in vivo these materials are non toxic, antigenically inactive, non-cancerous and evoke a direct contact with bone without an intervening connective tissue layer.[33] They can have resorbable and non-resorbable properties. The phosphate containing HPO_4^{2-} and PO_4^{3-} represent in general the biologically important calcium phosphates. Hydroxyapatite $(HA)(Ca_{10}(PO_4)_6(OH)_2)$ is the most stable form of Ca-P under physiological pH and body temperature and is more similar to bone tissue than tricalcium phosphate (TCP). However, resorbability and solubility of TCP is much higher compared to HA, which should be considered as non resorbable.[34]

1.6.1.1 Ca-P cement

Ca-P cements were first introduced in the early eighties. Ca-P cement is a novel material for bone repair. It is injectable, can be moulded into the required shape and is bone biocompatible.[35] The advantages of Ca-P cement include the in vivo moldability resulting in a seamless contact of the cement in the surrounding bone.[36] The scaffold architecture for bone grafting has to allow for initial cell attachment and subsequent migration into and through the matrix and for mass transfer of nutrients and metabolites and provide sufficient space for development and later remodeling of the organized tissue.[37] To achieve this, the bone biological properties of Ca-P cement can even be further improved by creating porosity in the material. The pores create inter-connectivity to allow tissue ingrowth and stabilization.[38]

1.6.1.2 Porosity of Ca-P cement

The porosity of Ca-P cements can influence the suspension rate of the material and its osteoconductive characteristics. Ca-P cements have essentially a microporous structure in which the micropores are smaller than 5μm. This pore size is too small for the infiltration and ingrowth of cells.

It is known that porosity has a positive influence on the degradation of Ca-P ceramics and determines the natural ingrowth of tissue. The disadvantage of porosity is that it results in less mechanical support.

Macropores are larger than 10 μm.[34] Macroporosity can be created by Ca-P cement with e.g. $NaHCO_3$ and NaH_2PO_4. Gas bubbles will be formed inside the material. As mentioned above, the interconnection between the pores is essential for tissue growth throughout the scaffold. The effect of different pore sizes of HA were observed in the study of Tsuruga et al.[39] Their results indicated that the optimal pore size for attachment, differentiation and growth of osteoblasts and vascularization is approximately 300-400 microns.[5,39]

1.6.2 Titanium

Titanium is well known for its excellent biocompatibility. This is expressed by two major observations: 1) a very favorable response of tissues to titanium surfaces, and 2) the absence of allergic reactions to titanium.[40,41] Bone cells and mineralized bone matrix are laid down on titanium surfaces without interposition of other tissues.[40] Porosity can be created in the titanium as well.

Although porous titanium mesh is nondegradable, interconnective porosity and flexibility are the advantages of the porous titanium fiber mesh above bulk titanium. Flexibility helps presumably to eradicate local forces by distributing the stresses between implant and tissue over a larger area.[41] The amount of bone ingrowth into the material can be influenced by

the porosity of the fiber mesh. This porosity can be varied during fabrication and allows a more normal restoration of the bone unlike nonporous implant materials.[41] Consequently, porous titanium fiber mesh offers several advantages over other materials by its uniformity and structural continuity, as well as by its strength, high porosity, low stiffness, corrosion resistance and high coefficient of friction.[42] To enhance the osteoconductive properties of the material, seeding stromal bone marrow cells into the mesh porosity or treating the titanium mesh with bone growth stimulating factors, like bone morphogenetic protein and transforming growth factor-ß1 are a solution.[43-46] Also, Ti-mesh has been shown to be an effective carrier for both osteogenic cells and BMPs in ectopic bone formation in vivo.[46,47] An alternative approach to the above mentioned ones can be the coupling of bioactive ligands, like RGD-peptides, to the titanium mesh surface.[48]

1.7 GROWTH FACTORS IN BONE HEALING

Numerous scaffold materials have been tested with recombinant Bone Morphogenetic Proteins (BMPs). These materials include organic and inorganic materials.
Bone contains several other mitogenic growth factors besides (BMPs) associated with bone healing, including Platelet Derived Growth factor (PDGF), Transforming Growth Factor-β (TGF-Beta), Insuline Like Growth Factor (IGF-I and II) and basic and acidic Fibroblast Growth Factor (bFGF and aFGF).[49]

1.7.1 Bone Morphogenic Proteins

Bone Morphogenic Proteins (BMPs) are growth factors involved in bone growth. Growth factors are polypeptides that are generally synthesized by specific tissue where they, in very low concentrations, act as local regulators of cell function, including cellular migration, proliferation, differentiation and apoptosis. Most growth factors are released as high molecular weight precursors, which are split by proteolysis and produce active factors, which are generally of low molecular weight. The growth factors elicit their action by binding the specific large transmembrane receptors on the cell surface of the target cell.

Bone Morphogenic Proteins (BMP) are members of the so-called Transforming Growth Factor (TGF)-ß super family that can exist in 5 subtypes of TGF-ß and 14 different kinds of Bone Morphogenetic Proteins (BMP). The proteins of the TGF-ß superfamily regulate many different biological processes including cell growth, differentiation and embryonic pattern formation.[50] BMP 1-16 are the presently known members of the BMP superfamily. They can be divided into different subgroups according to the structural similarity between the molecules within each group. BMP-1 is the only BMP that is not a member of the TGF-beta superfamily.
Various in vitro and in vivo (rodents, dogs, sheep, humans) studies have been done to establish the osteoinductive and bone formation enhancing effect of BMP. Especially, human BMP-2 and BMP-7 have been investigated extensively for bone engineering purposes.[51-55] Both are available in large quantities by human recombinant technology. BMPs play an important regulatory role in many steps in bone morphogenesis, like chemotaxis of osteoblasts, differentiation as well as mitosis of cartilage and bone producing cells.[56,57] The BMPs have been detected in cells that are involved in fracture healing.[52]

During the early phase of membranous-type fracture repair of long bones, BMP protein expression is localized in the thickened cambium layer of the periosteum and osteoblasts near the fractured bone segments.[58] Fracture repair stimulates a periosteal reaction and induces the synthesis of BMPs by immature periosteal cells. Initially, within several days after the fracture, periosteal cells and osteoblasts show an intense expression of bone morphogenetic proteins and their receptors. The expression of bone morphogenetic protein decreases when mature lamellar bone appears.[58]

Experimental research has shown that BMPs when added to human mesenchymal cells, lead to increased matrix production and increased alkaline phosphate and collagen I levels. They are the only growth factors with a known ability to stimulate the differentiation of mesenchymal stem cells in the chondro-and osteoblastic direction and only a subset of BMPs has the unique property of inducing de novo bone formation or osteoinduction by themselves.[58] Proliferation of the mesenchymal cells is not stimulated.[59,60] BMP has the ability to promote healing of Critical Sized Defects (CSD).
A carrier system of BMP can of course optimize the osteogenic activities of BMP. This to prevent rapid release of the BMP proteins from the area to stimulate the osteoprogenitor cells for an appropriate duration. Optimally, the subsequent degradation of the carrier material should proceed at the same rate as bone regeneration.

1.7.2 RGD-peptide

Another approach to enhance bone formation is the use of RGD-peptides. Arginine-glycine-aspartic acid sequence or RGD, is a small peptide ligand, which has high affinity for integrins. Integrins, which bind specifically to short peptide sequences like RGD, are responsible for cell responses. Recently, a lot of studies have demonstrated that these peptide modified surfaces influence cell responses in vitro. In this way, information can be transmitted to the nucleus through several cytoplasmic signaling pathways. RGD-peptides are known to increase the overall adhesiveness of the surface for osteoblasts.[61,62] In this way, they can essentially mimic cell attachment activity of the bone cells.[63,64] It has also been suggested that RGD-peptide coating enhances titanium rod osseointegration in the rat femur.[65]

1.7.3 PRP (Platelet Rich Plasma)

Finally, a recently suggested method to deliver growth factors in the bone healing process is the manufacturing of Platelet Rich Plasma (PRP). PRP is a volume of autologous plasma that has a platelet (thrombocytes) concentration above baseline (1×10^9 pl / ml).[66] Within thrombocytes/platelets all of the mitogenic growth factors are present, like Platelet Derived Growth Factor (PDGF), Transforming Growth Factor-β1 (TGF-β1) and β2 (TGF-β2), Vascular Endothelial Growth Factor (VEGF), Insulin Growth Factor (IGF) and Epidermal Growth Factors (EGF).[66-68] These growth factors are released from platelets after platelet breakdown and are known to play an important role in wound healing.[67,69-71]
These proteins act on target cells, resulting in the specific stimulation or inhibition of these cells. PRP is easily prepared from the patient's whole blood by centrifugation and separation of thrombocytes with the use of a cell separator. Also commercially available chair side appliances are available.[72-75] Depending on the production process, the concentration of thrombocytes in PRP is 3- to 20-fold greater than in whole blood.[66]
The positive effect of PRP can be mainly attributed to the effect of TGF-β and PDGF on cell proliferation, differentiation and angiogenesis. PRP stimulates the proliferation

and differentiation of osteoblasts and proliferation of capillaries.[76,77] The clinical use of platelet concentrates in PRP with autologous bone grafts has been shown to nearly double the rate of bone formation and to enhance bone density by 20% in some studies.[66] Recently, the efficacy of PRP combined with a polylactide scaffold and autologous bone graft, in a goat mandibular defect model, has been demonstrated.[78] The use of such scaffolds can further limit donor-site morbidity.

PRP is autogenous and already been widely used in clinical practice, although there is limited evidence and a lot of controversy about its working mechanism. The amount of PRP can be counted in a Coulter counter (Onyx/ Bürker). Although discontinuous cell separation is adequate for concentrating growth factors from whole blood and there is a correlation between the platelets counts in the PRP and the donor blood,[79] there is still considerable variability in the resulting concentrations of these growth factors.[80]

In the past years, some promising animal and clinical cases in which PRP treatment was applied in combination with autogeneous bone and biomaterials have been reported.[81-89] Fennis et al. showed that the addition of PRP improved bone healing considerably when using cortical scaffolds filled with a particulate cancellous anterior iliac crest bone graft in mandibular defects in goats.[78,90] Other studies could not confirm the positive effect of PRP preparations on bone formation in bone grafts.[91-95]

PRP has to be gelatinized to a platelet gel. This is a mixture of fibrogen, factor XIII, plasma proteins such as fibronectin and globulin, mixed with a clot initiator (human or bovine thrombin) and calcium chloride. The clot initiator forms the PRP into the gel which optimize growth factor release. Thrombin converts fibrogen into fibrin, whereafter calcium activates factor XIII. A cross-linking fibrin network will be created. This PRP-gel can be added to the bone graft or biomaterial. However, various studies have confirmed that the combination of PRP with a biomaterial alone does not lead to enhanced bone formation.[56,96,97]

Although clinical trials suggest that the combination of bone graft substitutes and growth factors such as contained in Platelet Rich Plasma (PRP) enhance bone density,[66] adverse effects of the PRP have to be evaluated as well. Finally, there has been some concern about a possible carcinogenic effect of PRP related to the stimulation of cellular proliferation and its local presence in high concentrations. A possible role of mitogenic growth factors in tumor growth has been described, but a carcinogenic effect of PRP is very unlikely, since the growth factors are merely differentiation factors and not mutagens. Differentiation factors are known to act on cell membranes in order to activate internal cytoplasmic signal proteins, which promote normal gene expression.[76]

Another consideration is the use of bovine thrombine and the risk of transmitting Bovine Spongiform Encephalopathy (BSE) or mad cow disease. Using recombinant human thrombine can eliminate this risk.

1.8 OBJECTIVE OF THIS THESIS

In many fields of medicine, there is a high need for bone graft substitutes. However, currently available "synthetic" bone grafts do not meet the requirements to replace the autogenous bone grafts and allografts for stable bone creation. On the other hand, calcium phosphates have excellent biochemical and biocompatible properties and have been used as bone defect filler. In addition, porous calcium phosphate cement appears to be a candidate carrier material in the creation of an osteoinductive bone graft substitute. Another promising material is titanium fiber mesh, which has excellent biochemical, biocompatible and mechanical properties.

The main objective of this thesis was to investigate the feasibility of porous Ca-P cement and titanium as a carrier material for growth factors, e.g. BMP in the creation of bone graft substitutes in a suitable cranial or critical size defect model. Beside the porosity, we hypothesized that the osteoconductive properties of these carrier materials could be further enhanced by PRP substitution or surface treatment with RGD.

Aims of this study were:

- Evaluation of the cranial and radial Critical Size Defect (CSD) of a New Zealand white rabbit animal model.
- Assessment of the suitability of porous Ca-P cement as a scaffold material for bone regeneration in cranial non weight bearing situations.
- Evaluation of the osteoconductive capacity of the porous Ca-P implants in a rabbit radius segmental defect in weight bearing situations.
- Comparison of the non-treated open defect size (control) and the defect filled with porous Ca-P cement in this weight bearing model.
- Measuring the bone strength in this weight bearing model after 12 weeks implantation time.
- Evaluation of the different torque/ torsional tests measurements in long bone segmental defects.
- Investigation of the suitability of porous calcium phosphate cement as a carrier material for rhBMP-2 at orthotopic location (cranial defect).
- Evaluation of rhBMP-2 loaded porous Ca-P cement at ectopic site in a rabbit animal model compared with the absorbable collagen sponge (ACS).
- Evaluation of the influence of RGD peptide sequence on porous titanium fiber mesh and on bone formation itself after different time periods (two, four and eight weeks post-implantation).
- Evaluation of the bone stimulative effect of PRP in a titanium fiber mesh scaffold on autologous bone graft in a weight bearing model.

REFERENCES

1) Heppenstall RB: Fracture healing. In Heppenstall RB, ed Fracture treatment and healing. Philadelphia, WB Saunders, 1980:35-64.
2) Hirschman A, Deutsch D, Hirschman M, Bab IA, Sela J, Muhlrad A. Neutral peptidase activities in matrix vesicles from bovine fetal alveolar bone and dog osteosarcoma. Calcif Tissue Int.1983.Sep;35(6):791-7.
3) Wuthier RE, Chin JE, Hale JE, Register TC, Hale LV, Ishikawa Y. Isolation and characterization of calcium-accumulating matrix vesicles from chondrocytes of chicken epiphyseal growth plate cartilage in primary culture. J Biol Chem. 1985 Dec 15;260(29):15972-9.
4) Marks SC, Hermey DC. Structure and development of bone. In Bilezikian JP, Raisz LG, Rodan GA; Principles in bone biology. Academic press, San Diego, p3-14.
5) Hoang Vu Nguyen, Bone and guided bone regeneration, A literature review. 2008: UMC Nijmegen, the Netherlands.
6) Bruder SP, Jaiswal N, Haynesworth SE. Growth kinetics, self-renewal, and the osteogenic potential of purified human mesenchymal stem cells during extensive subcultivation and following cryopreservation. J Cell Biochem. 1997 Feb;64(2):278-94.
7) Pittenger MF, Mackay AM, Beck SC, Jaiswal RK, Douglas R, Mosca JD, Moorman MA, Simonetti DW, Craig S, Marshak DR. Multilineage potential of adult human mesenchymal stem cells. Science. 1999 Apr 2;284(5411):143-7.
8) Noda M, Camilliere JJ. In vivo stimulation of bone formation by transforming growth factor-beta. Endocrinology. 1989 Jun;124(6):2991-4.
9) Osyczka AM, Nöth U, O'Connor J, Caterson EJ, Yoon K, Danielson KG, Tuan RS. Multilineage differentiation of adult human bone marrow progenitor cells transduced with human papilloma virus type 16 E6/E7 genes. Calcif Tissue Int. 2002 Nov;71(5):447-58. Epub 2002 Sep 18.
10) Allan EH, Ho PW, Umezawa A, Hata J, Makishima F, Gillespie MT, Martin TJ. Differentiation potential of a mouse bone marrow stromal cell line. J Cell Biochem. 2003 Sep 1;90(1):158-69.
11) Stein GS, Lian JB, Stein JL, Van Wijnen AJ, Montecino M. Transcriptional control of osteoblast growth and differentiation. Physiol Rev. 1996 Apr;76(2):593-629.
12) Jilka RL, Weinstein RS, Bellido T, Parfitt AM, Manolagas SC. Osteoblast programmed cell death (apoptosis): modulation by growth factors and cytokines. J Bone Miner Res. 1998 May;13(5):793-802.
13) Jones SJ, Gray C, Sakamaki H, Arora M, Boyde A, Gourdie R, Green C. The incidence and size of gap junctions between the bone cells in rat calvaria. Anat Embryol (Berl). 1993 Apr;187(4):343-52.
14) Aarden EM, Burger EH, Nijweide PJ. Function of osteocytes in bone. J Cell Biochem. 1994 Jul;55(3):287-99.
15) Klein-Nulend J, Burger EH, Semeins CM, Raisz LG, Pilbeam CC. Pulsating fluid flow stimulates prostaglandin release and inducible prostaglandin G/H synthase mRNA expression in primary mouse bone cells. J Bone Miner Res. 1997 Jan;12(1):45-51.
16) Kogianni G, Noble BS. The biology of osteocytes. Curr Osteoporos Rep. 2007 Jun;5(2):81-6.
17) Suda T, Takahashi N, Martin TJ. Modulation of osteoclast differentiation. Endocr Rev. 1992 Feb;13(1):66-80.
18) Woo SL, Lothringer KS, Akeson WH, Coutts RD, Woo YK, Simon BR, Gomez MA Less igid internal fixation plates: historical perspectives and new concepts. J Orthop Res. 1984;1(4):431-49.

19) Bos GD, Goldberg VM, Powell AE, Heiple KG, Zika JM. The effect of histocompatibility maching on canine frozen bone allografts. J Bone Joint Surg. 1983; 65(1), 89-96.
20) Damien CJ, Parsons JR. Bone graft and bone graft substitutes: a review of current technology and applications. J Appl Biomater. 1991 Fall;2(3):187-208.
21) Lane JM, Tomin E, Bostrom MP. Biosynthetic bone grafting. Clin Orthop Relat Res. 1999 Oct;(367 Suppl):S107-17.
22) Bauer TW, Muschler GF. Bone graft materials. An overview of the basic science. Clin Orthop Relat Res. 2000 Feb;(371):10-27.
23) Li RH, Wozney JM. Delivering on the promise of bone morphogenetic proteins. Trends Biotechnol. 2001 Jul;19(7):255-65.
24) Meijer GJ, de Bruijn JD, Koole R, van Blitterswijk CA. Cell-based bone tissue engineering. PLoS Med. 2007 Feb;4(2):e9.
25) Urist MR. Bone: formation by autoinduction. Science. 1965 Nov 12;150(698):893-9.
26) Fujimura K, Bessho,K, Kusumoto,K, Ogawa,Y, Iizuka,T. Experimental studies on bone inducing activity of composites of atelopeptide type I collagen as a carrier for ectopic osteoinduction by rhBMP-2. Biochem Biophys Res Commun 1995;208:316-322.
27) Si X, Jin,Y, Yang,L. Induction of new bone by ceramic bovine bone with recombinant human bone morphogenetic protein 2 and transforming growth factor beta. Int J Oral Maxillofac Surg 1998;27:310-4.
28) Murata M, Inoue,M, Arisue,M, Kuboki,Y, Nagai,N. Carrier-dependency of cellular differentiation induced by bone morphogenetic protein in ectopic sites. Int J Oral Maxillofac Surg 1998;27:391-6.
29) Omura S, Mizuki,N, Kawabe,R, Ota,S, Kobayashi,S, Fujita,K. A carrier for clinical use of recombinant human BMP-2: dehydrothermally cross-linked composite of fibrillar and denatured atelocollagen sponge. Int J Oral Maxillofac Surg 1998;27:129-34.
30) Yoshida K, Bessho,K, Fujimura,K, Kusumoto,K, Ogawa,Y, Tani,Y, Iizuka,T. Osteoinduction capability of recombinant human bone morphogenetic protein-2 in intramuscular and subcutaneous sites: an experimental study. J Craniomaxillofac Surg 1998;26:112-5.
31) Ripamonti U, Reddi AH. Periodontal regeneration: potential role of bone morphogenetic proteins. J Periodontal Res. 1994 Jul;29(4):225-35.
32) Hollinger J. Factors for osseous repair and delivery: Part II. J Craniofac Surg. 1993 Jul;4(3):135-41.
33) Kenny SM, Buggy M. Bone cements and fillers: a review. J Mater Sci Mater Med. 2003 Nov;14(11):923-38.
34) Ruhe PQ, Wolke JGH, Spauwen PHM, Jansen JA. Calcium Phosphate Ceramics of bone tissue engineering. CRC Biomediacal Engineering Handbook 2005, Section Tissue Engineering.
35) Ooms EM, Wolke JG, van der Waerden JP, Jansen JA. Trabecular bone response to injectable calcium phosphate (Ca-P) cement. J Biomed Mater Res. 2002 Jul;61(1):9-18.
36) Ooms EM, Wolke JG, van de Heuvel MT, Jeschke B, Jansen JA. Histological evaluation of the bone response to calcium phosphate cement implanted in cortical bone. Biomaterials. 2003 Mar;24(6):989-1000.
37) Hutmacher DW. Scaffolds in tissue engineering bone and cartilage. Biomaterials. 2000 Dec;21(24):2529-43.
38) Breitbart AS, Staffenberg DA, Thorne CH, Glat PM, Cunningham NS, Reddi AH, Ricci J, Steiner G. Tricalcium phosphate and osteogenin: a bioactive onlay bone graft substitute. Plast Reconstr Surg. 1995 Sep;96(3):699-708.
39) Tsuruga E, Takita H, Itoh H, Wakisaka Y, Kuboki Y. Pore size of porous hydroxyapatite as the cell-substratum controls BMP-induced osteogenesis. J Biochem. 1997 Feb;121(2):317-24.

40) Pohler OE. Unalloyed titanium for implants in bone surgery. Injury 31, 7, 2000.
41) Jansen JA, von Recum AF, van der Waerden JP, de Groot K. Soft tissue response to different types of sintered metal fibre-web materials. Biomaterials 13, 959, 1992.
42) Chang YS, Oka M, Kobayashi M, Gu HO, Li ZL, Nakamura T, Ikada Y. Significance of interstitial bone ingrowth underload-bearing conditions: a comparison between solid and porous implant materials. Biomaterials 17, 1141, 1996.
43) van den Dolder J, Farber E, Spauwen PHM, Jansen JA. Bone tissue reconstruction using titanium fiber mesh combined with rat bone marrow stromal cells. Biomaterials; 24, 1745, 2003.
44) Vehof JW, de Ruijter AE, Spauwen PHM, Jansen JA. Influence of rhBMP-2 on rat bone marrow stromal cells cultured on titanium fiber mesh. Tissue Eng. 7, 373, 2001.
45) Vehof JW, Haus MT, de Ruijter AE, Spauwen PHM, Jansen JA. Bone formation in transforming growth factor β-I-loaded titanium fiber mesh implants. Clin. Oral Implants Res. 13, 94, 2002.
46) Vehof JW, Madmood J, Tikita H, van't Hof MA, Kuboki Y, Spauwen PHM, Jansen JA. Ectopic bone formation in titanium mesh loaded with bone morphogenetic protein and coated with calcium phosphate. Plast. Reconstr. Surg. 108, 434, 2001.
47) Vehof JWM, Spauwen PHM, Jansen JA. Bone formation in CaP-coated titanium fiber mesh. Biomaterials 2000; 21: 2003-2009.
48) Massia SP, Hubbell JA. Covalent surface immobilization of Arg-Gly-Asp- and Tyr-Ile-Gly-Ser-Arg- containing peptides to obtain well-defined cell-adhesive substrates. Anal Biochem. 187, 292, 1990.
49) Solheim E. Growth factors in bone. International Orthopaedics (1998) 22:410-416.
50) Bonewald LF. Transforming growth factor–B. In Bilezikian JP, Raisz LG& Rodan GA; Principles in bone biology. Academic Press, San Diego, p 647-659.
51) Reddi AH. Cell biology and biochemistry of endochondral bone development. Coll Relat Res 1981;1:209-26.
52) Bostrom MP, Lane JM, Berberian WS, Missri AA, Tomin E, Weiland A, Doty SB, Glaser D, Rosen VM. Immunolocalization and expression of bone morphogenetic proteins 2 and 4 in fracture healing. J Orthop Res 1995;13:357-367.
53) Reddi AH. Bone morphogenetic proteins, bone marrow stromal cells, and mesenchymal stem cells. Maureen Owen revisited. Clin Orthop 1995;115-119.
54) Reddi AH. Role of morphogenetic proteins in skeletal tissue engineering and regeneration. Nat Biotechnol 1998;16:247-252.
55) Wozney JM, Rosen V, Celeste AJ, Mitsock LM, Whitters MJ, Kriz RW, Hewick RM, Wang EA. Novel regulators of bone formation: molecular clones and activities. Science 1988;242:1528-34.
56) Fürst G, Gruber R, Tangl S, Zechner W, Haas R, Mailath G, Sanroman F, Watzek G. Sinus grafting with autogenous platelet-rich plasma and bovine hydroxyapatite. A histomorphometric study in minipigs. Clin Oral Implants Res. 2003 Aug;14(4):500-8.
57) Groeneveld EH, Burger EH. Bone morphogenetic proteins in human bone regeneration. Eur J Endocrinol. 2000 Jan;142(1):9-21.
58) Bostrom MP. Expression of bone morphogenetic proteins in fracture healing. Clin Orthop Relat Res. 1998 Oct;(355 Suppl):S116-23.
59) Böttner M, Krieglstein K, Unsicker K. The transforming growth factor-betas: structure, signaling, and roles in nervous system development and functions. J Neurochem. 2000 Dec;75(6):2227-40.
60) Yamaguchi A, Katagiri T, Ikeda T, Wozney JM, Rosen V, Wang EA, Kahn AJ, Suda T, Yoshiki S. Recombinant human bone morphogenetic protein-2 stimulates osteoblastic maturation and inhibits myogenic differentiation in vitro. J Cell Biol. 1991 May;113(3):681-7.

61) Puleo DA, Bizios R. RGDS tetrapeptide binds to osteoblasts and inhibits fibronectin-mediated adhesion: Bone; 1991:12, 271.
62) Rezania A, Thomas CH, Branger AB, Waters CM, Healy KE. The detachment strength and morphology of bone cells contacting materials modified with a peptide sequence found within bone sialoprotein. J. Biomed. Mat. Res. 1997: 37, 9.
63) Pierschbacher MD, Ruoslahti E. Cell attachment activity of fibronectin can be duplicated by small synthetic fragments of the molecule. Nature: 1984;309, 30.
64) Pierschbacher MD, Ruoslahti E. Variants of the cell recognation site of fibronectin that retain attachment-promoting activity. Proc. Natl. Acad. Sci.USA. 1984; 81, 5985.
65) Ferris DM, Moodie GD, Dimond PM, Giorani CWD, Ehrlich MG, Valentini RF. RGD-coated titanium implants stimulate increased bone formation in vivo. Biomaterials. 1999; 20, 2323.
66) Marx RE, Carlson ER, Eichstadt RM, Schimmele SR, Strauss JE, Georgeft RN. Platelet Rich Plasma. Growth factor enhancement for bone grafts. Oral Surg Oral Med Oral Pathol Oral Radiol Endod. 1998; 85: 635-46.
67) Banks RE, Forbes MA, Kinsey SE et al. Release of the angiogenic cytokine VEGF from platelets: Significance for VEGF measurements and cancer biology. Br. J. of Cancer.1998; 77: 956.
68) Weibrich G, Kleis WKG, Hafner G. Growth factor levels in the platelet-rich plasma produced by two different methods: Curasan-type PRP kit versud PCCS PRP system. Int. J. Oral Maxillofac. Implants. 2002; 17: 184-190.
69) Seppä H, Grotendorst G, Seppä S, Schiffmann E, Martin GR. Platelet-derived growth factor in chemotactic for fibroblasts. J Cell Biol. 1982 Feb;92(2):584-8.
70) Maloney JP, Silliman CC, Ambruso DR, Wang J, Tuder RM, Voelkel NF. In vitro release of vascular endothelial growth factor during platelet aggregation. Am J Physiol. 1998 Sep;275 (3 Pt 2):H1054-61.
71) Kaplan DR, Chao FC, Stiles CD, Antoniades HN, Scher CD. Platelet alpha granules contain a growth factor for fibroblasts. Blood. 1979 Jun;53(6):1043-1052.
72) Zimmermann R, Jakubietz R, Jakubietz M, Strasser E, Schlegel A, Wiltfang J, Eckstein R. Different preparation methods to obtain platelet components as a source of growth factors for local application. Transfusion. 2001 Oct;41(10):1186-9.
73) O'Neill EM, Zalewski WM, Eaton LJ, Popovsky MA, Pivacek LE, Ragno G, Valeri CR. Autologous platelet-rich plasma isolated using the Haemonetics Cell Saver 5 and Haemonetics MCS+ for the preparation of platelet gel. Vox Sang. 2001 Oct;81(3):172-5.
74) Weibrich G, Kleis WK, Buch R, Hitzler WE, Hafner G. The Harvest Smart PRePTM system versus the Friadent-Schütze platelet-rich plasma kit. Clin Oral Implants Res. 2003 pr;14(2):233-9.
75) Weibrich G, Kleis WK Curasan PRP kit vs. PCCS PRP system. Collection efficiency and platelet counts of two different methods for the preparation of platelet-rich plasma. Clin Oral Implants Res. 2002 Aug;13(4):437-43.
76) Marx RE. Platelet-Rich Plasma (PRP): What Is PRP and What is not PRP? Implant Dentistry, volume 2001: 10; 4: 225-228.
77) Urist MR. The search for and discovery of bone morphogenic protein (BMP), Bone Grafts, Derivates and Substitute, Butterworth Heinemann, London, 1994.
78) Fennis JPM, Stoelinga PJW, Jansen JA. Mandibular reconstruction: a clinical and radiographic animal-study on the use of autogenous scaffolds and PRP. Int J Oral Maxillofac Surg. 2002;31(3): 281-6.
79) Weibrich G, Kleis WK, Hafner G, Hitzler WE, Wagner W. Comparison of platelet, leukocyte, and growth factor levels in point-of-care platelet-enriched plasma, prepared using a modified Curasan kit, with preparations received from a local blood bank. Clin Oral Implants Res. 2003 Jun;14(3):357-62.

80) Weibrich G, Kleis WK, Hafner G, Hitzler WE. Growth factor levels in platelet-rich plasma and correlations with donor age, sex, and platelet count. J Craniomaxillofac Surg. 2002 Apr;30(2):97-102.
81) Camargo PM, Lekovic V, Weinlaender M, Vasilic N, Madzarevic N, Kenney M. Platelet-rich plasma and bovine porous bone mineral combined with guided tissue regeneration in the treatment of intrabony defects in humans. Journal of Periodontal Research. 2002; 37: 300–306.
82) Hanna R, Trejo PM, Weltman RL. Treatment of intrabony defects with bovine derived xenograft alone and in combination with platelet-rich plasma: a randomized clinical trial. Journal of Periodontology. 2004; 75: 1668-77.
83) Kassolis JD, Rosen PS, Reynolds MA. Alveolar ridge and sinus augmentation utilizing platelet-rich plasma in combination with freeze-dried bone allograft: case series. Journal of Periodontolology. 2000; 71: 1654-61.
84) Lekovic V, Camargo PM, Weinlaender M, Vasilic N, Aleksic Z, Kenney EB. Effectiveness of a combination of platelet-rich plasma, bovine porous bone mineral and guide tissue regeneration in the treatment of mandibular grade II molar furcations in humans. Journal of Clinical Periodontology . 2003; 30: 746-751.
85) Nikolidakis D, van den Dolder J, Wolke JG, Stoelinga PJ, Jansen JA. The effect of platelet-rich plasma on the bone healing around calcium phosphate-coated and noncoated oral implants in trabecular bone. Tissue Engineering. 2006; 12: 2555-63.
86) Okuda K, Tai H, Tanabe K, Suzuki H, Sato T, Kawase T, Saito Y, Wolff LF, Yoshiex H. Platelet-rich plasma combined with a porous hydroxyapatite graft for the treatment of intrabony periodontal defects in humans: a comparative controlled clinical study. Journal of Periodontology. 2005; 76: 890-8.
87) Whitman DH, Berry RL, Green DM. Platelet gel: an autologous alternative to fibrin glue with applications in oral and maxillofacial surgery. Journal of Oral Maxillofacial Surgery. 1997; 55:1: 294-9.
88) Carlson ER. Bone grafting the jaws in the 21st century: the use of platelet-rich plasma and bone morphogenetic protein. Alpha Omegan. 2000 Aug-Sep;93(3):26-30.
89) Kassolis JD, Rosen PS, Reynolds MA. Alveolar ridge and sinus augmentation utilizing platelet-rich plasma in combination with freeze-dried bone allograft: case series. J Periodontol. 2000 Oct;71(10):1654-61.
90) Fennis JPM, Stoelinga PJW, Jansen JA. Mandibular reconstruction: a histological and histomorphometric study on the use of autogenous scaffolds, particulate cortico-cancellous bone grafts and platelet rich plasma in goats. Int J Oral Maxillofac Surg. 2004; 33(1):48-55.
91) Aghaloo TL, Moy PK, Freymiller EG. Evaluation of platelet-rich plasma in combination with freeze-dried bone in the rabbit cranium. A pilot study. Clin Oral Implants Res. 2005;16(2):250-7.
92) Jensen TB, Rahbek O, Overgaard S, Soballe K. No effect of platelet-rich plasma with frozen or processed bone allograft around noncemented implants. Int Orthop. 2005; 29(2):67-72.
93) Jung RE, Schmoekel HG, Zwahlen R, Kokovic V, Hammerle CHF, Weber FE. Platelet-rich plasma and fibrin as delivery systems for recombinant human bone morfogenetic protein-2. Clin.Oral Impl. Res. 2005 ;16: 676-682.
94) Raghoebar GM, Liem RS, Bos RR, van der Wal JE, Vissink A. Does platelet-rich plasma promote remodeling of autologous bone grafts used for augmentation of the maxillary sinus floor? Clin Oral Implants Res. 2005; 16(3):349-56.

95) Wiltfang J, Kloss FR, Kessler P, Nkenke E, Schultze-Mosgau S, Zimmermann R, Schlegel KA. Effects of platelet-rich plasma on bone healing in combination with autogenous bone and bone substitutes in critical-size defects. An animal experiment. Clin Oral Implants Res. 2004 Apr; 15(2):187-93.
96) Danesh-Meyer MJ, Filstein MR, Shanaman R. Histological evaluation of sinus augmentation using platelet rich plasma (PRP): a case series. J Int Acad Periodontol. 2001 Apr; 3(2):48-56.
97) Wiltfang J, Schlegel KA, Schultze-Mosgau S, Nkenke E, Zimmermann R, Kessler P. Sinus floor augmentation with beta-tricalciumphosphate (beta-TCP): does platelet-rich plasma promote its osseous integration and degradation? Clin Oral Implants Res. 2003 Apr; 14(2):213-8.

2

CLOSING CAPACITY OF CRANIAL BONE DEFECTS USING POROUS CALCIUM PHOSPHATE CEMENT IMPLANTS IN A RABBIT ANIMAL MODEL

H.C. Kroese-Deutman, J.G.C. Wolke, P.H.M. Spauwen and J.A. Jansen
J. Biomedical Materials Research Part A. 2006; 503-511.

CLOSING CAPACITY OF CRANIAL BONE DEFECTS USING POROUS CALCIUM PHOSPHATE CEMENT IMPLANTS IN A RABBIT ANIMAL MODEL

INTRODUCTION

Reconstruction of large bone defects (caused by e.g. excision of tumors, trauma and congenital malformations), can be difficult to perform and is associated with high complication rates. The areas, which have to resist mechanical pressure (weight bearing limbs), need extremely solid bone substance for a good reconstruction.

Standard procedure often involves bone transplantation (autografting). In general, this involves long-term surgical procedures with external fixation, which can be hindered by complications due mainly to poor local tissue conditions, limitations caused by the amount of donor bone material and skin, the size of the defect and the healing process itself.

Another problem is donor-site morbidity. Many complications such as infection, pain, loss of sensibility and haematoma have been described in this area.[1] It is not unusual that further surgical procedures have to take place due to these complications, often causing discomfort and disability.

Bone engineering offers an option to improve bone reconstruction procedures. This interdisciplinary field applies the principles of biology and engineering to the development of functional substitutes for damaged bone.[2] Bone engineering prevents donor-site morbidity and creates a scaffold on which it is possible to generate bone mass, this can contribute to the formation of lost or lacking bone.

Our research aimed to find the ideal scaffold material for bone regeneration, focusing on Calcium-Phosphate-Ceramics (CPC) developed by Brown and Chow in 1983.[3,4] Calcium-phosphate (Ca-P) cements are well-established materials used for bone repair. They consist of a mixture of powder (containing one or more compounds of calcium and/ or phosphate salts) and liquid and have a high compatibility and similarity with natural bone.[5,6,7,8] Ca-P cement is very osteoconductive and biodegradable[9,10] and furthermore, the cement formation it is easy to shape, injectable and can be maintained locally. This is why it is so effective for bone defects with an irregular form. The material provides mechanical support and serves as a substratum on which the cells and growth factors attach.[11]

To improve the quality of this scaffold material, the Department of Biomaterials of the University Medical Center Nijmegen has developed a porous Ca-P cement.[12] The porosity can be created either in vitro or in situ. It is anticipated that the porosity of the Ca-P cement will increase osteoconductivity and ensure cell colonisation and flow transport of nutrients and metabolic waste to enhance the activity of osteoinductive material.

In order to establish the clinical relevance of a bone substitute material it is useful to use a Critical Size Defect (CSD) model. In the literature, various definitions of the CSD exist and they indicate discrepancies in the size of the control defect.[13,14,15,16] One definition is that the CSD is the smallest size of a defect, which does not heal spontaneously when left untreated for a certain period of time.[17] Another definition is that a CSD is a defect, which has less than 10 percent bony regeneration during the lifetime of an animal.[18] For example, for adult New Zealand red rabbits, a CSD as created in the skull is assumed to be 15 mm in diameter after 24 weeks.[19] Hollinger et al confirmed that also untreated 15 mm cranial defects created in New Zealand white rabbits show less than 10 percent bone regeneration after 48 weeks.[20]

Confirmation of the critical sized nature of a bone defect is always a fundamental step in identifying the clinical relevance of bone replacing materials. In this way, the direct osteoconductive properties of implant materials can be determined. Therefore, the first objective of this study was to evaluate the cranial Critical Size Defect (CSD) of a New Zealand white rabbit, which has been defined as the smallest size of a defect that does not heal spontaneously when left untreated for a 12 week time period.[17] We choose a non weight-bearing defect for a start, in order to place the implants in weight-bearing defects (segmental defects of the radius) in the future. In view of this, circular defects with three different diameters (6, 9 and 15 mm) were created in the cranial skull. The second objective was to assess the suitability of porous Ca-P cement as a scaffold material for bone regeneration, using this rabbit model. A non-weight bearing location was chosen for the current study in order to exclude as much as possible interference with additional parameters, like the limited weight-bearing capacity of the tested porous Ca-P material.

MATERIALS AND METHODS

Preparation of porous calcium phosphate cement

In total, 30 disc-shaped porous calcium phosphate (Ca-P) cement implants were created by the CO_2 induction technique.[21] The implants were made out of Calcibon® (provided by Biomet Merck, Darmstadt, Germany). This used cement powder consisted of: 62.5wt% tricalcium phosphate (α-TCP), 26.8wt% dicalcium phosphate anhydrous (DCPA), 8.9wt% calcium carbonate ($CaCO_3$) and 1.8wt% hydroxyapatite (Hap). The cement liquid was a 2% aqueous solution of Na_2HPO_4. To generate macroporosity of the scaffold, $NaHCO_3$ was added for production of CO_2 gas in the cement. The ideal liquid/powder ratio for clinical applications of the cement has been shown to be 0.35 mL/g.[22] A syringe (Sherwood medical monoject 2 mL) was used for delivery of the cement.[23] One hundred and twenty µl aqueous Na_2HPO_4 (2% in weight) were added to the cement, which was placed in this syringe. The syringe was closed with an injection plunger and fixed in a mixing apparatus (Silamat® Vivadent, Schaan, Liechtenstein). Thereafter, 150µl NaH_2PO_4 (8%) were added in order to create gas bubbles inside the material and to generate macro-porosity. The total porosity of the various implants was determined by weighing and using the following formula:

$$E_{tot} = \left(1 - \frac{m}{V \times \rho_{HAP}}\right) \times 100\%$$

Where: E_{tot} = total porosity (%), m = average mass of the sample (g), V = volume of the sample (cm^3) and ρ_{HAP} = density of hydroxyapatite (g/cm^3).

In this way, the total porosity of the 6, 9 and 15 mm implants was calculated to be 71%, 74% and 74% respectively. The cement implants have an average pore diameter of 150 µm[12] Besides, a previous study already confirmed that. The newly formed cement was injected immediately into cylindrical Teflon moulds with three different diameters (6, 9 and 15 mm), to ensure a standardized shape of the implants. Subsequently, the samples were placed into an oven at 50°C for one hour. Afterwards, the surface of the discs was sandpapered to ensure the standardized height of 3 mm. Finally, the discs were sterilized by autoclaving for 15 minutes at 121°C.

Surgical procedure

In total, 40 adult female New Zealand rabbits (mean weight: 3334 gr; "de Vaan" farm, Bergharen, The Netherlands) were used. National guidelines for the care and use of laboratory animals were observed. Surgery was performed under general inhalation anesthesia. The anesthesia was induced by an intravenous injection of Hypnorm® (0.315 mg/ml fentanyl citrate and 10 mg/ml fluanisone) and atropine, while maintained by a mixture of nitrous oxide, oxygen and isoflurane through a constant volume ventilator. To reduce the peri-operative infection risk, antibiotic prophylaxis (Baytril 2.5%; Enrofloxacin, 5-10 mg/kg) was given to the rabbits. After anaesthesia, the animals were immobilized on their abdomen: The cranium was shaved and disinfected with povodine-iodine. From the nasal bone to the occipital protuberance, a longitudinal incision was made in the skull. Then, a midline incision was created in the periosteum, the periosteum was removed gently and lifted off the parietal skull with a blunt instrument. Subsequently, defects of different sizes were prepared with a dental-trephine bur (Table 1).

Group	Cranial size defects
I (n=10)	6 mm (pCa-P) 6 mm (control)
II (n=10)	9 mm (pCa-P) 9 mm (control)
III (n=10)	15 mm (pCa-P)
IV (n=10)	15 mm (control)

TABLE 1: *Design of the experiment: number of animals and defect size.*

The drill depth was always kept limited and the loosened cranial bone discs were removed carefully. In this way, full thickness holes were created without damaging the dura. The bone preparation was carried out using low rotation speed (max. 450 rpm) and using continuous internal cooling with physiologic saline. After these procedures, porous Ca-P-cement implants were inserted in the therefore chosen defects and the periosteum (Figure 1) and skin was closed (tensionless) using a vicryl 4.0 suture. Perioperativily, all the rabbits got Temgesic 0.05 mg/kg twice a day during two days for pain prevention.

As described in Table 1, a total of 40 animals were divided into four groups. Group one received 6 mm defects on both the right and left side of the cranium. The implant was placed alternately in the right or left defect, while the contralateral side was left open to serve as the control. Group 2 received 9 mm defects on the right and left side of the cranium, with the implant placed alternately in the right or left defect, and the contralateral side left open as the control. The third group received only one defect with a diameter of 15 mm in the middle of the cranium, because the skull is too fragile to bear two defects of this size. These single defects in the third group were filled with the 15 mm cement implants.

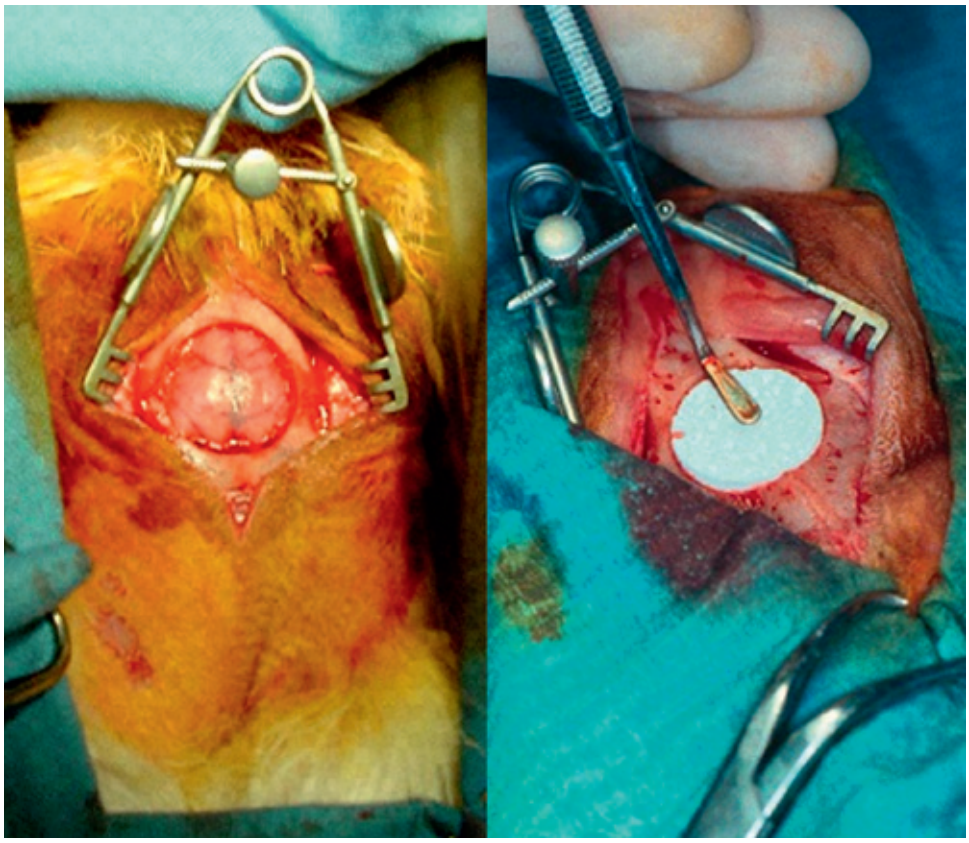

FIGURE 1: *Left: Empty 15 mm cranial defect of the rabbit.*
Right: Insertion of the porous Ca-P cement disc in the cranial defect.

Therefore there was an additional fourth group in which 15 mm defects were made in the cranium, which were left open, to serve as the control group of group III. The 15 mm defect size was chosen because it is assumed to be a critical sized defect (no spontaneous healing within 12 weeks[17], while the 5 and 9 mm defects were included as follow-up defects to evaluate the final osteoconductive properties of the porous Ca-P cement.

The rabbits were sacrificed 12 weeks postoperatively, and the skull containing the implants was used for radiological, histological and histomorphometrical evaluation.

Evaluation

Radiographic analysis

For all animals, an X-ray of the cranium was made after 12 weeks. The radiographs were made with a Siemens mobilett X-ray machine. The healing (closure) of the control defects of all groups were compared.

Histological and histomorphometrical evaluation

Directly after retrieval, specimens were fixed in 4% buffered formalin solution, dehydrated in a graded series of alcohol and embedded in methylmethacrylate (MMA). After polymerisation, non-decalcified thin (10 µm) transverse sections of the implant were prepared (at least three of each implant) using a modified sawing microtome technique.[24] Methylene blue and basic fuchsin were used for staining the sections. Histological examination of the slides was carried out using a light microscope (Leica BV, Rijswijk, the Netherlands) and using a concise description of the observed tissue reaction, i.e. histological appearance of the stability or degradation behavior of the implant, surrounding tissues and the tissue that has grown inside the implant porosity.

This histomorphometrical analysis was performed using computer based image analysis techniques (Leica® Quin Pro-image analysis system). Measurements were taken from three sections per porous Ca-P implant, and the results pooled to obtain an average for each implant, which was then used in the statistical evaluation.

The following parameters were used for digital analysis of the the cranial implants:

- The surface of the area where the implant is inserted, which is called the region of interest (ROI).
- The cement surface area. The cement surface area included micro-porosity of the cement, since pores smaller than 1 µm could not be distinguished histomorphometrically from cement particles.
- The bone surface area (%). This is the % of bone in the ROI.
- The macro-porosity (%), this is the ROI minus the cement surface area and bone surface area.
- Pore fill by bone (%), expressed as percentage of pore surface area occupied by bone.

Statistical analysis

Measurements from the histomorphometrical analysis were statistically evaluated using a One-Way Analysis of Variance (ANOVA) test[25] using GraphPad® Instat 3.05 software (Graphpad Software Inc., San Diego, CA, USA). Differences were considered significant at p-values less than 0.05.

RESULTS

Experimental animals:

In this study, three of the 40 animals did not survive the surgical procedure. One rabbit of the 9 mm cranial defect group + control group (after 23 days), and two rabbits of the porous Ca-P 15 diameter group (group III) died within 2 days of surgery. Their cause of death could not be determined to dural bleeding or oedema. This resulted in the following final numbers of retrieved animals per group: n=10 (Group I), n=9 (Group II), n=8 (Group III) and n=10 (Group IV). At retrieval, no inflammatory signs or adverse tissue reaction were observed. The porous Ca-P implants were clearly visible in the skull of the rabbit and covered by periosteum.

Radiographic analysis

The X-rays made after sacrifice suggested that two of the 6 mm control defects were closed after 12 weeks. In the 9 mm defects, three control defects appeared to be closed. In the 15 mm control group, all defects were still open and it was remarkable that the shape of the remained defect showed an oval central uncalcified area (Figure 2A).

In all Ca-P filled defects, the porous implants were always visible. In the 6 and 9 mm group, no signs of implant fracture or damage were observed. On the other hand, in the 15 mm group fracture lines were present (Figure 2B).

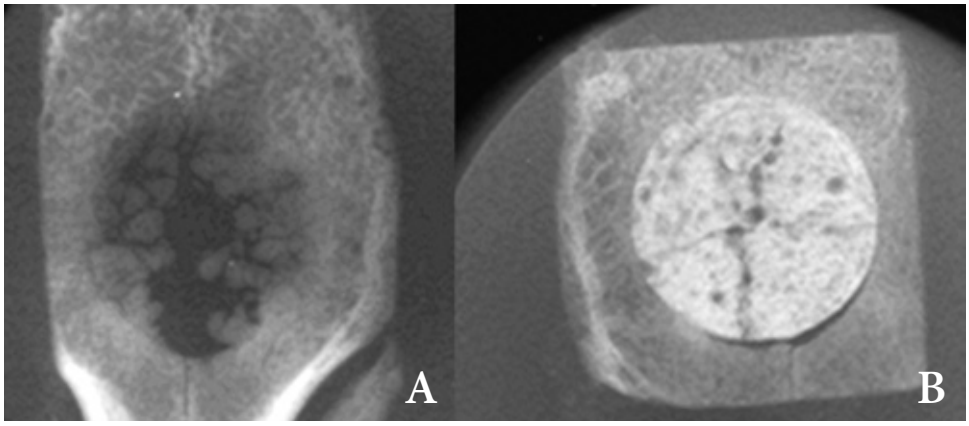

FIGURE 2: *Radiographic analysis.*

A: 15 mm open control defect, which is still open after 12 weeks implantation.

B: 15 mm porous Ca-P cement implant with a white aspect in which fracture lines are visible (also after 12 weeks implantation time).

Histology

Histologically there were no signs of inflammatory cells, necrosis or foreign body reaction. The cement was clearly visible and all control defects could be detected. All implants were surrounded by a thin fibrous capsula. Overviews of the sections of each group are shown in Figures 3 and 4. A more detailed picture of the bone formation in the porous Ca-P cement is shown in Figure 5.

Group I (6 mm)

After 12 weeks all of the porous Ca-P discs were completely covered and filled with bone (Figure 3A). Bone formation was seen in the pores and blood vessel ingrowth was present over the whole of the implant. Bone ingrowth was always seen to occur from one defect edge to the opposite one. It was characterized by the occurrence of osteoblasts, osteocytes and osteoclasts. There was excellent bone attachment to the surface of the porous Ca-P cement along the original defect, thus demonstrating a clear bone bridging aspect. Of the control defects, 3 of the 10 defects were left open after 12 weeks (Figure 4A). Both in open and closed defects, the ingrowth of new bone had proceeded form the defect walls to the center of the defect. The newly formed bone had a trabecular appearance and no discern could be made between the original and newly formed bone, which made it impossible to locate the previously created drill walls. In the open defects, the center of the defect was filled with fibrous tissue.

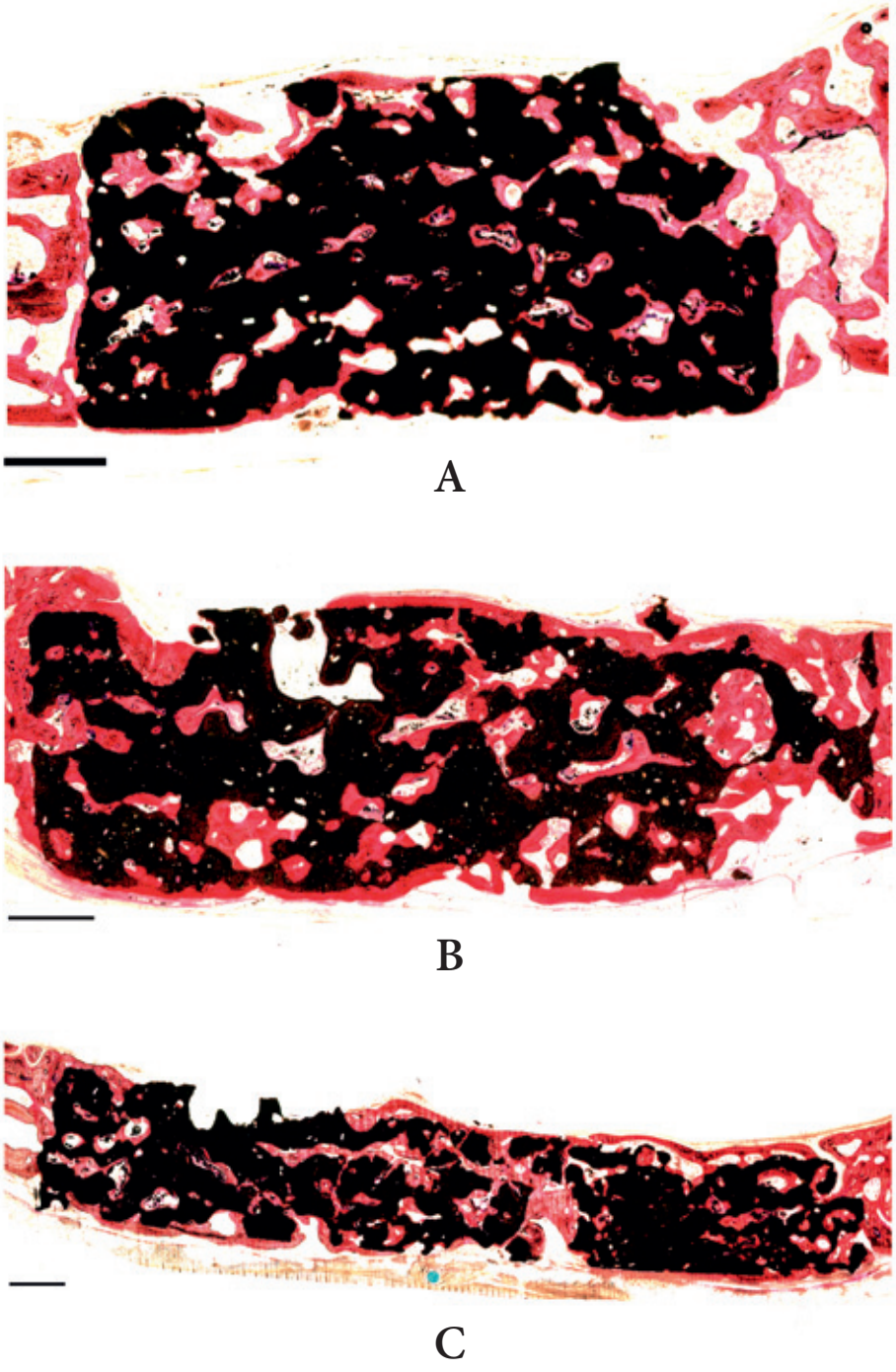

FIGURE 3: *Stained section of the 6, 9 and 15 mm porous Ca-P cement implant (original magnification 1.6x, bar represents 1 mm) in respectively A, B and C. The porous Ca-P in the middle has a dark aspect surrounded by bone formation developed over the implant.*

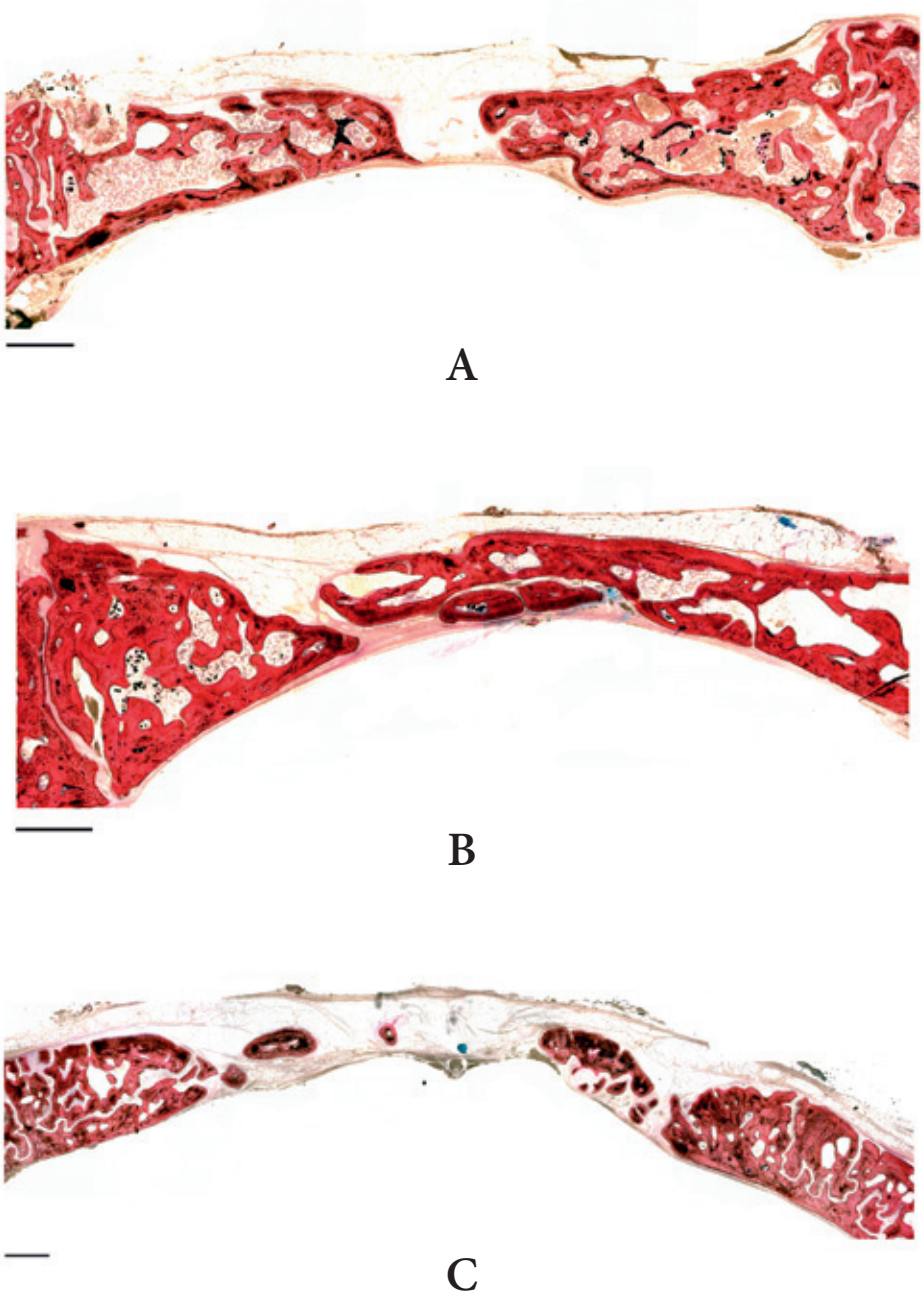

FIGURE 4: *Stained section of the 6, 9 and 15 mm control defect which are still open after 12 weeks implantation (original magnification 1,6x, bar represents 1 mm) in respectively A, B and C.*

Group II (9.0 mm)

In all the animals, bone formation was present over the whole of the porous Ca-P implant. Bone was seen also in the macropores, without any gap formation (Figure 3B). Osteocytes, osteoblasts and osteoclasts were visible in the implants, and a bone bridging aspect was seen, similar to the first group. Blood vessel ingrowth was present as well. In contrast to the first group, loose fragments of Ca-P were observed.

Of the control defects, three were closed and the other six were still open after 12 weeks (Figure 4B). The appearance of the closed and open defects was similar as described above for the 6 mm defects.

Group III and IV (15 mm)

In seven of the eight animals of group III bone bridging was present over the whole of the implant similar to that of groups I and II (Figure 3C). As in the first two groups, osteocytes, osteoblasts and osteoclasts and invasive blood vessel ingrowth were present in the implants. On the other hand, fracture lines and loose Ca-P fragments in the cement were now visible in about 90% of the prepared histological sections.

All control defects (n=10) were open after 12 weeks´ implantation time (Figure 4C). Relative less bone ingrowth was observed compared with the 6 and 9 mm control defects. As a consequence, a larger central open area was observed, which was again filled with fibrous tissue. The morphology of the ingrown bone and the remodeling of the drill walls were similar to the 6 and 9 mm control defects.

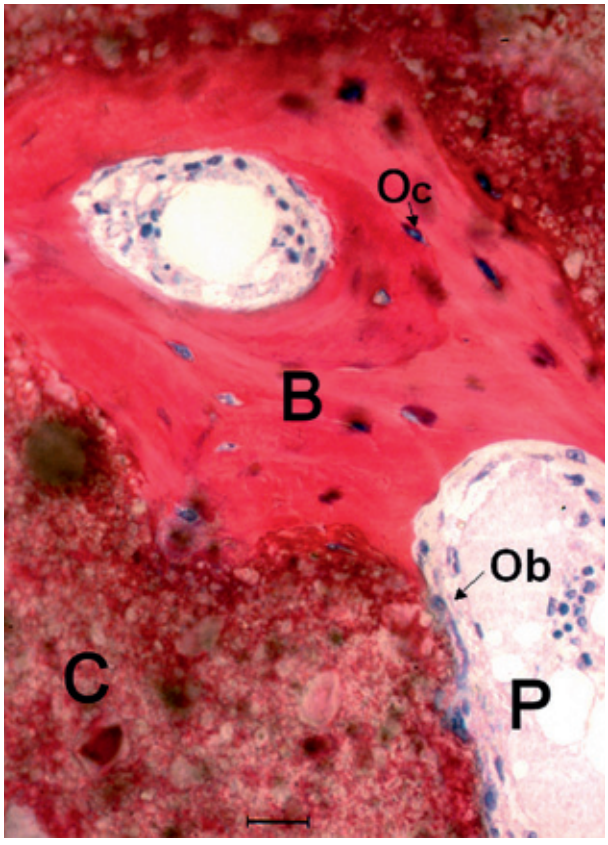

FIGURE 5*: Stained section of the porous Ca-P (original magnification 40x, bar represents 25 µm). Direct apposition of bone on the porous Ca-P cement surface is observed. C=Cement, P=Pore, B=Bone, Ob= Osteoblast, Oc= Osteocyte.*

Histomorphometry

A histomorphometrical analysis of bone ingrowth was only done for the cement filled defects, because it was impossible to locate the original drill walls. As a consequence, a proper definition of the Region of Interest was not allowed, which hampers correct measurements. The results of the histomorphometry analysis of the three porous Ca-P implant groups are listed in Table 2.

Groups with pCaP implants 12 weeks implantation time	n	Bone Surface area (%)	Postimplantation macro-porosity (%)	Porefill (%)
I: Porous Ca-P 6 mm	10	17 (±7%)	27 (±7%)	60 (±14)%
II: Porous Ca-P 9 mm	9	18 (±6%)	37 (±5%)	48 (±14%)
III: Porous Ca-P 15 mm	8	17 (±3%)	41 (±6%)	43 (±11%)
P value		0.95	0.0002	0.028

TABLE 2*: Histomorphometrical results of post-implantation macro-porosity, bone ingrowth, porefill and P-value; percentages for the three porous Ca-P implant groups after 12 weeks.*

Comparison of the data shows that no difference in bone surface area existed for the three different implant diameters. On the other hand, a statistical significant difference ($p<0.05$) was seen in pore fill percentage between the 6 mm and 15 mm group (60 ±14% vs 43 ±11%) after 12 weeks of implantation. Pore fill percentage was similar for the 9 mm and 15 mm implants. This corroborated with the calculated macro-porosity (= empty space after ingrowth of bone into the cement pores) as left in the implants. Significantly less ($p<0.05$) open space was left in the 6 mm implants compared with both the 9 mm and 15 implants, while no difference in post-implantation macro-porosity was found between the 9 mm and 15 mm implants.

DISCUSSION

As a basis for assessing the suitability of porous Ca-P cement as a bone regeneration material this experiment aimed to determine the cranial Critical Size Defect (CSD) of a New Zealand white rabbit. The results showed that defects of 15 mm failed to heal spontaneously; after 12 weeks all control defects with a diameter of 15 mm were still open.

It is known that the size of a CSD is depending on the breed and age of the used experimental animal model as well as the location of the defect. Therefore, in the current study, bone defects with varying diameter were created in the skull of only 3-month old New Zealand white rabbits. Determination of the critical defect size in this model and location can be valuable for other researchers studying the osteoconductive material goods of implants, although some discussion has arisen over whether testing an implant or graft in a non-critical size defect may also be meaningful, because delayed healing may occur due to the implant acting as a physical barrier.[26] Nevertheless, our results corroborate with studies as performed by Frame et al[19] (New Zealand reds) and Dodde[27]

(New Zealand whites, despite the fact that in these studies the animals were older (4 to 10 months compared to the 3 months old rabbits in our study). They also concluded that a defect size of 15 mm was the CSD.

The radiographs of the 15 mm control revealed that oval shaped gaps were left in the direction of the cranial skull lines (Figure 2A). Remarkably, this is the place where the sinus of the dura is located. It is known that the bone healing process is delayed when there is a haematoma in situ, and we assume that this could have been be the case in this experiment. Apparently, prevention of blood clot formation is important to stimulate the bone engineering process.

The X-ray data of the 6 mm control defects also showed a discrepancy compared with the histological observations, because the radiographs suggested that more defects were closed than seen in the light microscopical sections. Evidently, this is due to the fact that an X-ray image is a 2D representation of a 3D object. Consequently, overlapping structures and small differences in radiopacity of the ingrown tissue result in overestimation of defect closure.

Further, this study aimed to assess the characteristics of our scaffold material (porous Ca-P cement) when implanted in this animal model. Bone growth was seen in all three defect sizes in which implants were inserted and always seemed to extend from one defect edge to the opposite one. In view of this, the results provide evidence that porous Ca-P cement shows good osteoconductive properties without any sign of delayed or compromised healing when used for implants placed in a cranial defect of a rabbit. This was also confirmed in a previous study by Ruhé using the same animal model, in which 8 mm defects were made with an implantation time of 2 and 10 weeks.[11] Only, one of the 8 animals in the 15 mm porous Ca-P group showed no complete bridging of the skull defect. Strikingly, there was a large air bubble in this implant, which may be the reason that the formation of the bone bridge was delayed.

Also, all implants remained located in the created defect and maintained their shape and stability, with no signs of migration of the implant. Despite the overall good survival rate, two of the rabbits of the 15 mm defect group who received an implant died shortly after surgery. The reason for this could be the high pressure of the large diameter scaffold, which creates a high intracranial pressure. Alternatively, oedema, infection or intracranial bleedings, may have been the cause of death, although signs of these were not detectable during post-mortem examination. The death of one 9 mm defect rabbit was supposed not to be related to the surgery, because the animal died about 3.5 weeks after the installation of the implant.

As already mentioned, the defects in which porous CaP cement implants were placed, showed a complete bone bridging, as seen from the histological examination. We also noticed that the bone formed in porous Ca-P was covering a larger distance of the created defect compared to the open control groups. In contrast, the control defects showed bone formation only at the edges. Unfortunately we were not able to measure the amount of bone formation of the control groups because drill holes were not detectable in the histological sections. Marking the location of the drill holes of the control group with a metallic pin can be a way to overcome this in future experiments.

Previous studies described the degradation of Ca-P cements during implantation in bone defects.[28] Nevertheless, no clear sign of cement degradation was observed in our histological sections. Although, this observation agrees with another recent study of our group using the same cement composition and implant location, it contradicts with the results of Perez del Real et al, who used also the same cement composition and porosity preparation technique.[21] However, in this study, the cement was installed in defects

created in the trabecular bone of the femoral condyle of goats. Besides physico-chemical properties, the degradation rate of Ca-P ceramics is dependent on the local remodeling activity and bone conditions of the implant site. We suppose that this explains the current difference in results. Of course, it has to be noticed that poor mechanical properties are a disadvantage of the maintenance of highly porous Ca-P ceramic. This can be the reason for fracture lines in the 15 mm implants (visible during histological and radiological analysis (Figure 2B and 3C), which can be created during head injury against the cage walls as caused by the rabbit itself. Perhaps, a possible solution for this problem can be found by the preparation of mechanically stronger Ca-P cement composites, including the use of an in vivo degradable porogen, which is replaced during degradation by ingrowing bone.

CONCLUSION

The study showed that 15 mm is the Critical Size Defect (CSD) in an adult New Zealand white rabbit. The results also confirm that within the limitations of the study design, i.e. no comparison with other implant materials, porous Ca-P cement implants demonstrate excellent osteoconductive properties in non weight-bearing situations and bone bridging takes place over the total implant diameter.

Acknowledgement: This study has been supported by the NWO-AGIKO foundation.

REFERENCES

1) Hartman EHM, Spauwen PHM, and Jansen JA. Donor site complications in vascularised bone flap surgery. J of Invest. Surg. 2002; 15: 185-197.
2) Langer R, Vacanti JP. Tissue Engineering. Science 1993; 260:920-6.
3) Brown WE, Chow LC. US patent 1986; 4,612, 053.
4) Chow, LC. Development of self-setting calcium phosphate cements. J Ceram Soc Jpn (int Ed) 1991; 99:927-35.
5) Ishikawa K, Asaoka K. Estimation of ideal mechanical strength and critical porosity of calcium phosphate cement. J Biomed Mater Res. 1995 ; 29: 1537-43.
6) Khairoun I, Driessens FC, Boltong MG, Planell JA, Wenz R. Addition of cohesion promotors to calcium phosphate cements. Biomaterials 1999; 20: 393-8.
7) Brown WE, Chow LC. US patent 1985; 4, 518, 430.
8) Lee DD, Tofighi A, Aiolova M, Chakravarthy P, Catalano A, Majahad A, Knaack D. Alpha-BSM: a biomimetic bone substitute and drug delivery vehicle. Clin Orthop Relat Res. 1999;(367 Suppl):396-405.
9) Ooms EM, Wolke JGC, van der Waerden JPCM, Jansen JA. Trabecular bone response to injectable calcium phosphate (Ca-P) cement. J Biomed Mater Res. 2002; 61: 9-18.
10) Comuzzi L, Ooms EM, Jansen JA. Injectable calcium phosphate cement as a filler for bone defects around oral implants: an experimental study in goats. Clin Oral Implants Res. 2002; 13: 304-311.
11) Ruhé PQ, Kroese-Deutman HC, Wolke JG, Spauwen PHM, Jansen JA. Bone inductive properties of rhBMP-2 loaded porous calcium phosphate cement implants in cranial defects in rabbits. Biomaterials 2004; 2123-32.
12) del Real RP, Wolke JGC, Vallet-Regi M, Jansen JA. A new method to produce macropores in calcium phosphate cements. Biomaterials 2002; 23: 3673-80.
13) Chang SC, Chuang H, Chen YR, Yang LC, Chen JK, Mardini S, Chung HY, Lu YL, Ma WC, Lou J. Cranial repair using BMP-2 gene engineered bone marrow stromal cells. J Surg Res; 2004 Jun 1;119(1):85-91.
14) Lundgren D, Nyman S, Mathisen T, Isaksson S, Klinge B. Guided bone regeneration of cranial defects, using biodegradable barriers: an experimental pilot study in the rabbit. J Craniomaxillofac Surg; 1992;20(6):257-60.
15) Levy FE, Hollinger JO, Szachowicz EH. Effect of a bioresorbable film on regeneration of cranial bone. Plast Reconstr Surg; 1994;93(2):307-11; discussion 312.
16) Clokie CM, Moghadam H, Jackson MT, Sandor GK. Closure of critical sized defects with allogenic and alloplastic bone substitutes. J Craniofac Surg. 2002;13(1):111-21; 122-3.
17) Bos GD, Goldberg VM, Powell AE, Heiple KG, Zika JM. The effect of histocompatibility maching on canine frozen bone allografts. J Bone Joint Surg. 1983; 65(1), 89-96.
18) Hollinger JO, Kleinschmidt JC. The critical size defect as an experimental model to test bone repair materials. J Craniofac Surg ; 1990; 1(1):60-8.
19) Frame JW. A convenient animal model for testing bone substitute materials. J. Oral surg. 1980; 38, 176.
20) Hollinger JO, Schmitz JP, Mizgala JW, Hassler C. An evaluation of two configurations of tricalcium phosphate for treating craniotomies. J Biomed Mater Res. 1989; 23(1):17-29.
21) del Real RP, Ooms EM, Wolke JGC, Vallet-Regi M, Jansen JA. In vivo bone response to porous calcium phosphate cement. J Biomed Mater Res. 2003; 65A: 30-36.

22) Wolke JGC, Ooms EM, Jansen JA. In vivo resorption behaviour of a high strength injectable calcium-phosphate cement. Bioceramics 2000; 13: 793-796.
23) Munting E, Mirtchi AA, LeMaitre J. Bone repair of defects filled with a phosphocalcic hydraulic cement: an in vivo study. J. Mater. Med. 1993; 4: 337-344.
24) van der Lubbe HB, Klein CP, de Groot K. A simple method for preparing thin (10 microM) histological sections of undecalcified plastic embedded bone with implants. Stain Technol 1988; 63: 171-6.
25) Armitage P, Berry G. Statistical methods in medical research (2nd ed.). London: Blackwell Scientific; 1988: 120.
26) Melcher AH, Irving JT. The effect of implanting various substances into artificially created circumscribed defects in rat femurs. J Bone Joint Surg ; 1963 : 45B: 162-175.
27) Dodde R 2nd, Yavuzer, R, Bier UC, Alkadri A, Jackson IT. Spontaneous bone healing in the rabbit. J Craniofac Surg ; 11: 346-9, 2000.
28) Yuan H, Li Y, de Bruijn JD, de Groot K, Zhang X. Tissue responses of calcium phosphate cement: a study in dogs. Biomaterials 2000; 21: 1283-90.

3

TORQUE TESTING AS A METHOD TO DETERMINE THE REGENERATION OF SEGMENTAL BONE DEFECTS IN RABBITS PROVIDED WITH POROUS CALCIUM PHOSPHATE CEMENT

H.C. Kroese-Deutman, J.G.C.Wolke, P.H.M. Spauwen and J.A. Jansen
In submission Tissue Engineering part C: Methods (2009).

TORQUE TESTING AS A METHOD TO DETERMINE THE REGENERATION OF SEGMENTAL BONE DEFECTS IN RABBITS PROVIDED WITH POROUS CALCIUM PHOSPHATE CEMENT

INTRODUCTION

Reconstruction of large segmental bone defects caused by excision of tumors, trauma and congenital malformations, are complex procedures for reconstructive surgeons. Especially areas, which have to resist a lot of mechanical load (like weight bearing limbs), are difficult to reconstruct. It is not uncommon that a second or a third surgical procedure has to be performed due to complications, e.g. infection, pain, loss of sensibility and hematoma. Problems that occur during the healing process can even lead to amputation of the limb.

This study was focused on the use of calcium phosphate (Ca-P) cement, as a synthetic bone grafting material. An important advantage of this material is that can be injected and shaped, which makes it very effective for the restoration of large bone defects with an irregular or abnormal shape. After setting, the material provides mechanical support and serves as a scaffold upon which the cells attach, proliferate and undergo differentiation due to its high similarity and compatibility with natural bone.[1-4] In addition, Ca-P cement can be provided with a porosity, which is anticipated to increase the osteoconductivity and to enhance the degradation of the material.[5,6] Also, the material can be used as a delivery system for the supplementary release of growth factors to further boost bone formation.[7]

In order to determine the clinical relevance of Ca-P cement as a bone substitute material in a weight-bearing situation, the current study aimed on the use of a rabbit segmental defect model. The mid-diaphyseal radius was chosen as the area in which to create non-critical as well as an assumed Critical Size Defect (CSD). It is claimed that this model does not need any kind of internal or external fixation because the maintained intact ulna provides sufficient stability.[8,9,10-12] A CSD is defined as the smallest size of a defect, which does not heal spontaneously when left untreated for a certain period of time.[13] There is a lot of variation in literature in the definition of a segmental CSD as made in rabbits.

The CSD of a radius or ulna, has been defined as 15 mm or 20 mm.[8,9,14-19] In this study, defect sizes of 5, 10 and 15 mm were used. The defects in both radii of each animal, were left open or filled with a tubular shaped porous Ca-P cement implant of the same size. The hypothesis was that the empty 15 segmental defects would stay open during a 12 week healing period. This in contrast to the porous Ca-P cement filled 15 mm defects, which were supposed to become closed due to the osteoconductive properties of the cement material. Five and 10 mm defects without Ca-P cement implants were also included as controls. Further, it was decided to evaluate the final bone regenerative capacity as present in all conditions not only by X-ray imaging and histological analysis, but to put special emphasis on mechanical testing as a methodological approach to determine final bone regeneration. For the mechanical studies, a torsional approach was used, which is considered as an appropriate method to measure the strength of the healed bone in long bone segmental defect models. A review of the literature shows that such a torque test can be performed in different ways.[8,20,21] Some studies test the total ulna-radius complex, while others separate the radius or ulna and test the single bone alone. It can be questioned whether such a separation is feasible without damaging the regenerated tissue. Therefore, we decided to maintain the complete ulna-radius complex during the torque assay.

MATERIALS AND METHODS

Preparation of porous calcium phosphate cement

In total, 30 porous calcium phosphate (pCa-P) cement implants were created by a CO_2 induction technique.[22] The implants were tubular-shaped with a diameter of 4.2 mm and length of resp. 5, 10 and 15 mm. Specific designed Teflon moulds were used to prepare the implants. The implants were made out of Calcibon® (provided by Biomet Merck, Darmstadt, Germany). This cement consists of a mixture of 62.5wt% tricalcium phosphate (α-TCP), 26.8wt% anhydrous dicalcium phosphate (DCPA), 8.9wt% calcium carbonate ($CaCO_3$) and 1.8 wt% hydroxyapatite (HA). The ideal liquid/powder ratio for clinical applications of the cement has been shown to be 0.35 mL/g23. To create porosity $NaHCO_3$ was added to the cement powder. All components (0.5 G of standards powder plus 0.05 g of $NaHCO_3$) were placed into a syringe (Sherwood medical monoject 2 mL) with aqueous Na_2HPO_4 (2%). The syringe was closed with an injection plunger and fixed in a mixing apparatus (Silamat® Vivadent, Schaan, Liechtenstein). After a mixing time of 15 sec, the plunger was removed and NaH_2PO_4 (8%) aqueous solution was added. Thereafter, the syringe was shaken again for 2 sec. Finally, the mixed cement was injected immediately into the respective Teflon moulds to ensure the standardized shape of the implants. Subsequently, the samples were placed in an oven at 50°C for 1 h.

After cooling, the implants were sandpapered to ensure a standardized size. Subsequently, the specimens were sterilized by autoclaving for 15 minutes at 121°C.

Surgical procedure

A total of 30 adult female New Zealand white rabbits (2, 5-3, 5 kg), 6 months of age, were used. National guidelines for the care and use of laboratory animals were respected. The rabbits were divided in 3 groups (5, 10 and 15 mm defects with or without pCa-P implant) as described in Table 1.

Group number	Segmental defects of the radius (bilaterally)
I n=10 (1†)	5 mm (Ca-P +control)
II n=10	10 mm (Ca-P +control)
III n=10 (1†)	15 mm (Ca-P +control)

TABLE 1: *Design of the experiment showing the number of animals and bilateral defect sizes.*

Surgery was performed under general inhalation anesthesia. The anesthesia was induced by an intravenous injection of Hypnorm® (0.315 mg/ml fentanyl citrate and 10 mg/ml fluanisone) (Abbeyvet Export Ltd, Leeds, UK) and atropine, and maintained by a mixture of nitrous oxide, isoflurane, and oxygen through a constant volume ventilator. To reduce the peri-operative infection risk, antibiotic prophylaxis (Baytril® 2.5% (KPV Pharma, Kiel, Germany) was given. Preoperatively, all rabbits received Finadyne® (Schering-Plough, Segre, France) 0.02 mg/kg twice a day during two days for pain treatment. An extra 40 ml fluid was administered before surgery to prevent dehydration.

After induction of anesthesia, the animals were immobilized in a prone position. In each animal the front legs were shaved and disinfected with povidone-iodine. A 4.5 cm longitudinal skin incision was made at the dorsal part along the radius. After dissecting the muscles, the radius was exposed. The periosteum was partially pushed off and a 5, 10 or 15 mm segmental defect was created in the mid diaphyseal part of the radius using a diamond-bladed dental drill with continuous saline cooling.

In all groups, bilateral segmental radial defects of the same size, were made in both radii. The porous Ca-P cement implants were pressed into place, according to a randomization scheme in the left or right limb, while the other limb served as the control group (Figure 1). After finishing this procedure, the muscle layers and the skin were closed in separate layers with a Vicryl 4.0 suture.

The rabbits were sacrificed 12 weeks postoperatively for radiological, mechanical and histological evaluation. Of each experimental group, 6 of the ulna-radius complexes were used for torque testing. The remaining ulna-radius complexes were taken directly for histological evaluation. Further, the specimens as subjected to mechanical testing were after application of the torsional load also prepared for histological analysis.

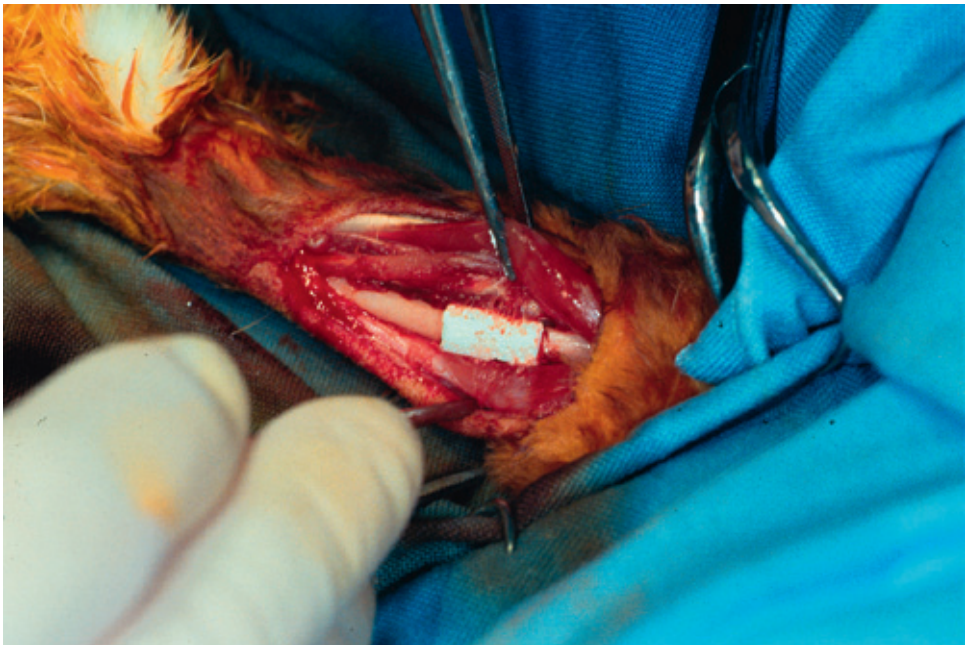

FIGURE 1: *Implantation of the scaffold in the radius.*

Radiographic analysis

A medio-lateral X-ray of the ulna-radius complex was made immediately after surgery (day 0), at 2 weeks and 12 weeks postoperatively. The radiographs were made with a Siemens Mobilett X-ray machine. The obtained X-ray images were only used for a subjective description of the bone healing characteristics such as callus formation, quality of union and bone remodelling in the three different experimental groups.

Mechanical testing (Torque test)

After harvesting, the ulna-radius complexes of 18 rabbits (six of each experimental group) were dissected free of all soft tissue. The ulna and the radius were connected to each other due to the fibrosis and new bone formation. A dental plaster was used to fix the specimen for mechanical testing (Figure 2A, 2B). Therefore, both ends of the forearm were placed in square formed moulds, which were filled with dental plaster. After setting, these square models fitted precisely in the torque apparatus (Instron, Norwood, USA). Before mechanical testing, two transcortical cuts were made as distal as possible at the lateral ends of the ulna using an oscillating saw. This was done to eliminate the mechanical contribution of the ulna and to isolate the radius during torque testing. Separation of the radius from the ulna was not an option due to ulnar hypertrophy, scar tissue formation and fibrous fusion.[24] The experimental groups were also compared to twelve non-operated complete bone samples as retrieved from rabbits of the same age.

An Instron torque apparatus was used to measure the maximum stress, which could be submitted to the ulna-radius complex (values of ultimate torque/ torque at failure) with or without porous Ca-P cement. The torque speed was 5 mm/minute. The angular displacement at torque failure could also be extracted from the data. With these measurements the energy absorbed and the stiffness of the specimens were calculated:

Torque = *Force* × *real distance (N.mm)*
Energy = *Force* × *real distance* × *degree (N.mm* × *°)*
Stiffness = *Torque / degree (N.mm / °)*

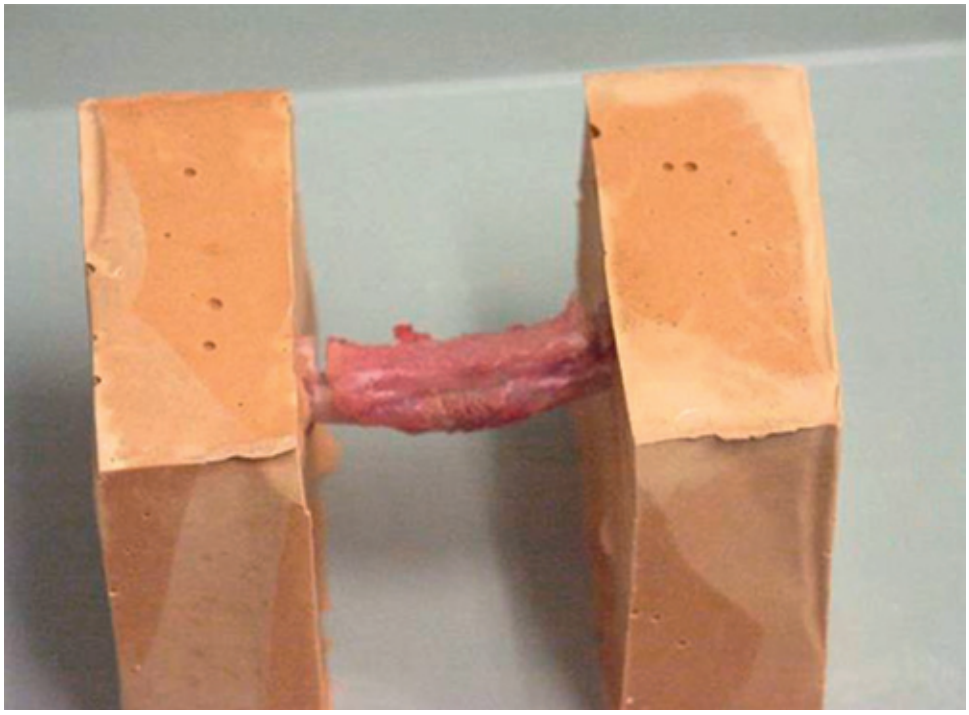

FIGURE 2A*: Torque test measurement. The ulna-radius complex fixated in the dental plaster.*

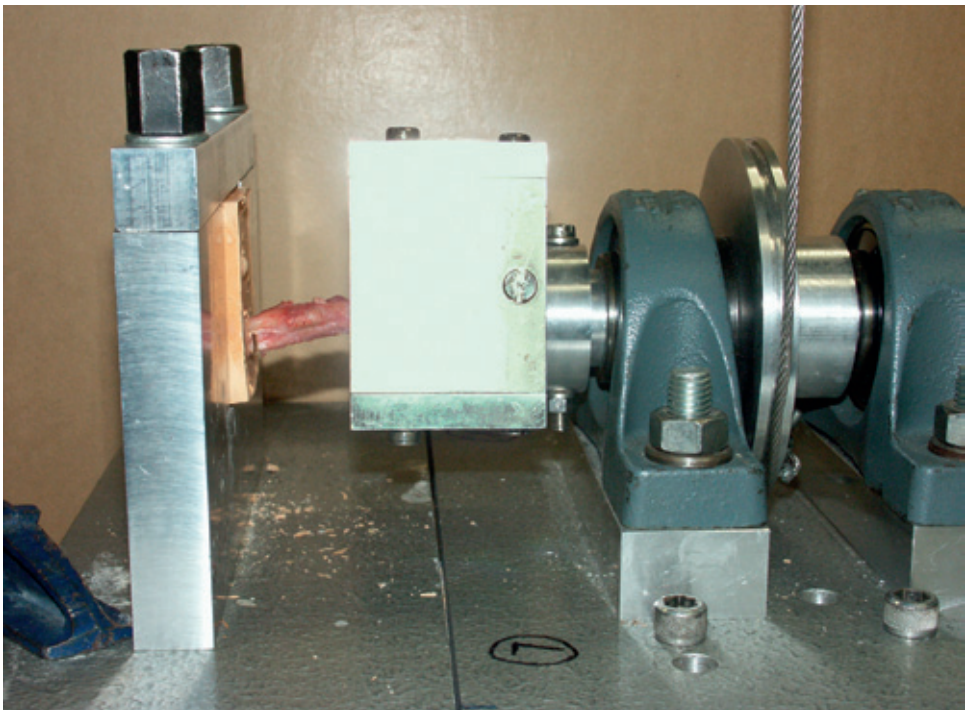

FIGURE 2B: *Torque test measurement. An Instron apparatus was used to measure the maximum stress as could be submitted to the bone structure.*

Histological evaluation

All the samples for histological examination (also the specimens as included after torque testing) were fixated in 4% phosphate-buffered formalin solution, dehydrated in a graded series of ethanol and embedded in methylmethacrylate (MMA). After polymerization, thin longitudinal sections (10 µm) were prepared (at least three per implant) in a transversal plane with a sawing microtome technique.[25] These sections were stained with methylene blue/ basic fuchsin and examined with a light microscope for concise histological description (Leica BV, Rijswijk, the Netherlands).

Statistical analysis

All data are reported as means and standard deviations. Measurements from the mechanical testing were statistically evaluated using a paired T-test (GraphPad® Instat 3.05 software, San Diego, CA, USA).[26] Differences were considered statistically significant at p-values less than 0.05.

RESULTS

In this study, two of the animals died directly after the surgical procedure (one animal of the 5 mm defect group and one of the 15 mm defect group). The remaining (n=28) survived the 12 weeks and were able to walk within three hours after surgery. The rabbits remained in good health, did not lose weight, did not show any direct wound complications, and the total ulna-radius complex could be taken out for further investigation at the end of the study.

Radiographic analysis

The radiographs taken directly after surgery confirmed that all implants were installed correctly. At two weeks, the X-rays showed a minimal amount of bone healing in all three groups.

After 12 weeks implantation time, the radiographs showed bone bridging over the total length of the defects of all three porous Ca-P cement groups (5, 10 and 15 mm defects) (Figure 3B). The porous Ca-P cement implants also remained in place according to X-ray examination and were clearly visible in the radius of the rabbit. One of the 15 mm implants showed a fracture line through the implant.

In the control group (no implants), all 5 mm defects were closed. In group II (10 mm), one out of 10 control defects was still open. In the third group (15 mm), 7 out of 9 control defects appeared to be still open (Figure 3A-2). Results are presented in Table 2. The two 15 mm control defects that were closed, showed a tiny bone bridge at the ulnar side of the radius.

FIGURE 3A+B*: Radiographic analysis of the 15 mm implant after 2 and 12 weeks of implantation.*

FIGURE 3A-1*: Control 15 mm after 2 weeks.*

FIGURE 3A-2*: Control 15 mm after 12 weeks.*

FIGURE 3B-1*: 15 mm porous Ca-P cement after 2 weeks.*

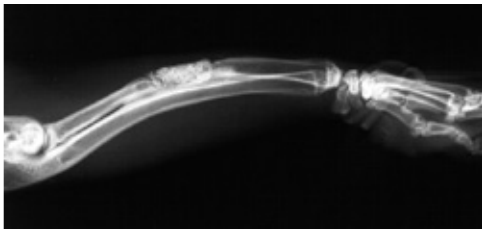

FIGURE 3B-2*: 15 mm porous Ca-P cement after 12 weeks.*

X-ray after 12 weeks	Closed	Open
5 mm (n=9) Ca-P	9	0
5 mm (n=9) control	9	0
10 mm (n=10) Ca-P	10	0
10 mm (n=10) control	9	1
15 mm (n=9) Ca-P	9	0
15 mm (n=9) control	2	7

TABLE 2: *Radiology results after 2 and 12 weeks. The numbers of open and closed defects are presented.*

Mechanical testing (Torque test)

Of each experimental group 6 ulna-radius complexes were used. In addition, the same test was carried out with an intact bone group as retrieved from rabbits of the same age (n=12).

During the torque tests, 2 animals of the 10 mm group and one of each 15 mm group were excluded of this paired test, due to technical failure during the torque test in one of the ulna-radius complexes (fracture of the dental plaster as used for the fixation of the ulna-radius complex or unstable fixation of the ulna-radius complexes in this dental plaster). The ultimate forces and distances were measured and the calculated torque, theta, stiffness and energy were calculated (see Table 3).

Statistical analysis of the torque measurements using the T-test showed that the 5 and 10 mm defects with our without pCa-P implants achieved similar values at 12 weeks of implantation (p value in the 5 mm group (n=6) was 0.13 (95% confidence interval of difference: -69.3 and 399.2), in the 10 mm (n=4) group p=0.71 (95% confidence interval of difference: –472.5 and 365.5). There was also no statistically significant difference with the retrieved non-operated bone samples. Further comparison suggested that the torsion data for the 15 mm open defect were lower compared with the filled 15 mm defect as well as the non-operated specimens (15 mm group (n=5) p=0.11 (95% confidence interval of difference: –499.2 and 73.3). However, a significant difference

could only be proven for the non-operated samples (p=0.03).

	Force N (±SD)	Real distance (±SD)	Torque N.mm (±SD)	Theta Degrees (±SD)	Stiffness N.mm/ degrees (±SD)	Energy N.mm × degrees (±SD)
Ca-P 5 mm	8.8 (±2.8)	21.6 (±5.9)	469.0 (±152.2)	23.2 (±6.3)	20.2 (±3.7)	10868.6 (±5873.7)
Open 5 mm	10.7 (±3.0)	25.8 (±5.2)	634.0 (±106.7)	27.6 (±5.6)	22.9 (±8.0)	17526.0 (±3174.2)
Ca-P 10 mm	11.7 (±2.4)	26.1 (±2.9)	628.1 (±129.5)	27.9 (±3.1)	22.5 (±4.8)	17545.3 (±4548.8)
Open 10 mm	11.5 (±4.0)	21.2 (±3.8)	616.3 (±212.9)	22.7 (±4.0)	27.2 (±6.9)	13992.67 (±6878.6)
Ca-P 15 mm	9.5 (±4.4)	20.2 (±5.2)	508.3 (±238.4)	21.6 (±5.5)	23.5 (±7.6)	10995.4 (±8118.8)
Open 15 mm	5.7 (±3.4)	18.2 (±15.4)	305.0 (±181.6)	19.5 (±16.5)	15.6 (±6.4)	5947.2 (±8002.4)
No defect	10.6 (±2.3)	23.7 (±4.3)	566.0 (±123.2)	25.4 (±4.6)	22.3 (±6.3)	14387.7 (±5262.4)

TABLE 3: *Torque test results. Torque, Stiffness and Energy are calculated.*
Torque = Force × real distance (N.mm)
Energy = Force × real distance × degree (N.mm × °)
Stiffness = Torque / degree (N.mm / °)

Histology

Group I (5 mm)

After 12 weeks, residues of the Ca-P were visible, but not in all the samples. One of the implants showed an old hematoma, without signs of infection. Ingrowth of blood vessels was observed throughout the porosity of the pCa-P implants. At the implant-ulna border, new bone formation had occurred, which resulted in fusion between the pCa-P implant and ulnar bone. Also at the original defect border, the newly formed bone was in contact with the porous Ca-P surface. Only occasionally, intervening fibrous tissue was present between the radius defect border and the implant surface. Bone formation had penetrated through all scaffolds, but the amount of bone varied. In the newly formed bone osteoblasts and osteocytes could be detected.

All empty control defects showed regeneration of the radius and were completely closed with new bone tissue. In addition, fusion of ulnar and new radial bone was seen in almost all samples.

FIGURE 4A+B: *Histology results after 12 weeks' implantation time.*

FIGURE 4A-1: *10 mm control defect. Magnification: 1.6x.*

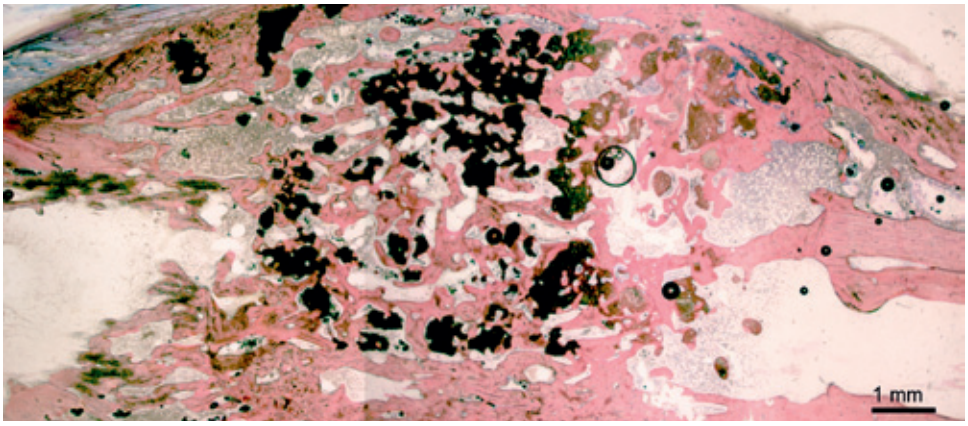

FIGURE 4A-2: *10 mm p Ca-P implant. Magnification: 1.6x.*

Group II (10 mm)

In 9 out of 10 specimens, bone formation had penetrated into and through the porous Ca-P implants (Figure 4A-2). However, the amount of bone varied between the various specimens. Bone formation was associated with the ingrowth of blood vessels. An intervening soft tissue layer was present at radial defect border of three samples and no bone ingrowth from this side was observed. Some bone tissue and fibrocartilagenous tissue was interposed between the pCa-P implant and ulna. Further examination revealed also that two of the scaffolds showed some displacement out of the defect.

Bone regeneration in the open control defects was similar to the group I defects, but in two of the open control defects there was no bone bridging. The rest of the non-filled defects (n=7) were completely closed histologically (Figure 4A-1).

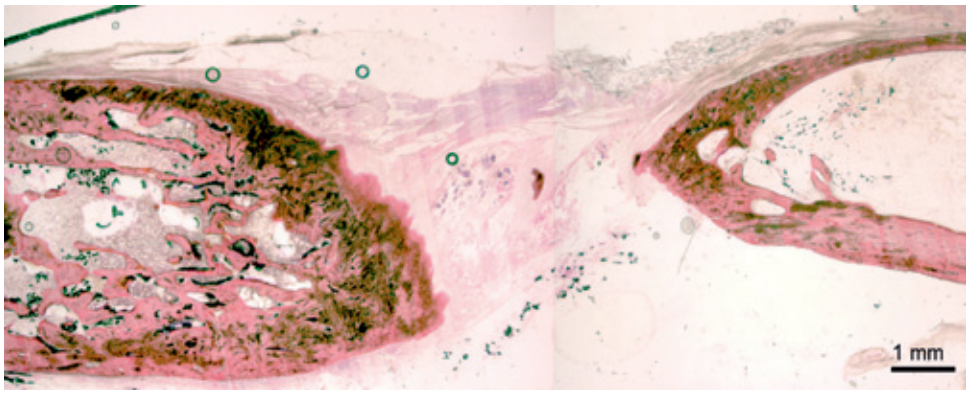

FIGURE 4B-1: *15 mm control defects. Magnification: 1.6x.*

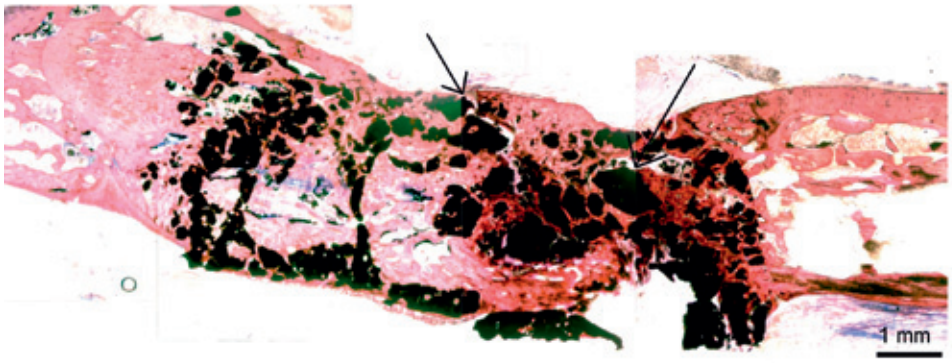

FIGURE 4B-2: *15mm p Ca-P implant. Magnification: 1.6x a fracture line is visible (arrows).*

Group III (15 mm)

The pCa-P cement implants were still in place after 12 weeks of implantation and all specimens showed bone formation throughout the Ca-P implant porosity (Figure 4B-2). Again, blood vessel ingrowth was observed in these implants. Fibrocartilagenous and limited bone tissue had formed in the area between the pCa-P implant and ulna. Further, an intervening soft tissue layer at the implant- radial defect border was present in two samples. Although bone was still present in the implant porosity of these implants, ingrowth did not occur from the edges. Two of the implants were found to be displaced and two of them showed fracture lines, without dislocation.

The sections of the empty control defects showed that seven of these defects were still open after 12 weeks. Only in two out of 9, bone bridging was visible histologically, but bone formation at the ulnar surface was limited.

DISCUSSION

This study aimed to assess the bone healing supporting characteristics of porous Ca-P cement when implanted in a rabbit segmental defect model. Bone formation into the cement porosity was seen in all three defect sizes in which implants were inserted. In view of this, the results provide evidence that porous Ca-P cement shows osteoconductive properties. A similar observation was done in a previous study dealing with the regeneration of large sized cranial defects of rabbits.[6,27] In addition, the torque measurements revealed that all pCa-P filled defects obtained the same mechanical strength as non-operated radii. Further, we have to emphasize that we decided to use the Ca-P cement in a pre-set form in order to avoid experimental variation due to differences in implant shape or total amount of implant material.

The torque or torsional test is described as a method to measure the strength of bone and is preferred to evaluate the mechanical properties of bone associated with fracture healing. Therefore, torsional testing is a frequently used technique to evaluate bone healing in long bone segmental defect models, because bone fails in torsion at the weakest point along the shaft.

It has to be emphasized that there are different approaches to perform a torque test. In some studies, separation of the radius or ulna is performed.[14,28-31] For example, Cook et al created 15 mm defects in the ulna of a rabbit, isolated the ulna carefully from the radius and placed the distal ends in an aluminum sleeve.[28] As the ulna has a curved shape, the ulna had to be mounted eccentrically to keep the axis of the ulnar rotation coaxial with the testing device.[28] The measured average torsional strength and energy absorption of the healed ulna defect was comparable to the intact ulna after 12 weeks' implantation time. Beck et al created 15 mm segmental defects in the rabbit radius and augmented the defects with a combination of bone marrow and TGFß1.[14] They isolated the radii using bone rongeurs when the ulna was fused to the operated radius and thereafter mechanical testing was carried out.[14] They also removed one centimeter of the distal and proximal radius before fixing them into the mechanical testing apparatus. However, it has to be noticed that when the distal bone fragments are removed, the torque results can be influenced because the angle of rotation changes more when the length of the radius is shorter. Also, Mori et al isolated the radius carefully from the ulna of a rabbit and cut it into a 5-cm-long sample.[30] Subsequently, both ends were fixed in a square mold.[30] In this 24 week study, no statistically significant differences were found between ulnae regenerated by rhBMP-2/PLGA capsules and the intact contralateral bones.

The difficulties that occur when the radius and ulna are separated before mechanical testing is especially evident in the study of Sheller et al, who created non-critical sized defects in the radii and non-critical sized defects in the ulnae of New Zealand White rabbits.[29] All ulnae and radii were separated before torsional testing was done. Finally, they observed that six out of 16 control bones could not be tested as they were either fractured due to the separation process or had no bridging. When 37,5% of the control samples are lost, as was the case in Sheller's experiment, it might be difficult to draw any conclusion. In addition, bone formation outside the defect site and bone not spanning the defect might be difficult to distinguish during the separation process, which can as well influence the final measurements. In agreement with the above mentioned, it will be clear that in the present experiment separation of the bones would have influenced the test results because histological examination of the samples revealed some bone, but also fibrocartilagenous s tissue located in the area between the radius and ulna. Also, bone overgrowth (i.e. osseoconduction over the implant surface) is difficult to discern macroscopically. This gives

the additional risk of removing too much of the newly formed bone, which results in an unreliable measurement.

Similar to the technique as used by Wheeler et al [8], we potted the ulna-radius complex in dental plaster and made transcortical incisions as close as possible near the embedding of the ulna in the plaster. This was done to eliminate the mechanical contribution of the ulna. Nevertheless, it has to be questioned whether this discontinuous ulna segment has still no effect on the fracture torque or stiffness of the radius (Figure 5). For example, our histological analysis showed that bone and cartilagenous tissue formation had occurred in the area between the radius and ulna, which can influence the outcome of the measurements. Further, there is always the risk of additional experimental flaws, like variability of the transcortical incisions, fracture of the dental plaster and instability of the fixation.

Due to these limitations of a torsional test, other methods have been suggested to measure the strength of newly formed bone in a segmental defect. An alternative approach is the use of a compression test, but separation of the ulna and radius is still required in this method as a load is applied vertically to the specimen along the longitudinal axis of the ulna or radius. Of importance is also that in this test, the angle of the radius and the fixation of the bone in the instrument can influence the measurements. Besides compression, a bending test can be done, but the disadvantages of this method are that: (1) there are no equal loads to all sections of the bone, and (2) the test is relatively insensitive to specimen length and orientation.[32,33,34]

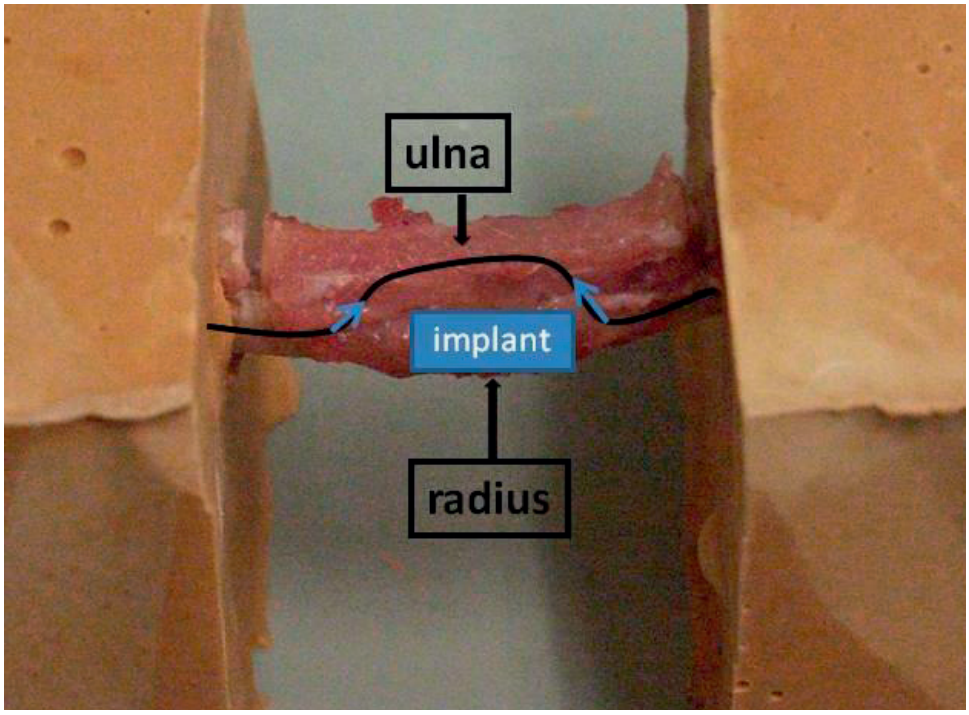

FIGURE 5: *The ulna-radius complex after creation of the transcortical incisions. The discontinuous ulna segment can affect the torque because of fusion in the area between radius and ulna.*

Besides the applied mechanical test method, there are a lot of other variables that can influence the outcome of mechanical assays. For example, anatomical differences, which cause angular variation between the radius and ulna, can influence the measurements as well as the inherent strength of a radius will vary from rabbit to rabbit. Also, the mechanical properties of the scaffold material are important, e.g. the use of a mechanically strong material is mechanically strong will result in less displacement or impression compared to weaker scaffold materials. All these limitations were present in the current study and could not be excluded, which can explain the high standard deviation in the measurements as well as the lack of a significant difference for the 15 mm open defect.

To assess the suitability of porous Ca-P cement as a bone substituting material, this experiment aimed on the creation of a CSD defect in the radius of New Zealand white rabbits. The radiology results showed that two of the 15 mm control defects showed signs of spontaneous closure, which was confirmed by the histological analysis. As a consequence, the created 15 mm defect cannot convincingly be considered as critical-sized. The size of a CSD is known to depend on the breed and age of the used experimental animal model as well as the location of the defect. Also the surgical technique, such as the experience and skills of the surgeon, the used saline cooling, the way to treat the periosteum (whether it is taken away of lifted), and removal or maintenance of the interosseus membrane are of main importance. For example, Sheller et al reported that a segmental defect could elicit bone formation from the periosteum of the nearby radius when an ulna defect is created.[29]

Considering the histological evaluation, a limitation in the study design was that we were not able to quantify the amount of bone formation and cement degradation. The torqued specimens showed fracturing of the pCa-P implants, which prevented the performance of reliable histomorphometrical measurements, while the number of non-torqued specimens was too limited to allow appropriate statistical analysis. In addition, no clear sign of cement degradation was observed in the histological sections, which corroborates with our previous study dealing with rabbit cranial defects.[27] An explanation for this lack of degradation can be the used animal model, as significant degradation of Ca-P cement has been reported in studies with different animal species.[22,35]

CONCLUSIONS

Within the limitation of the study design, porous Ca-P cement implants demonstrated osteoconductive properties and confirmed to be a suitable scaffold material in a weight bearing situation. Nevertheless, the results have to be interpreted with care, as the torque testing revealed that several variables can interfere with the study outcome. Also, this study confirmed again that a 15 mm radius defect is not a CSD in female New Zealand white rabbits of six month of age (weight 2.5-3.5 kg).

Acknowledgement: This study has been supported by the NWO-AGIKO foundation. We also like to thank E. Bronkhorst for his statistical support and Vincent Cuypers for his histological advises.

REFERENCES

1) Ishikawa K, Asaoka K. Estimation of ideal mechanical strength and critical porosity of calcium phosphate cement. J Biomed Mater Res. 1995;29:1537-43.
2) Khairoun I, Driessens FC, Boltong MG, Planell JA, Wenz R. Addition of cohesion promotors to calcium phosphate cements. Biomaterials 1999; 20: 393-8.
3) Brown WE, Chow LC. US patent 1985;4, 518,430.
4) Lee DD, Tofighi A, Aiolova M, Crakravarthy P, Catalona A, Majahad A, Knaack D. Alpha-BSM: a biomimetic bone substitute and drug delivery vehicle. Clin. Orthop Relat Res. 1999;(367 Suppl):396-405.
5) Ooms EM, Wolke JGC, van der Waerden JPCM, Jansen JA. Trabecular bone response to injectable calcium phosphate (Ca-P) cement. J Biomed Mater Res. 2002;61:9-18.
6) Comuzzi L, Ooms EM, Jansen JA. Injectable calcium phosphate cement as a filler for bone defects around oral implants: an experimental study in goats. Clin Oral Implants Res. 2002;13:304-311.
7) Ruhé PQ, Kroese-Deutman HC, Wolke JG, Spauwen PHM, Jansen JA. Bone inductive properties of rh-BMP-2 loaded porous calcium phosphate cement implants in cranial defects in rabbits. Biomaterials 2004;2123-32.
8) Wheeler DL, Chamberland DL, Schmitt JM, Buck DC, Brekke JH, Hollinger JO, Joh SP, Suh KW. Radiomorphometry and biomechanical assessment of recombinant human bone morphogenetic protein 2 and polymer in rabbit radius ostectomy model. J Biomed Mater Res. 1998;43(4):365-73.
9) Meinig RP. Polylactide membranes in the treatment of segmental diaphyseal defects: animal model experiments in the rabbit radius, sheep tibia, Yucatan minipig radius, and goat tibia. Injury. 2002 Aug; 33 Suppl 2:B58-65.
10) Bodde EWH, Spauwen PHM, Mikos AG, Jansen JA. Closing capacity of segmental radius defects in rabbits. J Biomed Mater Res A. 2008 Apr;85(1):206-17.
11) Hedberg EL, Kroese-Deutman HC, Shih CK, Crowther RS, Carney DH, Mikos AG, Jansen JA. Effect of varied release kinetics of the osteogenic thrombin peptide TP508 from biodegradable, polymeric scaffolds on bone formation in vivo. J Biomed Mater Res A. 2005 Mar 15;72A(4):343-53.
12) Geiger F, Berger I, Lorenz H, Wall O, Eckhardt C, Simank HG, Richter W. Vascular endothelial growth factor gene-activated matrix (VEGF165-GAM) enhances osteogenesis and angiogenesis in large segmental bone defects. J Bone Miner Res. 2005 Nov;20(11):2028-35.
13) Bos GD, Goldberg VM, Powell AE, Heiple KG, Zika JM. The effect of histocompatibility maching on canine frozen bone allografts. J Bone Joint Surg. 1983; 65(1), 89-96.
14) Beck LS, Wong RL, DeGuzman L, Lee WP, Ongpipattanakul B, Nguyen TH. Combination of bone marrow and TGF-beta1 augment the healing of critical-sized bone defects. J Pharm Sci. 1998 Nov;87(11):1379-86.
15) Zegzula HD, Buck DC, Brekke J, Wozney JM, Hollinger JO. Bone formation with use of rhBMP-2 (recombinant human bone morphogenetic protein-2). J Bone Joint Surg Am. 1997 Dec;79(12):1778-90.
16) Nyman R, Magnusson M, Sennerby L, Nyman S, Lundgren D. Membrane-guided bone regeneration. Segmental radius defects studied in the rabbit. Acta Orthop Scand. 1995 Apr;66(2):169-73.
17) Kaito T, Myoui A, Takaoka K, Saito N, Nishikawa M, Tamai N, Ohgushi H, Yoshikawa H. Potentiation of the activity of bone morphogenetic protein-2 in bone regeneration by a PLA-PEG/hydroxyapatite composite. Biomaterials. 2005 Jan;26(1):73-9.

18) Geiger F, Bertram H, Berger I, Lorenz H, Wall O, Eckhardt C, Simank HG, Richter W. Vascular endothelial growth factor gene-activated matrix (VEGF165-GAM) enhances osteogenesis and angiogenesis in large segmental bone defects. J Bone Miner Res. 2005 Nov;20(11):2028-35. Epub 2005 Jul 5.
19) Yamamoto M, Takahashi Y, Tabata Y. Enhanced bone regeneration at a segmental bone defect by controlled release of bone morphogenetic protein-2 from a biodegradable hydrogel. Tissue Eng. 2006 May;12(5):1305-11.
20) White AA 3rd, Panjabi MM, Southwick WO. The four biomechanical stages of fracture repair. J. Bone Joint Surg Am. 1977 Mar;59(2):188-92.
21) Cook SD, Salkeld SL, Patron LP, Sargent MC, Rueger DC. Healing course of primate ulna segmental defects treated with osteogenic protein-1.
22) del Real RP, Ooms EM, Wolke JGC, Vallet-Regi M, Jansen JA. In vivo bone response to porous calcium phosphate cement. J Biomed Mater Res. 2003; 65A: 30-36.
23) Wolke JGC, Ooms EM, Jansen JA. In vivo resorption behaviour of a high strength injectable calcium-phosphate cement. Bioceramics 2000; 13: 793-796.
24) Hollinger JO, Kleinschmidt JC. The critical size defect as an experimental model to test bone repair materials. J Craniofac Surg ; 1990; 1(1):60-8.31
25) van der Lubbe HB, Klein CP, de Groot K. A Simple method for preparing thin (10 microM) histological sections of uncalcified plastic embedded bone with implants. Stain Technol 1988 ; 63 : 171-6.
26) Armitage P, Berry G. Statistical methods in medical research (2nd ed). Blackwell Scientific, London; 1988: 120.
27) Kroese-Deutman HC, Wolke JHG, Spauwen PHM, Jansen JA. Closing capacity of cranial bone defects using porous calcium phosphate cement implants in a rabbit animal model. J Biomed Mater Res A. 2006 Dec 1;79(3):503-11.
28) Cook SD, Baffes GC, Wolfe MW, Sampath TK, Rueger DC, Whitecloud TS 3rd. The effect of recombinant human osteogenic protein-1 on healing of large segmental bone defects. J Bone Joint Surg Am. 1994 Jun;76(6):827-38.
29) Sheller MR, Crowther RS, Kinney JH, Yang J, Di Jorio S, Breuting T, Carney DH, Ryaby JT. Repair of rabbit segmental defects with the thrombin peptide, TP508. J Orthop Res. 2004 Sep;22(5):1094-9.
30) Mori M, Isobe M, Yamazaki Y, Ishihara K, Nakabayashi N. Restoration of segmental bone defects in rabbit radius by biodegradable capsules containing recombinant human bone morphogenetic protein-2. J Biomed Mater Res. 2000 May;50(2):191-8.
31) Bolander ME, Balian G. The use of demineralized bone matrix in the repair of segmental defects. Augmentation with extracted matrix proteins and a comparison with autologous grafts. J Bone Joint Surg Am. 1986 Oct;68(8):1264-74.
32) Burstein AH, Frankel VH. A Standard test for laboratory animal bone. J. Biomech. 1971; 4:155-158.
33) Levenston ME, Beaupre GS, Van der Meulen MCH. Improved method for analysis of whole bone torsion tests. J. Bone Min Res.1994 ; 9 :1459-1465 .
34) Nash TJ, Howlett CR, Martin C, Steele J, Johnson KA, Hicklin DJ. Effect of platelet-derived growth factor on tibial osteotomies in rabbits. Bone. 1994 Mar-Apr;15(2):203-8.
35) Yuan H, Li Y, de Bruijn JD, de Groot K, Zhang X. Tissue responses of calcium phosphate cement: a study in dogs. Biomaterials 2000; 21: 1283-90.

4

BONE INDUCTIVE PROPERTIES OF rhBMP-2 LOADED POROUS CALCIUM PHOSPHATE CEMENT IMPLANTS IN CRANIAL DEFECTS IN RABBITS

P.Q. Ruhé, H.C. Kroese-Deutman, J.G.C. Wolke, P.H.M. Spauwen, J.A. Jansen
Biomaterials, 25: 2123-2132, 2004.

BONE INDUCTIVE PROPERTIES OF rhBMP-2 LOADED POROUS CALCIUM PHOSPHATE CEMENT IMPLANTS IN CRANIAL DEFECTS IN RABBITS

INTRODUCTION

The use of autologous bone grafts is considered to be the golden standard for repair and reconstruction of bone. To overcome the disadvantages of this technique, such as (1) the low availability of transplantable tissue, (2) postoperative morbidity, and (3) lack of functional shape of the transplant, several alternatives to autologous bone have been investigated. One of these is tissue engineered synthetic bone graft substitute (BGS). In this concept, a BGS consists of an osteoconductive scaffold material combined with osteogenic cells and/or osteoinductive proteins.

A lot of prerequisites have been postulated for the ideal scaffold material with regard to mechanical properties, biocompatibility, biodegradability, absence of allergic reactions, disease transmission, delivery of the osteoinductive factor, gross architecture, shaping, clinical handling, and regulatory issues. Nevertheless, none of the currently available scaffold materials meets all of the formulated demands.

Calcium phosphate (Ca-P) cements have been studied extensively.[1-5] Besides the clinical advantage that this cement can be injected directly into a bone defect, it shows a fast deposition of new bone at the cement surface and is considered to be extremely biocompatible.[6,7] To enhance tissue ingrowth and degradation rate of the cement, we have recently developed a method to increase the porosity of the cement by creating macropores.[8] In an animal study in goats, the degradation rate was shown to increase up to 80% in ten weeks.[9]

Osteoinductive proteins play an important role in bone regeneration. These proteins belong to the Transforming Growth Factor (TGF)-ß super family. Currently fifteen different Bone Morphogenetic Proteins (BMPs) have been identified.[10] Various in vitro and in vivo (rodents, dogs, sheep, humans) studies have been done to establish the osteoinductive effect of BMP.[11-18] Especially human BMP-2 has been investigated thoroughly for bone engineering purposes. This homodimeric protein can be produced by human recombinant technology since 1988 and consists of two polypeptide chains of more than 400 amino acids.[16,19] A region with seven cystine amino acids located near the C-terminus plays a crucial role in the protein function.[19] Recent investigations showed that the so-called cystine knot is located in the core of the complex three dimensional structure.[20,21] More insights into the primary steps of BMP receptor activation have been provided with the characterization of two receptor binding epitopes for high affinity BMP receptors.[20,22] Binding of BMP to cell surface receptors on mesenchymal cells activates a BMP signaling cascade that results in gene expression and leads to differentiation of the mesenchymal cells into chondrocytes or osteoblasts.[21] The role of biomaterials on the osteoinductive activity of BMP is not completely clear. The biomaterial itself might directly influence cellular differentiation[23] and it might potentiate the activity of BMP by binding the protein and presenting it to target cells in a "bound" form.[24,25] On the other hand, slowly released BMP may provide a physiological concentration of free protein in the vicinity of the implant, what may attract target cells to the implant-site by chemotaxis.[26] The ideal retention/release rates for growth factors have not been established yet.

Although in several studies the combination of growth factors with calcium phosphate ceramics, like hydroxyapatite and tricalciumphosphate, has been reported,[18,27-33] to our knowledge only a few studies have been carried out with Ca-P cement and osteoinductive proteins.[34-38] The Ca-P cements used in these studies did not have a macroporous structure and growth factors were mostly added to the cement before setting.

To our knowledge, this is the first study with macroporous Ca-P cement and rhBMP-2. We hypothesize that: 1) Porous Ca-P cement is an appropriate candidate scaffold material for bone engineering purposes. 2) Bone formation in porous Ca-P cement can be enhanced by lyophilization of rhBMP-2 on the scaffold surface. 3) Porous rhBMP-2 loaded Ca-P cement discs show degradation after implantation in cranial defects in rabbits for ten weeks.

MATERIALS AND METHODS

Porous calcium phosphate cement implants

Thirty-six disc-shaped porous calcium phosphate (Ca-P) cement implants were prepared by a CO_2 induction technique as previously described.[8] The discs were made out of Calcibon® (Biomet Merck, Darmstadt, Germany). This cement consists of a mixture of 62.5wt% tricalcium phosphate (α-TCP), 26.8wt% dicalcium phosphate anhydrous (DCPA), 8.9wt% calcium carbonate ($CaCO_3$) and 1.8wt% hydroxyapatite (Hap). An aqueous solution of Na_2HPO_4 (2wt%) was used as the liquid component. To generate macroporosity of the scaffold, $NaHCO_3$ was added for production of CO_2 gas in the cement. After mixing, the cement was immediately injected in a cylindrical mould of 2.7 mm height and 8.0 mm diameter. The discs were air dried in a furnace at 50°C for 1 h. Thereafter, the surface of the discs was carefully ground with fine sand-paper to ensure a standardized height of 2.7 mm. Finally, the discs were removed from the moulds and sterilized by autoclaving for 15 min at 121°C. Average weight was 108 ±7 mg/disc. The total porosity of the discs was 75% as was calculated with the formula: $\text{porosity}(\%) = 100 \times \{1-(\text{disc weight}/[\text{cement density} \times \text{disc volume}])\}$. Histomorphometrical analysis of the discs before implantation revealed that the macroporosity was 36%. In a previously published paper, it was shown that the microporosity (pores < 1 μm) of this cement is 39%.[8]

Absorbable collagen sponge implants

As positive reference material for administration of rhBMP-2, sterile absorbable collagen sponge (ACS) was used as provided by Dr. D.W.R. Hall (Yamanouchi Europe BV, Leiderdorp, The Netherlands). Under sterile conditions the ACS sheets (thickness 3.5 mm) were moistened with H_2O to induce the common shrinkage of the material and the sheets were lyophilized subsequently. Thereafter, discs were punched out of the lyophilized sheets with sterile 8 mm biopsy punches (Stiefel Laboratories BV, Veendam, The Netherlands) under sterile conditions.

rhBMP-2 loading

Eighteen porous Ca-P cement implants were loaded with rhBMP-2 (Yamanouchi Europe BV, Leiderdorp, The Netherlands) one day prior to implantation. Thereafter, the Ca-P discs were placed in a sterile Eppendorf® tube under sterile conditions and 25 μL of diluted rhBMP-2 (0.2 mg/ml PBS/BSA[0.1%]) was added to each side of the implant to achieve a total dose of 10 μg per implant. The specimens were lyophilized and stored at 4°C until implantation.

Eighteen ACS discs were loaded with rhBMP-2 on the day of implantation as prescribed by the provider. To achieve a total dose of 10 µg rhBMP-2 per implant with a soak-load of 30%, 50 µL of the diluted rhBMP-2 solution (0.2 mg/ml PBS/BSA[0.1%]) was pipetted carefully onto the discs of ACS. The ACS discs were allowed to soak-load for minimally 15 min before being inserted into the cranial defects. Care was taken not to squeeze the discs.

Surgical procedure for cranial implants:

Fifty-four healthy skeletally mature female New Zealand White rabbits with a weight between 2.8 - 3.2 kg were used as experimental animals. National guidelines for the care and use of laboratory animals were observed.

Surgery was performed under general inhalation anesthesia. The anesthesia was induced by an intravenous injection of Hypnorm® (0.315 mg/ml fentanyl citrate and 10 mg/ml fluanisone) and atropine, while maintained by a mixture of nitrous oxide, isoflurane, and oxygen through a constant volume ventilator. To reduce the peri-operative infection risk, the rabbits received antibiotic prophylaxis [Baytril® 2.5% (Enrofloxacin), 5-10 mg/kg].

For the insertion of the implants, the animals were immobilized in ventral position. The skull was shaved, washed and disinfected with povidone-iodine. A longitudinal incision was made down to the periosteum from the nasal bone to the occipital protuberance. Subsequently, a midline incision was made in the periosteum. The periosteum was undermined and lifted off the parietal skull. The defect was drilled in the parietal calvarial bone with a dental trephine burr (ACE Dental Implant System, Brockton, MA, USA) with an outer diameter of 8.0 mm and continuous internal and external cooling with physiologic saline. Care was taken to make a full thickness defect without damaging the underlying dura. Following insertion of the implants (Fig. 1A and 1B), the periosteum was closed using non-resorbable Prolene® 4-0 sutures. Finally, the skin was closed intracutaneously using resorbable Vicryl® 4-0 suture material. Implantation periods were two and ten weeks. At the end of each implantation period, euthanasia was performed with an overdose of Nembutal® (pentobarbital).

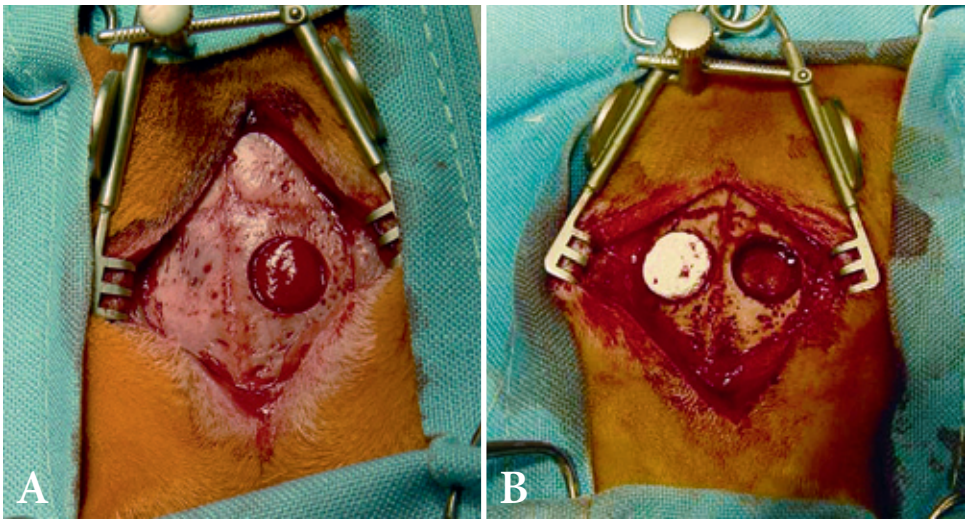

FIGURE 1A: *rhBMP-2 loaded ACS implant inserted in cranial defect.*
FIGURE 1B: *Porous Ca-P cement implant inserted in cranial defect (left) and empty defect (right).*

In this way, a total of fifty-four implants were placed into the fifty-four rabbit skulls: eighteen rhBMP-2 loaded Ca-P cement implants, eighteen unloaded Ca-P cement implants and eighteen rhBMP-2 loaded ACS implants (n=9 for each implant and time period). In the group of rabbits that received an unloaded Ca-P cement implant, an additional defect was drilled in the contralateral parietal bone, which was left open and served as control (empty defect). In this group, no rhBMP-2 was administered. Therefore, there was no cross-over effect of rhBMP-2.

Sequential quadruple fluorochrome labeling, i.e. tetracycline (yellow), alizerin-complexon (red), calcein (green) and tetracycline (yellow), was performed in four rabbits of each group at respectively one, three, seven and nine weeks postoperatively. All labels were administered subcutaneously at 25 mg/kg body weight. Parallel to this study, a separate study was performed in the same animals where identical experimental groups were implanted subcutaneously.

Implant retrieval and histological preparations.

Directly after euthanasia, implants with the surrounding tissues were retrieved and fixed in 4% phosphate-buffered formaldehyde solution (pH=7.4). Subsequently, the tissue blocks were dehydrated in ethanol and embedded in methylmethacrylate. Following polymerization undecalcified 10-µm-thick sections were prepared in a transverse direction to the implant's axis using a modified sawing microtome technique.[39] At least three sections of each implant were stained with methylene blue/basic fuchsin and examined with a light microscope. Two additional unstained 30-µm-thick sections of the fluorochrome-labeled specimens were prepared for reflectant fluorescence microscopy.

Histological and histomorphometrical evaluation

A light microscope (Leica Microsystems AG, Wetzlar, Germany) was used for histological evaluation. This evaluation consisted of a morphological description of three sections per implant.

Further, all sections that contained Ca-P cement implants were used for histomorphometrical evaluation using computer based image analysis techniques (Leica® Qwin Pro-image analysis system, Wetzlar, Germany). Digital analysis determined the following parameters:

1. The surface of the area within the defect edges and the thickness of the implant, which was called region of interest (ROI).
2. Cement surface area [%], indicative for the macroporosity.
3. Total bone area in Ca-P specimens [%], defined as the index of the surface area of bone and the ROI. This parameter was subdivided in: A. Bone inside the cement (BIC), defined as bone formed within the implant edges. B. Bone outside the cement (BOC) defined as newly formed bone deposited outside the implant at either skin- or cerebral side.
4. Pore fill [%], defined as the index of BIC and the surface area of macropores.

The results are based on the average of the separate measurements of three sections per implant. We have to emphasize that no histomorphometrical measurements were done for the ACS implants. A quantitative comparison of parameters for this group would be unreliable since no proper ROI, in terms of implant thickness and area, could be defined for the spongy ACS.

A reflectant fluorescence microscope equipped with an excitation filter of 470-490 nm (Leica Microsystems AG, Wetzlar, Germany) was used for fluorescent microscopical assessment.

Statistical analysis

All measurements of rhBMP-2 loaded and unloaded porous Ca-P cement implants were statistically evaluated with GraphPad® Instat 3.05 software (GraphPad Software Inc, San Diego, CA, USA), using an unpaired T-test with Welch correction.

RESULTS

Experimental animals

During the experiment, all fifty-four rabbits remained in good health and did not show any wound complications. At the end of the two implantation periods, a total of fifty-four implants and eighteen empty control defects could be retrieved. At retrieval, the implants were all covered by periosteum. No inflammatory signs or adverse tissue reaction could be observed. Bone formation could be seen macroscopically in most of the specimens.

Light microscopy

Light microscopic analysis of the sections revealed various amounts of bone formation between implants, groups and time periods. In all sections, the original defect edge was still visible. Little or no inflammatory multinucleated cells were observed on the cement surface. Representative sections are depicted in Figure 2.

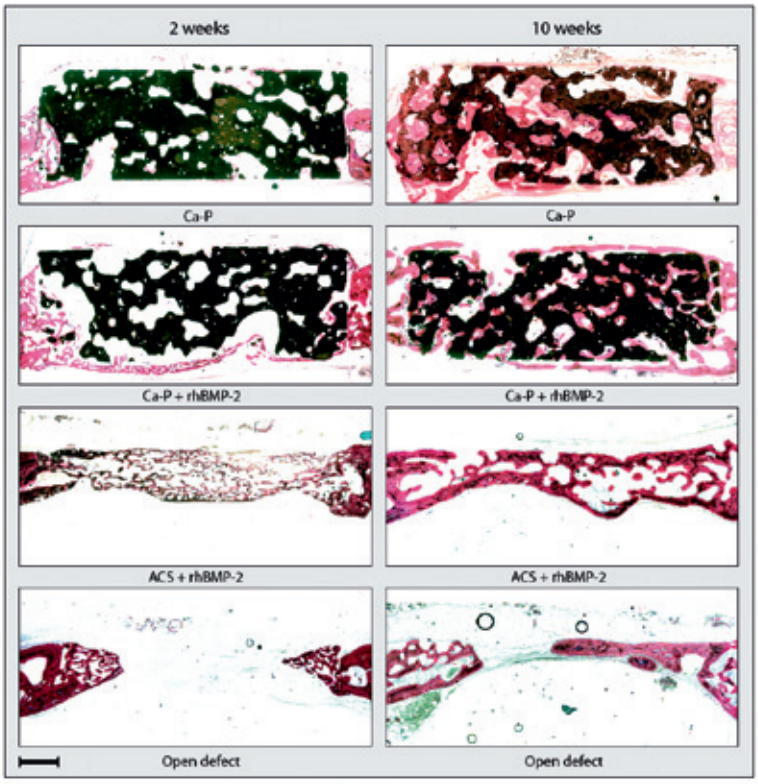

FIGURE 2:
Overview of representative sections of implants and empty defects after two and ten weeks (original magnification 2.5x).

Two weeks specimens

Two weeks postoperatively, none of the empty defects was closed completely. Primary bone ingrowth from the defect edge to the defect center covered about half of the defect diameter. In the ACS group, all defects were completely closed after two weeks of implantation. The new-formed primary bone was characterized by the presence of osteoblasts, osteocytes and small blood vessels and had a structure, comparable with the new bone formation in the empty defects. Microscopically, no collagen left from the ACS material could be observed. The newly formed bone layer was thinner than the originally inserted ACS material and thinner than the surrounding skull bone in all sections.

Light microscopy showed that the macropores in the Ca-P cement implants were irregularly formed and had a channel-like rather than a spherical structure. In three unloaded Ca-P cement implants, some fracturing of the scaffolds occurred. In these sections, fracture lines in the Ca-P cement and loose Ca-P fragments were observed. However, the outline of these discs was not affected. All other implants had maintained their integrity. Fibrous encapsulation of the Ca-P cement implants was not observed. Bone ingrowth from the skull bone into the macropores of the cement was present in all implants. Also, direct bone contact with the cement and layers of osteoblast-like cells were observed in all sections. At the interface, no inflammatory cells or fibrous tissue were present between bone and cement. Further inside the implant, macropores were filled with loose connective tissue and blood vessels. Remarkably, all rhBMP-2 loaded Ca-P implants were surrounded by a thin layer of primary bone outside the cement at the cerebral side of the implant, the skin side or both sides. This callus-like tissue was characterized by the frequent absence of contact between bone and cement. In eight out of nine implants, the bone outside the cement covered the defect completely. A very limited formation of bone outside the cement was also observed in three of the unloaded Ca-P cement implants.

Ten weeks specimens

Ten weeks postoperatively, average bone ingrowth in the empty defects covered about 75% of the defect diameter. One of the empty defects was closed completely by a thin layer of new trabecular bone. In the ACS group, all defects were completely closed. The primary bone of the two weeks ACS implants was now replaced by a more cortical-like structure. Occasionally, the newly formed bone was difficult to discern from the original skull bone. Further, we noticed that in four of the nine specimens the newly deposited bone was not formed according the original skull contour and lacked the finally required shape. Microscopically, the ACS appeared to have degraded completely.

All of the Ca-P cement scaffolds were intact and had maintained their integrity. Bone bridging between the Ca-P implant and skull occurred in all specimens. Bone ingrowth in both the rhBMP-2 loaded and unloaded Ca-P cement scaffolds had increased dramatically compared to the two weeks implants. Complete closure of the defect was observed in all rhBMP-2 loaded specimens and in seven unloaded specimens. The deposited bone had a more lamellar appearance than after two weeks of implantation. Bone formation in the cement porosity was characterized by the presence of osteoblast- as well as osteocyte-like cells embedded in a mineralized matrix (Fig. 3). Also, bone remodeling and bone marrow-like tissue were observed. Osteoclast-like cells and foreign body giant cells were noticed occasionally. Formation of bone outside the Ca-P cement was present in eight of

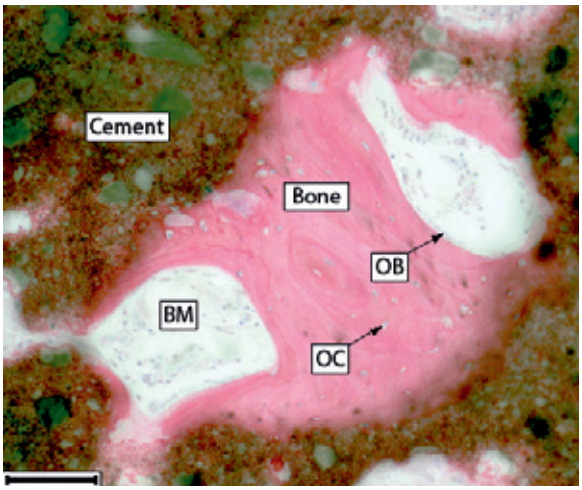

FIGURE 3:
Light microscopic aspect of bone formation in the center of a rhBMP-2 loaded Ca-P cement scaffold after ten weeks of implantation. Bone formation is characterized by the presence of osteocyte-like cells (OC) embedded in the matrix and the layer of cubical osteoblast-like cells (OB) at the matrix surface. Bone marrow-like tissue (BM) is observed in the macropores. Original magnification 10x. Bar represents 100 µm.

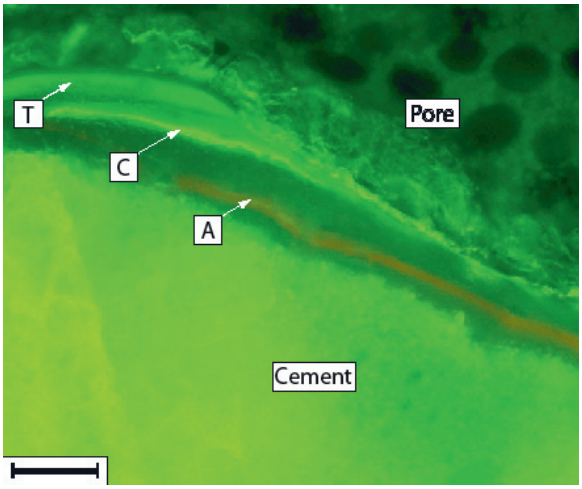

FIGURE 4:
Fluorescence microscopy of bone formation in the center of a rhBMP-2 loaded Ca-P cement scaffold. Formation of bone started at the cement surface and proceeded into the macropore. A= alizerine complexon label (red), administered after three weeks of implantation. C= calcein label (green), administered after seven weeks of implantation. T= tetracycline label (yellow), administered after nine weeks of implantation. Original magnification 20x. Bar represents 50 µm.

the nine rhBMP-2 loaded Ca-P scaffolds. Unlike the two weeks sections, the bone outside the cement was frequently in direct contact with the Ca-P cement. In the unloaded group, formation of bone outside the scaffold was very limited in four of the nine scaffolds. Here, direct bone- Ca-P cement contact existed also. Finally, in both the rhBMP-2 loaded and non-loaded Ca-P cements implants no clear indication for cement degradation was observed.

Fluorescence microscopy

Results of fluorescence microscopy are depicted in Figure 4. Tetracycline labels, that were administered one and nine weeks post-operatively, were scarcely observed. Analysis of the fluorescence labels revealed that formation of bone started at the cement surface and proceeded into the macropores.

Histomorphometry

The results of the histomorphometrical analysis of the Ca-P specimens are shown in Figures 5 and 6.

Measurement of cement surface before implantation revealed a cement/ROI ratio of 63.6 ±0.3%, indicative for a macroporosity of the scaffold of 36.4 ±0.3%. After two and ten weeks of implantation, the macroporosity was not significantly changed ($p>0.05$).

In the histomorphometrical analysis, we discerned total bone formation in bone inside the cement (BIC) and bone outside the cement (BOC). In the rhBMP-2 loaded group, total bone surface area increased from 8.9 ±7.1% (BIC: 3.2 ±1.9%; BOC: 5.7 ±5.3%) after two weeks to 27.4 ±6.2% (BIC: 19.5 ±3.6%; BOC: 7.9 ±3.3%) after ten weeks. In the unloaded group, total bone surface area increased from 3.2 ±1.9% (BIC: 2.4 ±1.2%; BOC: 0.8 ±1.1%) after two weeks to 16.6 ±5.1% (BIC: 14.2 ±4.4%; BOC: 2.4 ±1.6%) after ten weeks. Statistical testing revealed that these increases were significant ($p< 0.0001$) for both groups. Comparison between loaded and unloaded groups showed that total bone surface area was significantly higher in the rhBMP-2 loaded group after two weeks ($p< 0.05$) and after ten weeks ($p< 0.005$).

After two weeks of implantation, pore fill in the rhBMP-2 group (9.3 ±3.7%) was not significantly different from the unloaded group (8.3 ±4.0%). After ten weeks, pore fill was significantly higher ($p< 0.05$) in the rhBMP-2 group (53.0 ±5.4 vs. 43.1 ±10.4).

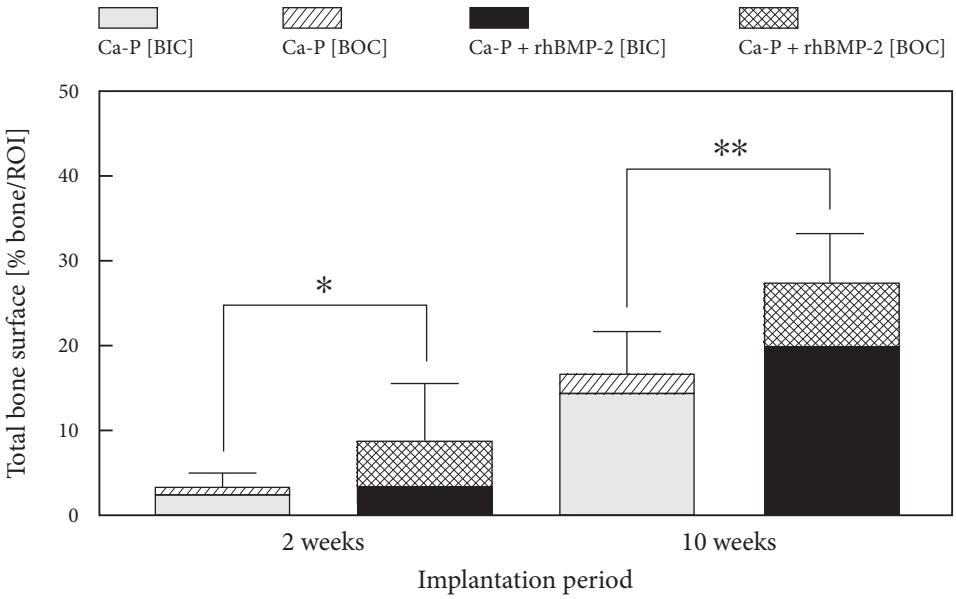

FIGURE 5:

*Total bone surface in porous Ca-P cement scaffolds, expressed as the index of the surface area occupied by bone and the region of interest (ROI). Total bone formation is subdivided in bone inside the Ca-P cement (BIC) and bone outside the Ca-P cement (BOC). Error bars represent means ± standard deviation for n=9. * = p< 0.05 ** = p< 0.005.*

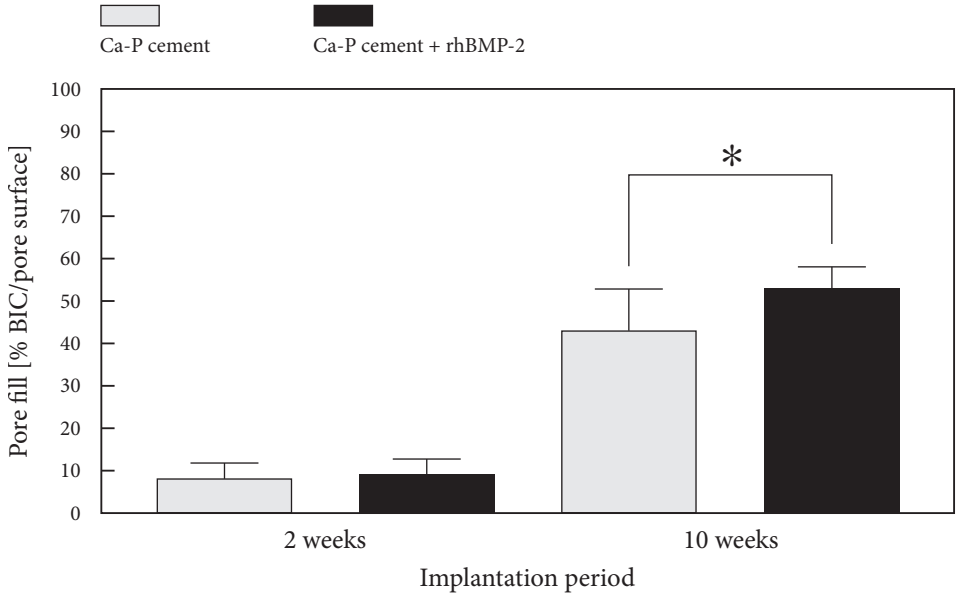

FIGURE 6:
*Pore fill percentage, expressed as the index of the surface area occupied by bone inside the Ca-P cement (BIC) and the pore surface area. Error bars represent means ± standard deviation for n=9. * = p< 0.05.*

DISCUSSION

This study focuses on the osteoinductive properties of rhBMP-2 loaded porous Ca-P cement in cranial defects in rabbits. The critical size of cranial defects in rabbits has been reported to measure 15 mm in diameter for implantation periods up to twenty-four weeks.[40,41] This corroborates with our findings in previous research, which showed that 7.3 mm cranial defects are non-critical size defects for implantation periods of eight weeks.[42] In the current study, one open defect had closed completely after ten weeks and the remaining eight defects showed a tendency to complete closure. However, it should be noticed that we did not intend to create a critical size defect in the current study. Our aim was to investigate whether lyophilized rhBMP-2 on a porous Ca-P cement scaffold surface stimulated bone formation.

rhBMP-2 loaded ACS was used in this study as positive reference material for rhBMP-2 bone induction. Unloaded ACS was not included since the carrier material was not under investigation in this study, and has been investigated thoroughly.[35,43-46] The loaded ACS proved to be a powerful osteoinductive positive reference, as bone bridging was observed in all ACS filled defects after two weeks of implantation. Unfortunately, histomorphometrical comparison of ACS and Ca-P cement implants was impossible due to the indefinable region of interest (ROI) in the ACS group. We underline the importance of the ROI for histomorphometry and we refrain from quantitative comparison if this parameter is insecure. However, the qualitative histological analysis revealed that in four of the ACS implants, the new deposited bone showed some variety in contour and did not match the desired shape. We presume that this is due to the flaccid aspect of the collagen sponge. Despite the excellent

osteoinductive properties, this lack of shape maintenance is a drawback of the rhBMP-2 loaded ACS as a scaffold material for bone engineering.

The complete closure of all defects filled with unloaded Ca-P cement indicates that porous Ca-P cement did not hamper the physiologic bone healing response. Biocompatibility of porous Ca-P cement was confirmed by histological analysis of the sections. Formation of fibrous capsule around the implant was observed in none of the sections. In agreement with previous studies, few multinucleated inflammatory cells were seen on the cement surface.[9] Loose connective tissue and blood vessel ingrowth occurred in all macropores throughout the scaffolds. The macropores in this ceramic can thus be regarded as completely interconnected.

Fluorescence microscopy revealed that formation of bone started at the cement surface and proceeded into the macropores. This observation agrees with previously described bone deposition in porous ceramics[47] and emphasizes again the beneficial effect, which Ca-P ceramics of a specific geometry and composition can have on bone healing.

The histomorphometrical analysis showed that after ten weeks of implantation pore fill and total bone surface area were significantly higher in the rhBMP-2 loaded Ca-P cement scaffolds than in the unloaded scaffolds. This confirms that administration of rhBMP-2 can indeed enhance the formation of bone in porous Ca-P cement scaffolds. As the defects created in the current study were non-critical size and bone formation also occurred without administration of growth factor, we assume that the significance of bone formation induced by rhBMP-2 will increase in clinically more relevant (critical size) defects. Nevertheless, we have to emphasize that the unloaded Ca-P cement scaffolds also supported a fair amount of bone formation inside the cement porosity. We suggest that this is due to the osteoconductive qualities of the macroporous Ca-P cement.

Perhaps the most striking difference between the loaded and unloaded implants was the early callus-like bone formation outside the cement as occurred in all of the rhBMP-2 loaded two weeks implants. To determine whether this bone formation was induced by a relatively high concentration of growth factor in the surrounding tissues, we assessed the in vitro rhBMP-2 release profile from Ca-P cement with ^{125}I labeled rhBMP-2 in an additional study according to previously described methods (fig. 7).[48] The results showed that our Ca-P cement scaffolds showed no initial burst release. Instead, there was a very limited release of the loaded rhBMP-2 of accumulatively 9.7 ±0.9% after 28 days. In other studies, limited release of growth factors from Ca-P cement in vitro has been reported also.[37,49] It is known from column chromatography separation techniques, that ceramics exhibit a high binding affinity for proteins. However, the exact binding mechanism of rhBMP-2 on a ceramic surface is not known to our knowledge. Therefore, it remains unclear how the protein is attached to the ceramic surface, and whether the receptor binding epitopes maintain their accessibility. Binding of BMP on a biomaterial has even been suggested to potentiate the activity of the protein.[24] Unfortunately, no data are available on the activity of "bound" rhBMP-2 on ceramic surface. Evidently, the limited release of rhBMP-2 in vitro does not explain the formation of bone outside the scaffold, unless the early physiologic callus formation is very sensitive to induction by rhBMP-2. On the other hand, we noticed that Li et al reported slow release of rhBMP-2 from a Ca-P cement in vitro, whereas in vivo release was significantly faster.[37] Therefore, the in vitro release profile as determined in the current study can still be an underestimation of the in vivo release and the subsequent concentration of growth factor in the surrounding tissues.

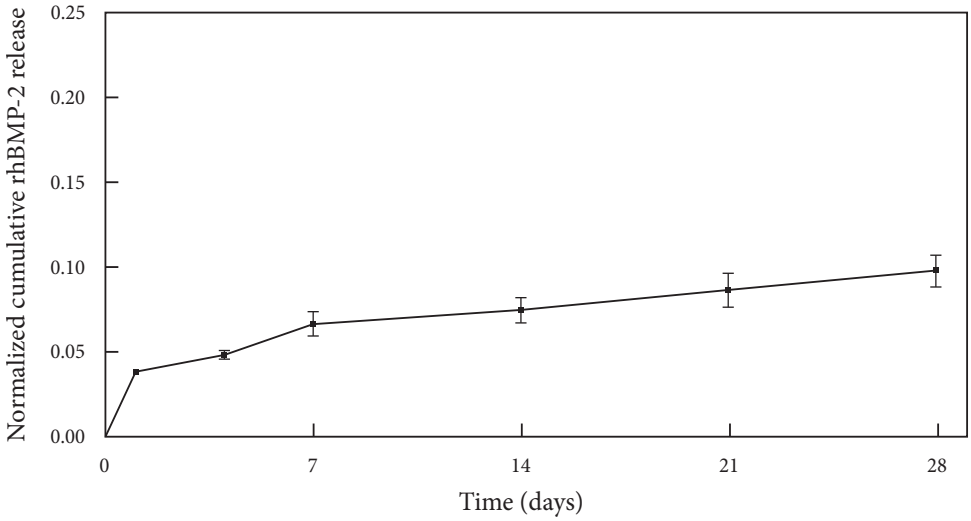

FIGURE 7:
In vitro release profile of ^{125}I rhBMP-2 from porous Ca-P cement scaffolds. Iodination of rhBMP-2 and the release assay were carried out according to previously described methods.[48] Error bars represent means ± standard deviation for n=3.

In a previous study, we have demonstrated that degradation of porous Ca-P cement can reach up to 80% after ten weeks.[9] In that study, a trabecular condylar defect in goats was filled with a Ca-P cylinder. In contrast, in the current animal model no degradation of the cement was observed after ten weeks of implantation. Initial bone-implant contact surface area was relatively large in the cylinder shaped defect in the goat study and relatively small in the current study. Therefore, in the current study there was less initial bone ingrowth and a longer time was needed before the cement was completely surrounded by bone. Consequently, the manifestation of osteoclasts and degradation of the Ca-P cement might occur later. This confirms that the degradation rate of porous Ca-P cement is influenced by various factors such as species, implantation site and implant geometry.

CONCLUSIONS

We conclude that porous Ca-P cement is an appropriate candidate scaffold material for bone engineering purposes. This material reveals excellent osteoconductive properties and maintains its shape and stability during the formation of new bone. Bone formation in porous Ca-P cement scaffolds can be enhanced by lyophilization of rhBMP-2 on the scaffolds. Degradation of porous Ca-P cement is species-, implantation site- and implant dimension-specific.

Acknowledgement: The authors thank Dr. D.W.R. Hall of Yamanouchi Europe BV, Leiderdorp, The Netherlands for kindly supplying the rhBMP-2.

REFERENCES

1) Driessens FC, Planell JA, Boltong MG, Khairoun I, Ginebra MP. Osteotransductive bone cements. Proc Inst Mech Eng [H], 212: 427-435, 1998.
2) Friedman CD, Costantino PD, Takagi S, Chow LC. BoneSource hydroxyapatite cement: a novel biomaterial for craniofacial skeletal tissue engineering and reconstruction. J Biomed Mater Res, 43: 428-432, 1998.
3) Fukase Y, Eanes ED, Takagi S, Chow LC, Brown WE. Setting reactions and compressive strengths of calcium phosphate cements. J Dent Res, 69: 1852-1856, 1990.
4) Ishikawa K, Asaoka K. Estimation of ideal mechanical strength and critical porosity of calcium phosphate cement. J Biomed Mater Res, 29: 1537-1543, 1995.
5) Khairoun I, Driessens FC, Boltong MG, Planell JA, Wenz R. Addition of cohesion promotors to calcium phosphate cements. Biomaterials, 20: 393-398, 1999.
6) Comuzzi L, Ooms E, Jansen JA. Injectable calcium phosphate cement as a filler for bone defects around oral implants: an experimental study in goats. Clin Oral Implants Res, 13: 304-311, 2002.
7) Ooms EM, Wolke JG, van der Waerden JP, Jansen JA. Trabecular bone response to injectable calcium phosphate (Ca-P) cement. J Biomed Mater Res, 61: 9-18, 2002.
8) del Real RP, Wolke JG, Vallet-Regi M, Jansen JA. A new method to produce macropores in calcium phosphate cements. Biomaterials, 23: 3673-80, 2002.
9) del Real RP, Ooms E, Wolke J, Vallet-Regi M, Jansen JA. In vivo bone response to porous calcium phosphate cement. J Biomed Mater Res, 65A: 30-36, 2003.
10) Groeneveld EH, Burger EH. Bone morphogenetic proteins in human bone regeneration. Eur J Endocrinol, 142: 9-21, 2000.
11) Boyne PJ, Marx RE, Nevins M, Triplett G, Lazaro E, Lilly LC, Alder M, Nummikoski PA. Feasibility study evaluating rhBMP-2/absorbable collagen sponge for maxillary sinus floor augmentation. Int J Periodontics Restorative Dent, 17: 11-25, 1997.
12) Gerhart TN, Kirker-Head CA, Kriz MJ, Holtrop ME, Hennig GE, Hipp J, Schelling SH, Wang E. Healing segmental femoral defects in sheep using recombinant human bone morphogenetic protein. Clin Orthop Relat Res, 317-326, 1993.
13) Riley EH, Lane JM, Urist MR, Lyons KM, Lieberman JR. Bone morphogenetic protein-2: biology and applications. Clin Orthop, 39-46, 1996.
14) Sandhu HS, Kanim LE, Kabo JM, Toth JM, Zeegen EN, Liu D, Delamarter RB, Dawson EG. Effective doses of recombinant human bone morphogenetic protein-2 in experimental spinal fusion. Spine, 21: 2115-2122, 1996.
15) Uludag H, D'Augusta D, Golden J, Li J, Timony G, Riedel R, Wozney JM. Implantation of recombinant human bone morphogenetic proteins with biomaterial carriers: A correlation between protein pharmacokinetics and osteoinduction in the rat ectopic model. J Biomed Mater Res, 50: 227-38, 2000.
16) Wang EA, Rosen V, D'Alessandro JS, Bauduy M, Cordes P, Harada T, Israel DI, Hewick RM, Kerns KM, LaPan P et al. Recombinant human bone morphogenetic protein induces bone formation. Proc Natl Acad Sci U S A, 87: 2220-4, 1990.
17) Wozney JM. The bone morphogenetic protein family: multifunctional cellular regulators in the embryo and adult. Eur J Oral Sci, 106 Suppl 1: 160-6, 1998.
18) Yoshida K, Bessho K, Fujimura K, Konishi Y, Kusumoto K, Ogawa Y, Iizuka T. Enhancement by recombinant human bone morphogenetic protein-2 of bone formation by means of porous hydroxyapatite in mandibular bone defects. J Dent Res, 78: 1505-10, 1999.

19) Wozney JM, Rosen V, Celeste AJ, Mitsock LM, Whitters MJ, Kriz RW, Hewick RM, Wang E. A. Novel regulators of bone formation: molecular clones and activities. Science, 242: 1528-34, 1988.
20) Kirsch T, Sebald W, Dreyer MK. Crystal structure of the BMP-2-BRIA ectodomain complex. Nat Struct Biol, 7: 492-6, 2000.
21) Reddi AH. Bone morphogenetic proteins: from basic science to clinical applications. J Bone Joint Surg Am, 83-A Suppl 1: 1-6, 2001.
22) Nickel J, Dreyer MK, Kirsch T, Sebald W. The crystal structure of the BMP-2:BMPR-IA complex and the generation of BMP-2 antagonists. J Bone Joint Surg Am, 83-A Suppl 1: 7-14, 2001.
23) Anselme K. Osteoblast adhesion on biomaterials. Biomaterials, 21: 667-81, 2000.
24) Reddi AH, Cunningham NS. Initiation and promotion of bone differentiation by bone morphogenetic proteins. J Bone Miner Res, 8 Suppl 2: 499-502, 1993.
25) Uludag H, Gao T, Porter TJ, Friess W, Wozney JM. Delivery systems for BMPs: factors contributing to protein retention at an application site. J Bone Joint Surg Am, 83-A Suppl 1: 128-35, 2001.
26) Cunningham NS, Paralkar V, Reddi AH. Osteogenin and recombinant bone morphogenetic protein 2B are chemotactic for human monocytes and stimulate transforming growth factor beta 1 mRNA expression. Proc Natl Acad Sci U S A, 89: 11740-4, 1992.
27) Gombotz WR, PankeySC, Bouchard LS, Phan DH, Puolakkainen PA. Stimulation of bone healing by transforming growth factor-beta 1 released from polymeric or ceramic implants. J Appl Biomater, 5: 141-50, 1994.
28) Kuboki Y, Jin Q, Takita H. Geometry of carriers controlling phenotypic expression in BMP-induced osteogenesis and chondrogenesis. J Bone Joint Surg Am, 83-A Suppl 1: 105-15, 2001.
29) Kusumoto K, Bessho K, Fujimura K, Konishi Y, Ogawa Y, Iizuka T. Self-regenerating bone implant: ectopic osteoinduction following intramuscular implantation of a combination of rhBMP-2, atelopeptide type I collagen and porous hydroxyapatite. J Craniomaxillofac Surg, 24: 360-5, 1996.
30) Laffargue P, Fialdes P, Frayssinet P, Rtaimate M, Hildebrand HF, Marchandise X. Adsorption and release of insulin-like growth factor-I on porous tricalcium phosphate implant. J Biomed Mater Res, 49: 415-21, 2000.
31) Lind M, Overgaard S, Soballe K, Nguyen T, Ongpipattanakul B, Bunger C. Transforming growth factor-beta 1 enhances bone healing to unloaded tricalcium phosphate coated implants: an experimental study in dogs. J Orthop Res, 14: 343-50, 1996.
32) Ono I, Inoue M, Kuboki Y. Promotion of the osteogenetic activity of recombinant human bone morphogenetic protein by prostaglandin E1. Bone, 19: 581-8, 1996.
33) Si X, Jin Y, Yang L. Induction of new bone by ceramic bovine bone with recombinant human bone morphogenetic protein 2 and transforming growth factor beta. Int J Oral Maxillofac Surg, 27: 310-4, 1998.
34) Blom EJ, Klein-Nulend J, Yin L, van Waas MA, Burger EH. Transforming growth factor-beta1 incorporated in calcium phosphate cement stimulates osteotransductivity in rat calvarial bone defects. Clin Oral Implants Res, 12: 609-16, 2001.
35) Blumenthal NM, Koh-Kunst G, Alves ME, Miranda D, Sorensen RG, Wozney JM, Wikesjo UM. Effect of surgical implantation of recombinant human bone morphogenetic protein-2 in a bioabsorbable collagen sponge or calcium phosphate putty carrier in intrabony periodontal defects in the baboon. J Periodontol, 73: 1494-1506, 2002.
36) Lee DD, Tofighi A, Aiolova M, Chakravarthy P, CatalanoA, Majahad A, Knaack D. Alpha-BSM: a biomimetic bone substitute and drug delivery vehicle. Clin Orthop, 396-405, 1999.

37) Li RH, D'Augusta D, Blake C, Bouxsein M, Wozney JM, Li J, Stevens M, Kim H, Seeherman H. rhBMP-2 delivery and efficacy in an injectable calcium phosphate based matrix. The 28th International Symposium on Controlled Release of Bioactive Materials San Diego, Abstract # 6130: 2001.
38) Ohura K, Hamanishi C, Tanaka S, Matsuda N. Healing of segmental bone defects in rats induced by a beta-TCP-MCPM cement combined with rhBMP-2. J Biomed Mater Res, 44: 168-75, 1999.
39) van der Lubbe HB, Klein CP, de Groot KA. Simple method for preparing thin (10 microM) histological sections of undecalcified plastic embedded bone with implants. Stain Technol, 63: 171-6, 1988.
40) Dodde R, Yavuzer R, Bier UC, Alkadri A, Jackson IT. Spontaneous bone healing in the rabbit. J Craniofac Surg, 11: 346-9, 2000.
41) Frame JW. A convenient animal model for testing bone substitute materials. J Oral Surg, 38: 176-80, 1980.
42) Vehof JW, Haus MT, de Ruijter AE, Spauwen PH, Jansen JA. Bone formation in transforming growth factor beta-I-loaded titanium fiber mesh implants. Clin Oral Implants Res, 13: 94-102, 2002.
43) Choi SH, Kim CK, Cho KS, Huh JS, Sorensen RG, Wozney JM, Wikesjo UM. Effect of recombinant human bone morphogenetic protein-2/absorbable collagen sponge (rhBMP-2/ACS) on healing in 3-wall intrabony defects in dogs. J Periodontol, 73: 63-72, 2002.
44) Li G, Bouxsein ML, Luppen C, Li XJ, Wood M, Seeherman HJ, Wozney JM, Simpson H. Bone consolidation is enhanced by rhBMP-2 in a rabbit model of distraction osteogenesis. J Orthop Res, 20: 779-788, 2002.
45) Pluhar GE, Manley PA, Heiner JP Jr, Seeherman HJ, Markel MD. The effect of recombinant human bone morphogenetic protein-2 on femoral reconstruction with an intercalary allograft in a dog model. J Orthop Res, 19: 308-317, 2001.
46) Welch RD, Jones AL, Bucholz RW, Reinert CM, Tjia JS, Pierce WA, Wozney JM, Li XJ. Effect of recombinant human bone morphogenetic protein-2 on fracture healing in a goat tibial fracture model. J Bone Miner Res, 13: 1483-90, 1998.
47) Kuboki Y, Takita H, Kobayashi D, Tsuruga E, Inoue M, Murata M, Nagai N, Dohi Y, Ohgushi H. BMP-induced osteogenesis on the surface of hydroxyapatite with geometrically feasible and nonfeasible structures: topology of osteogenesis. J Biomed Mater Res, 39: 190-9, 1998.
48) Ruhe PQ, Hedberg EL, Padron NT, Spauwen PH, Jansen JA, Mikos AG. rhBMP-2 release from injectable poly(DL-lactic-co-glycolic acid)/calcium-phosphate cement composites. J Bone Joint Surg Am, 85-A Suppl 3: 75-81, 2003.
49) Blom EJ, Klein-Nulend J, Wolke JG, Kurashina K, van Waas MA, Burger EH. Transforming growth factor-beta1 incorporation in an alpha-tricalcium phosphate/dicalcium phosphate dihydrate/tetracalcium phosphate monoxide cement: release characteristics and physicochemical properties. Biomaterials, 23: 1261-8, 2002.

4

5

BONE INDUCTIVE PROPERTIES OF rhBMP-2 LOADED POROUS CALCIUM PHOSPHATE CEMENT IMPLANTS INSERTED AT AN ECTOPIC SITE IN RABBITS

H.C. Kroese-Deutman, P.Q. Ruhé, P.H.M. Spauwen and J.A. Jansen
Biomaterials. 2005;26(10):1131-8.

BONE INDUCTIVE PROPERTIES OF rhBMP-2 LOADED POROUS CALCIUM PHOSPHATE CEMENT IMPLANTS INSERTED AT AN ECTOPIC SITE IN RABBITS

INTRODUCTION

Bone tissue is one of the most frequently used tissues for transplantation. The vast demand for bone is due to various reasons, i.e. to fill defects caused by trauma or tumor resection, reconstruction of congenital malformation and age related decrease of bone mass. Autogenous bone is the treatment-of-choice to restore and augment osseous structures. Unfortunately, insufficient autogenous bone is available for reconstruction in many cases.

Furthermore, autografting is associated with donor-site morbidity. Many complications like infection, pain, loss of sensibility and hematoma have been described.[1] Therefore, several alternatives to autogenous bone have been investigated. One of these are the so called synthetic Bone Graft Substitutes (BGSs).[2-5] A BGS could be engineered directly at the recipient site (orthotopically) or, depending on medical implications such as radiation therapy or unfavorable local physical conditions, it could be prefabricated ectopically in subcutaneous or intramuscular pockets before being transplanted to the recipient site.

Calcium phosphate (Ca-P) cement is one of the materials currently under investigation for its potential as BGS.[6-9] An advantage of cement-like Ca-P materials is that they can be injected directly into a bone defect and can be shaped and molded to fit the required shape. Further, Ca-P cements are considered to be extremely biocompatible and show fast deposition of new bone at their surface.[10,11] Recently, a method has been developed within our laboratory to increase the porosity of the cement by creating macropores.[12] In this way, the degradation rate and tissue ingrowth of the cement were enhanced.[13]

Besides the scaffold material, another important component in bone regeneration are osteoinductive factors like Bone Morphogenetic Protein (e.g. BMP-2). BMP's play an important regulatory role in many steps in bone morphogenesis like chemotaxis, differentiation as well as mitosis of cartilage and bone producing cells.[14] At this moment 15 different kinds of BMPs are known,[15] which belong to the Transforming Growth Factor (TGF)-β gene super family. Research especially focuses on the bone regenerating properties of BMP-2 and BMP-7.[14,16-19] Both factors are available in large quantities by human recombinant technology. BMP-2 also showed osteogenic activity at intramuscular[20,21] and subcutaneous sites.[22-24]

Osteoinductive proteins require an appropriate carrier material as delivery vehicle.[25] However, the role of biomaterials on the osteoinductive activity of BMP is not completely clear. A material itself might potentiate the activity of BMP by binding the protein and presenting it to target cells in a "bound" form.[26,27] For several biomaterials, a correlation between growth factor retention and osteoinductivity has been reported.[28] On the other hand, slowly released BMP may provide a physiological concentration of free protein in the vicinity of the implant, what may attract target cells to the implant-site by chemotaxis.[29] The optimal retention/release rates for growth factors and their carriers have not been established yet.

In the present study, we hypothesized that rhBMP-2 loaded porous Ca-P cement can induce bone in an ectopic site. rhBMP-2 loaded as well as unloaded pre-set porous Ca-P cement discs were implanted subcutaneously in the rabbit model and compared with the current standard for rhBMP-2 delivery, absorbable collagen sponge (ACS).

MATERIALS AND METHODS

Porous calcium phosphate cement implants

In total, 36 disc-shaped porous calcium phosphate (Ca-P) cement implants were created by the CO_2 induction technique.[12] The implants were made out of Calcibon® (Biomet Merck, Darmstadt, Germany). This cement consists of a mixture of 62.5wt% tricalcium phosphate (α-TCP), 26.8wt% dicalcium phosphate anhydrous (DCPA), 8.9wt% calcium carbonate ($CaCO_3$) and 1.8wt% hydroxyapatite (Hap).

Hundred-twenty μl of an aqueous Na_2HPO_4 (2% in weight) solution was added to the cement, which was placed in a syringe. The syringe was closed with an injection plunger and fixed in a mixing apparatus (Silamat® Vivadent, Schaan, Liechtenstein). Thereafter, 150μl NaH_2PO_4 (8%) was added in order to create gas bubbles inside the material and to generate macroporosity. The newly formed cement was injected immediately into a cylindrical mold to ensure a standardized shape of the implants (discs of 2.7 mm height and 8.0 mm diameter, weight 0.11gr/ disc). The samples were placed into an oven at 50°C for one hour. Afterwards, the surface of the discs was sandpapered to ensure a standardized height of 2.7 mm. Finally, the discs were air dried and sterilized by autoclaving for 15 minutes at 121°C.

The average weight of the discs was 108 ± 7 mg. Channel –like macropores varying from 100μm to more than 1000μm in length could be detected. Histomorphometrical analysis of the discs before implantation showed that the volumetric macroporosity was 36%. Previously, the microporosity (pores<1 μm) of this cement was shown to be 39%.[12]

Absorbable Collagen Sponge (ACS) implants

Sterile Absorbable Collagen Sponge (ACS) loaded with rhBMP-2, was used as a reference material (provided by Yamanouchi Europe BV). Under sterile conditions, discs were punched out of lyophilized ACS sheets with 8 mm biopsy punches (Stiefel Laboratories BV, Veendam, The Netherlands). Prior to this procedure, the material was moistened with H_2O under sterile conditions to induce common shrinkage of the material.

rhBMP-2 loading

The stock solutions of rhBMP-2 (1 mg/ml) were stored frozen at -20°C before use. This solution was thawed slowly to refrigeration temperature and was diluted with 4000 μL buffer to give a total volume of 5000 μL (rhBMP-2 concentration 0.2 mg/ml). The dilution buffer (pH 7.2) for both the Ca-P implants and the ACS implants was PBS/ BSA (0.1%).

One day before implantation, eighteen calcium phosphate implants were loaded with this rhBMP-2 concentration. Twenty-five μL of diluted rhBMP-2 (0.2 mg/ml) was administered to each side of the sterile porous Ca-P implants, which were placed in a sterile Eppendorf® tube. In this way, a total dose of 10 μg per implant was achieved. Thereafter, the specimens were lyophilized and stored at 4°C until surgery took place.

In all, fifty μL of the diluted rhBMP-2 solution (0.2 mg/ml) was pipetted carefully onto the 8 mm diameter cylindrical pieces of the ACS. In this way, 10 μg of rhBMP was present per implant (30% soak-load). The ACS discs were allowed to soak-load for minimally 15 minutes before they were implanted subcutaneously. Care was taken not to squeeze the discs to prevent the loss of growth factor.

Surgical procedure

Fifty-four female New Zealand White rabbits, each weighing 2.8 –3.2 kg, were used ("De Vaan" farm, Bergharen, The Netherlands). National guidelines for the care and use of laboratory animals were observed. The animals were divided into three groups of 18 animals (Table 1). Each animal received one subcutaneous implant to prevent cross-over effects of rhBMP-2.

Group	No. of rabbits	Implant	Sacrifice of rabbits	
			2 weeks	10 weeks
I	18	Porous Ca-P cement	9	9
II	18	Porous Ca-P cement + rhBMP-2	9	9
III	18	ACS + rhBMP-2	9	9

TABLE 1: *Implantation scheme.*

Surgery was performed under general inhalation anesthesia and sterile conditions. The rabbits received antibiotic prophylaxis (Baytril (2.5% Enrofloxacin), 5-10 mg/kg) before surgery. The anesthesia was initiated by an intramuscular injection of 0.5 ml/kg Hypnorm® (0.315 mg/ml fentanyl citrate and 10 mg/ml fluanisone) and 0.25 mg atropine. Thereafter, the rabbits were intubated and connected to an inhalation ventilator with a constant volume of a mixture of nitrous oxide, isoflurane, and oxygen.

Before the insertion of the subcutaneous implants, each animal was immobilized in the ventral position and mid dorsum, the skin was shaved and marked with a small tattoo to indicate the implantation site. Subsequently, the skin was washed and disinfected with povidone-iodine. Paravertebral, at one side of the spinal column, a longitudinal incision of about 1.5 cm was made through the full thickness of the skin. Subsequently, a subcutaneous pocket towards the tattoo was created by blunt dissection with a pair of scissors. The implant then was inserted in this pocket close to the tattoo. Finally, the skin was closed intracutaneously using resorbable Vicryl® 4-0 suture material. A total of 54 implants were inserted this way.

Two weeks after implantation, nine animals of each group were euthanized by an overdose of Nembutal®. The remaining nine rabbits were euthanized after ten weeks of implantation.

At the time of euthanasia the implants with surrounding tissue were retrieved for histological analysis. Parallel to this study, a separate study was performed in the same animals where identical experimental groups were implanted in the rabbit's skull.

Fluorochrome labeling

Twelve rabbits of the ten week implantation period (four of each group) received in vivo fluorochromes that adsorb to bone mineral during the time they are present in the blood circulation. Four markers were administered subcutaneously at timed intervals (1, 3, 7 and 9 weeks) to deposit at the mineralizing surface of the bone (Table 2).

Postoperative administration (weeks)	Fluorochrome	Colour	Dose
1	Tetracycline	Yellow	25 mg/Kg sc
3	Alizerin-Complexon	Red	25 mg/Kg sc
7	Calcein	Green	25 mg/Kg sc
9	Tetracycline	Yellow	25 mg/Kg sc

TABLE 2: *Scheme for administration of fluorochromes to 12 rabbits (four of each group).*

Histological preparations

Directly after retrieval, specimens were fixed in 4% buffered formalin solution, dehydrated in a graded series of alcohol and embedded in methylmethacrylate (MMA). After polymerisation, non-decalcified thin (10 μm) transverse sections of the implant were prepared (at least three of each implant) using a modified sawing microtome technique.[30] Methylene blue and basic fuchsin were used for staining the sections. Two extra unstained slides (10 μm) were made of the specimens where fluorochrome labeling analysis was indicated.

Histological and histomorphometrical evaluation

The histological evaluation consisted of a concise description of the observed specimens and a histomorphometrical analysis of the tissue response using a light microscope (Leica Microsystems AG, Wetzlar, Germany). The Leica® Qwin Pro-image analysis system (Wetzlar, Germany) was used for the computer based image analysis techniques (histomorphometrical evaluation). A reflectant fluorescence microscope equipped with an excitation filter of 470-490 nm (Leica Microsystems AG, Wetzlar, Germany) was used for the fluorochrome labeling analysis.

All Ca-P cement scaffolds were digitally analyzed. The quantitative measurements were performed for all three digitalized sections per implant. Results were based on the average of these measurements. ACS implants were not evaluated with this method, because no ACS residue or subsequent bone formation could be retrieved after two and ten weeks of implantation (see also Results section).

The following parameters were assessed for histomorphometrical analysis:

- The surface of the area where the implant is inserted, which is called the region of interest (ROI).
- The bone surface area and the cement surface area (expressed as a percentage of the ROI). The cement surface area included microporosity of the cement, since pores smaller than 1 μm could not be distinguished histomorphometrically from cement particles.
- The (macro)pore surface area (%), calculated from the ROI minus the cement surface area and bone surface area.
- Pore fill by bone (%), expressed as percentage of pore surface area occupied by bone.

Statistical analysis

Data for all parameters of the of rhBMP-2 loaded and unloaded porous Ca-P cement implants were compared among and within groups using an unpaired T-test with Welch correction. All statistical analyses were performed with GraphPad® Instat 3.05 software (GraphPad Software Inc, San Diego, CA, USA). Differences were considered significant at p-values less than 0.05.

RESULTS

Experimental animals

In this study, all 54 animals survived the procedure without any signs of disease or wound complications. Thirty-six porous Ca-P implants (group I and II) could be retrieved. At retrieval, no inflammatory signs or adverse tissue reaction could be observed. All implants were surrounded by a thin fibrous capsule.

On the contrary, none of the ACS implants (group III) could be detected and even after microscopical evaluation of the area surrounding the tattoo, no ACS residue or signs of bone formation were observed.

Light microscopy

Two weeks specimens

Analysis revealed that all Ca-P cement implants had maintained their shape. A thin fibrous capsule surrounded the implants. Ingrowth of blood vessels and loose connective tissue were present in all macropores throughout the scaffolds. Little or no inflammatory cells could be observed at the cement surface. None of the porous Ca-P implants (group I and II) showed bone or cartilage formation after two weeks (figure 1A and 1B).

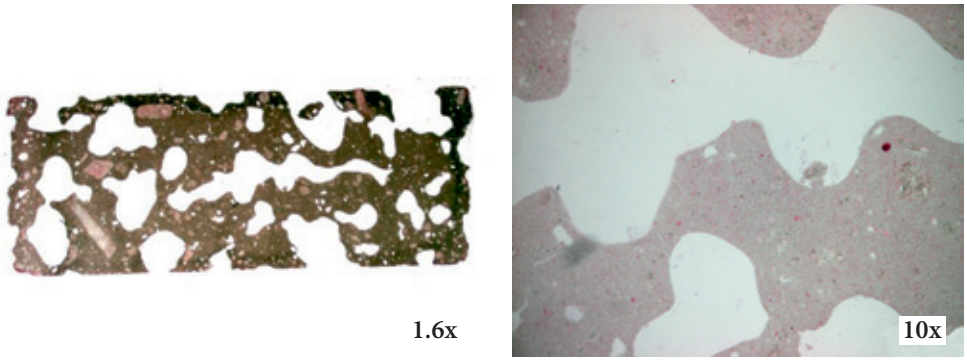

FIGURE 1A+B:

Light microscopical aspect of the subcutaneous porous CaP+rhBMP-2 implant after 2 weeks. There are no signs of bone formation yet (original magnification 1.6x respectively 10x).

Ten weeks specimens

Ten weeks postoperatively, all Ca-P implants had maintained their shape. The fibrous capsule around the discs had a more mature appearance and blood vessel ingrowth was more prominent than in the two weeks sections. Bone formation was present in the rhBMP-2 loaded group. Bone formation in this group was characterized by the presence of osteoblasts and osteocyte-like cells embedded in the matrix (figure 2A, 2B and 3). The newly formed bone had a lamellar appearance. Bone remodeling was seen in some sections. Bone formation was diffusely spread throughout the macropores of the whole implant. Formation of cartilage or bone outside the cement was not observed in any of the Ca-P cement scaffolds.

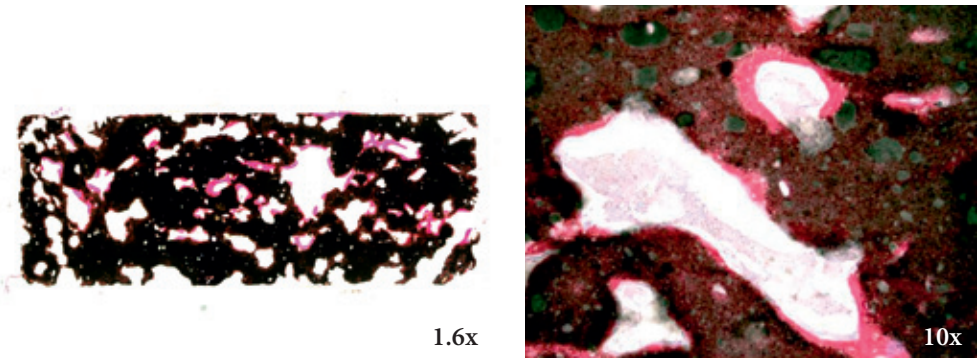

FIGURE 2A+B:
Light microscopical aspect of the subcutaneous porous Ca-P +rhBMP-2 implant after 10 weeks of implantation. Bone formation is to be seen in the cement scaffolds (original magnification 1.6x respectively 10x).

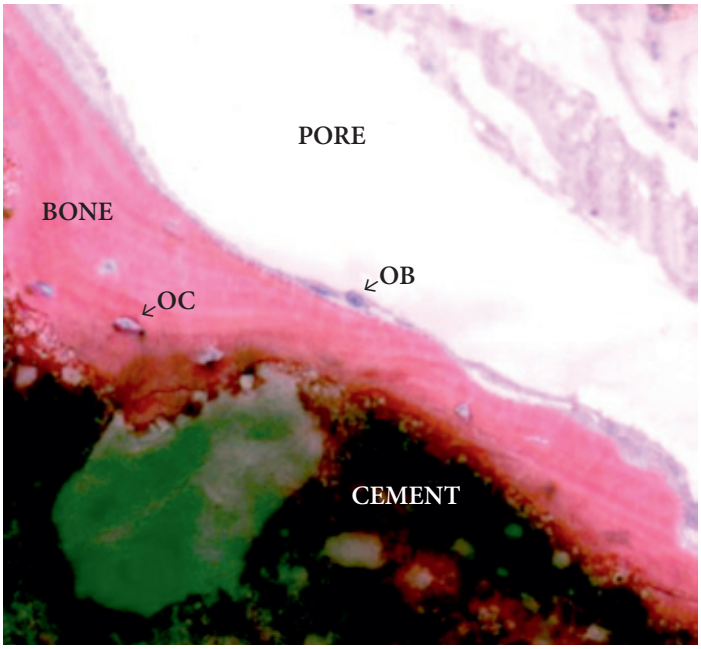

FIGURE 3:
Light microscopical aspect of the subcutaneous porous Ca-P +rhBMP-2 implant after 10 weeks of implantation. Direct apposition of bone on the Ca-P cement surface is observed. OC= osteocyte; OB= osteoblast (original magnification 20x).

Fluorescence microscopy

The first yellow Tetracycline label and the red Alizerin-Complexon label, administered after one and three weeks respectively, were not detected. On the other hand, the green Calcein label and the second yellow Tetracycline label, indicative for bone formation after seven and nine weeks, were clearly visible in the bone formation in the rhBMP-2 loaded Ca-P cement implants (figure 4).

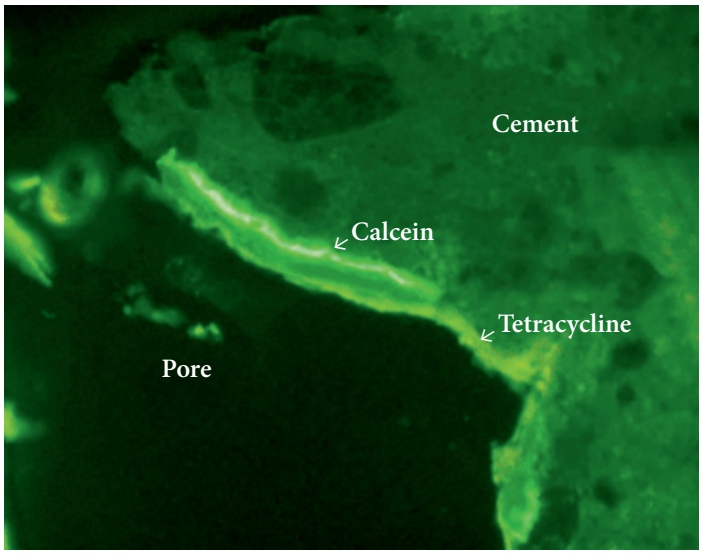

FIGURE 4:

Results of fluorescence microscopy inside a fluorochrome labelled rhBMP-2 loaded Ca-P cement (10 weeks). Formation of bone started at the cement surface and proceeded into the macropore. C=calcein label, administered after seven weeks of implantation (green). T=tetracycline label, administered after nine weeks of implantation (yellow). (original magnification 20x).

Histomorphometry

Histomorphometrical results are summarized in table 3. As previously described, bone formation was only present in the ten weeks rhBMP-2 group. In this group, total bone surface was 7±3% of the scaffold's ROI. This resembled a pore fill percentage of 18±6%. After two and ten weeks of implantation, the macroporosity was not significantly changed in both groups.

	Bone surface (% of ROI)	**Pore fill (%)**
Porous Ca-P	0 ± 0%	0 ± 0%
Porous Ca-P + rhBMP-2	7 ± 3% **	18 ± 6% **

TABLE 3: *Histomorphometrical analysis of ectopic bone formation after 10 weeks of implantation (means ± standard deviation for n=9 ** p<0.05).*

DISCUSSION

In this study, we investigated the osteoinductive characteristics of rhBMP-2 loaded and unloaded porous preset Ca-P cement discs at an ectopic site in rabbits. As reference material, rhBMP-2 loaded ACS discs were implanted similarly.

After two and ten weeks, implants were retrieved from their subcutaneous pockets. All Ca-P discs had maintained their shape and stability. This observation suggests that the mechanical properties of this porous Ca-P cement are sufficient to serve as scaffold material for subcutaneous bone engineering. On the contrary, none of the ACS discs could be retrieved. Despite widespread searching, no ACS residue or subcutaneous bone formation were observed. Bone formation in the vicinity of the tattoo could not be confirmed histologically. Therefore, we conclude that the ACS has been degraded completely within two weeks. This rapid degradation of the ACS sponge was also observed in the cranial defect study that was performed in the same rabbits.[31] In contrast to studies dealing with rhBMP-2 loaded ACS in subcutaneous pockets in rats[28,32], ectopic bone formation was not observed in the rhBMP-2 loaded ACS implants. We assume that the absence of bone formation in the current study is due to the spongy nature of the ACS, which causes rapid dispersion of the rhBMP-2 directly after implantation. This explanation is supported by the findings of Friess et al[33], who reported that the fraction of rhBMP-2 retained in the ACS in subcutaneous sites is less than 10% after 10 days, which is perhaps too low to induce bone formation. Further the implantation site could have an effect on ectopic bone formation. For example, Yoshida et al described that subcutaneous implantation is less favorable for rhBMP-2 induced bone formation compared to intramuscular or intermuscular implantation.[24] This suggests that although rhBMP-2 loaded ACS is a powerful osteoinductive material in other locations[34,35], it could be less suitable for subcutaneous prefabrication of bone graft substitutes.

Histomorphometrical analysis determined that bone formation in the rhBMP-2 loaded porous Ca-P cement discs reached a pore fill of 18 ±6% after ten weeks of implantation. As the two weeks light microscopical sections did not show bone deposition or cartilage formation, and the three weeks fluorescent Alizerin-Complexon label was never observed, it could be supposed that direct bone formation started after three weeks of implantation. Some studies even suggested that calcium phosphate biomaterials show osteoinductive characteristics in soft tissues without administration of growth factors or osteoblastic cells.[36,37] However, this suggestion could not be confirmed by the present study because unloaded porous Ca-P cement discs did not show any bone formation after subcutaneous implantation up to ten weeks.

The sequence of the fluorescent labels also confirmed that bone formation started at the cement surface and subsequently proceeded into the center of the macropores. This observation agrees with previously reported bone deposition in porous ceramics[31,38] and illustrates the osteocompatibility of porous Ca-P cement. Furthermore, it is opposite to bone formation in other scaffold materials like titanium fiber mesh, which is reported to start in the center of the pore.[39,40]

Finally, histomorphometrical analysis included quantification of the cement surface as indicator of macroporosity and implant degradation. Degradation of the cement was not observed in this study. In previous studies, degradation of similar porous Ca-P cement varied from none to 80% after ten weeks.[13,31] It is known that the presence of bone –and thus osteoclasts- is essential for degradation of Ca-P material. Ideally, bone formation and scaffold degradation follow one another progressively until the biomaterial has been replaced completely by new bone. As long as bone formation is not extensive enough to

supply mechanical strength, the scaffold material should not be degraded too quickly to assure stability of the construct. We think that the limited extent of bone formation in the rhBMP-2 loaded Ca-P cement discs after ten weeks does not justify significant degradation of the Ca-P cement at this phase. Furthermore, in the orthotopic implants, no degradation of the porous Ca-P cement discs was observed either, while these implants showed an extensive bone fill up to 53.0 ±5.4%.[31] This is in contrast to a previous study in goats, where porous Ca-P cement implants inserted in the femoral condyle showed 80% degradation within ten weeks.[13] This illustrates that degradation of Ca-P cement depends on various parameters such as implant dimension, species and implantation site.

CONCLUSIONS

In summary, we conclude that porous Ca-P cement is a suitable carrier material for ectopic bone engineering. Although the amount of bone formation in this study was limited, porous Ca-P cement in combination with rhBMP2 revealed osteoinductive properties and maintained its shape and stability during subcutaneous implantation in New Zealand white rabbits for ten weeks.

Acknowledgement: Yamanouchi Europe BV provided the rhBMP-2.
This study has been supported by the NWO-AGIKO foundation.

REFERENCES

1) Hartman EH, Spauwen PH, Jansen JA. Donor-site complications in vascularized bone flap surgery. J Invest Surg 2002;15:185-197.
2) Hollinger JO, Schmitz JP, Mizgala JW, Hassler C. An evaluation of two configurations of tricalcium phosphate for treating craniotomies. J Biomed Mater Res 1989;23:17-29.
3) Bostman OM. Absorbable implants for the fixation of fractures. J Bone Joint Surg Am 1991;73:148-153.
4) Schwartz Z, Braun G, Kohavi D, Brooks B, Amir D, Sela J, Boyan B. Effects of hydroxyapatite implants on primary mineralization during rat tibial healing: biochemical and morphometric analyses. J Biomed Mater Res 1993;27:1029-1038.
5) Costantino PD, Friedman CD. Synthetic bone graft substitutes. Otolaryngol Clin North Am 1994;27:1037-74.
6) Ishikawa K, Asaoka K. Estimation of ideal mechanical strength and critical porosity of calcium phosphate cement. J Biomed Mater Res 1995;29:1537-1543.
7) Khairoun I, Driessens FC, Boltong MG, Planell JA, Wenz R. Addition of cohesion promotors to calcium phosphate cements. Biomaterials 1999;20:393-398.
8) Lee DD, Tofighi A, Aiolova M, Chakravarthy P, Catalano A, Majahad A, Knaack D. Alpha-BSM: a biomimetic bone substitute and drug delivery vehicle. Clin Orthop 1999;396-405.
9) Brown WE, Chow LC. Dental restorative cement pastes. US. Patent 4,518,430. 1985.
10) Comuzzi L, Ooms E, Jansen JA. Injectable calcium phosphate cement as a filler for bone defects around oral implants: an experimental study in goats. Clin Oral Implants Res 2002;13:304-311.
11) Ooms EM, Wolke JG, van der Waerden JP, Jansen JA. Trabecular bone response to injectable calcium phosphate (Ca-P) cement. J Biomed Mater Res 2002;61:9-18.
12) del Real RP, Wolke JG, Vallet-Regi M, Jansen JA. A new method to produce macropores in calcium phosphate cements. Biomaterials 2002;23:3673-80.
13) del Real RP, Ooms E, Wolke J, Vallet-Regi M, Jansen JA. In vivo bone response to porous calcium phosphate cement. J Biomed Mater Res 2003;65A:30-36.
14) Reddi AH. Cell biology and biochemistry of endochondral bone development. Coll Relat Res 1981;1:209-26.
15) Groeneveld EH, Burger EH. Bone morphogenetic proteins in human bone regeneration. Eur J Endocrinol 2000;142:9-21.
16) Bostrom MP, Lane JM, Berberian WS, Missri AA, Tomin E, Weiland A, Doty SB, Glaser D, Rosen VM. Immunolocalization and expression of bone morphogenetic proteins 2 and 4 in fracture healing. J Orthop Res 1995;13:357-367.
17) Reddi AH. Bone morphogenetic proteins, bone marrow stromal cells, and mesenchymal stem cells. Maureen Owen revisited. Clin Orthop 1995;115-119.
18) Reddi AH. Role of morphogenetic proteins in skeletal tissue engineering and regeneration. Nat Biotechnol 1998;16:247-252.
19) Wozney JM, Rosen V, Celeste AJ, Mitsock LM, Whitters MJ, Kriz RW, Hewick RM, Wang EA. Novel regulators of bone formation: molecular clones and activities. Science 1988;242:1528-34.
20) Fujimura K, Bessho K, Kusumoto K, Ogawa Y, Iizuka T. Experimental studies on bone inducing activity of composites of atelopeptide type I collagen as a carrier for ectopic osteoinduction by rhBMP-2. Biochem Biophys Res Commun 1995;208:316-322.
21) Si X, Jin Y, Yang L. Induction of new bone by ceramic bovine bone with recombinant human bone morphogenetic protein 2 and transforming growth factor beta. Int J Oral Maxillofac Surg 1998;27:310-4.

22) Murata M, Inoue M, Arisue M, Kuboki Y, Nagai N. Carrier-dependency of cellular differentiation induced by bone morphogenetic protein in ectopic sites. Int J Oral Maxillofac Surg 1998;27:391-6.
23) Omura S, Mizuki N, Kawabe R, Ota S, Kobayashi S, Fujita K. A carrier for clinical use of recombinant human BMP-2: dehydrothermally cross-linked composite of fibrillar and denatured atelocollagen sponge. Int J Oral Maxillofac Surg 1998;27:129-34.
24) Yoshida K, Bessho K, Fujimura K, Kusumoto K, Ogawa Y, Tani Y, Iizuka T. Osteoinduction capability of recombinant human bone morphogenetic protein-2 in intramuscular and subcutaneous sites: an experimental study. J Craniomaxillofac Surg 1998;26:112-5.
25) Lucas PA, Syftestad GT, Goldberg VM, Caplan AI. Ectopic induction of cartilage and bone by water-soluble proteins from bovine bone using a collagenous delivery vehicle. J Biomed Mater Res 1989;23:23-39.
26) Reddi AH, Cunningham NS. Initiation and promotion of bone differentiation by bone morphogenetic proteins. J Bone Miner Res 1993;8 Suppl 2:499-502.
27) Uludag H, Gao T, Porter TJ, Friess W, Wozney JM. Delivery systems for BMPs: factors contributing to protein retention at an application site. J Bone Joint Surg Am 2001;83-A Suppl 1:128-35.
28) Uludag H, D'Augusta D, Golden J, Li J, Timony G, Riedel R, Wozney JM. Implantation of recombinant human bone morphogenetic proteins with biomaterial carriers: A correlation between protein pharmacokinetics and osteoinduction in the rat ectopic model. J Biomed Mater Res 2000;50:227-38.
29) Cunningham NS, Paralkar V, Reddi AH. Osteogenin and recombinant bone morphogenetic protein 2B are chemotactic for human monocytes and stimulate transforming growth factor beta 1 mRNA expression. Proc Natl Acad Sci U S A 1992;89:11740-4.
30) van der Lubbe HB, Klein CP, de Groot K. A simple method for preparing thin (10 microM) histological sections of undecalcified plastic embedded bone with implants. Stain Technol 1988;63:171-6.
31) Ruhe PQ, Kroese-Deutman HC, Wolke JG, Spauwen PH, Jansen JA. Bone inductive properties of rhBMP-2 loaded porous calcium phosphate cement implants in cranial defects in rabbits. Biomaterials 2004;25:2123-2132.
32) Uludag H, D'Augusta D, Palmer R, Timony G, Wozney J. Characterization of rhBMP-2 pharmacokinetics implanted with biomaterial carriers in the rat ectopic model. J Biomed Mater Res 1999;46:193-202.
33) Friess W, Uludag H, Foskett S, Biron R, Sargeant C. Characterization of absorbable collagen sponges as rhBMP-2 carriers. Int J Pharm 1999;187:91-9.
34) Tatakis DN, Koh A, Jin L, Wozney JM, Rohrer MD, Wikesjo UM. Peri-implant bone regeneration using recombinant human bone morphogenetic protein-2 in a canine model: a dose-response study. J Periodontal Res 2002;37:93-100.
35) Welch RD, Jones AL, Bucholz RW, Reinert CM, Tjia JS, Pierce WA, Wozney JM, Li XJ. Effect of recombinant human bone morphogenetic protein-2 on fracture healing in a goat tibial fracture model. J Bone Miner Res 1998;13:1483-90.
36) Ripamonti U, Crooks JaKAN. Sintered porous hydroxyapatites with intrinsic osteoinductive activity: geometric induction of bone formation. S Afr J Sci 1999;95:335-343.
37) Yuan H, Kurashina K, de Bruijn JD, Li Y, de Groot K, Zhang X. A preliminary study on osteoinduction of two kinds of calcium phosphate ceramics. Biomaterials 1999;20:1799-1806.
38) Kuboki Y, Takita H, Kobayashi D, Tsuruga E, Inoue M, Murata M, Nagai N, Dohi Y, Ohgushi H. BMP-induced osteogenesis on the surface of hydroxyapatite with geometrically feasible and nonfeasible structures: topology of osteogenesis. J Biomed Mater Res 1998;39:190-9.

39) Vehof JW, Spauwen PH, Jansen JA. Bone formation in calcium-phosphate-coated titanium mesh. Biomaterials 2000;21:2003-9.
40) Vehof JW, Haus MT, de Ruijter AE, Spauwen PH, Jansen JA. Bone formation in transforming growth factor beta-I-loaded titanium fiber mesh implants. Clin Oral Implants Res 2002;13:94-102.

6

THE INFLUENCE OF RGD-LOADED TITANIUM IMPLANTS ON BONE FORMATION IN VIVO

H.C. Kroese-Deutman, J. van den Dolder, P.H.M. Spauwen and J.A. Jansen
Tissue Eng. 2005;11(11-12):1867-75.

THE INFLUENCE OF RGD-LOADED TITANIUM IMPLANTS ON BONE FORMATION IN VIVO

INTRODUCTION

In the field of bone regeneration, naturally derived and synthetic polymers, ceramics, metals and composites are being used. Occasionally, these so-called scaffold materials are also provided with growth factors as well as stromal cells in order to enhance their bone forming capacity. The demands upon the scaffold properties largely depend on the site of application and the function that has to be restored. For example, the ideal scaffold material is biocompatible and biodegradable, can be shaped easily, possesses interconnective porosity, is osteoconductive and promotes angiogenesis.[1]

Unfortunately, none of the currently used materials meets all of the properties postulated. Some of the materials show an undesirable inflammatory response or foreign body reaction. These reactions are associated with a reduced osteoinductive response. Other materials show a lack of structural support and good mechanical characteristics.

In view of the above mentioned, in our laboratory a series of studies is ongoing where we explore the feasibility and efficacy of titanium fiber mesh as scaffold material for bone reconstructive purposes. Titanium is well known for its excellent biocompatibility. This is expressed by two major observations: (1) a very favorable response of tissues to titanium surfaces, and (2) the absence of allergic reactions to titanium.[2,3] For example, bone cells and mineralized bone matrix are laid down on titanium surfaces without interposition of other tissues.[2]

The porous titanium fiber mesh as used in our studies has several advantages above bulk titanium, like its flexibility and interconnective porosity. Flexibility helps presumably to eliminate focal stresses by distributing the stresses between implant and tissue over a larger area.[3] The porosity of the fiber mesh can be varied during the fabrication, which can influence the amount of bone ingrowth into the material and allows a more normal restoration of the bone unlike nonporous implant materials.

Proper bone growth also requires initial stability. The frictional characteristics of porous titanium fiber mesh when contacting bone exceeds solid-metal materials available today. In the early post-operative period these frictional and structural properties allow a high initial stability of the construct.

Consequently, porous titanium fiber mesh offers several advantages over other materials by its uniformity and structural continuity, as well as by its strength, low stiffness, high porosity, corrosion resistance and high coefficient of friction.[4] Nevertheless, previous studies have shown that the osteoconductive properties of the material are still insufficient to allow complete closure of cranial defects in rats.[5] Stromal bone marrow cells have been seeded into the mesh porosity to overcome this problem.[5] Although the data confirmed that this technique supports the bone formation inside the mesh, this cell-based approach is laborious and the outcome not completely predictable. Therefore, titanium mesh has also been treated with bone growth stimulating factors, such as bone morphogenetic protein and transforming growth factor-ß1.[6-8] Despite favorable results in rats, the disadvantage of the use of such morphogens is the cost and reproducibility of the results in larger animals and humans.

An alternative approach to the above mentioned ones can be the coupling of ligands, like peptides, to the titanium mesh surface.[9]

The organic component of bone is composed of numerous extracellular matrix proteins that serve multiple roles in bone formation and homeostasis, ranging from simple cell-attachment to binding of hydroxyapatite. These extracellular matrix proteins interact with a heterodimeric cell membrane receptor family, known as integrins that use multiple intracellular signaling pathways. Arginine-glycine-aspartic acid or RGD is a small peptide ligand, which has high affinity for these integrins and is the most extensively studied integrin-stimulating peptide. It is known, that RGD peptides increase the overall adhesiveness of the surface for osteoblasts.[10,11] In this way, they can essentially mimic cell attachment activity of the bone cells.[12,13] It has also been suggested that RGD peptide coating enhances titanium rod osseointegration in the rat and goat femur.[14,15]

In the current study, the influence of RGD peptide sequence on porous titanium fiber mesh and on bone formation itself was investigated. We evaluated the osteoconductive properties of porous titanium fiber mesh, coated with or without RGD-sequence, in a rabbit non-critical size cranial defect model. We hypothesized that adding this cycled RGD-peptide to the titanium fiber mesh would enhance the osteoconductive properties of this carrier material. In the study design, an empty control defect was included in order to follow the regular healing process of the non-critical sized cranial defect.

MATERIALS AND METHODS

Implant preparation

Sintered titanium fiber mesh implants (Bekaert N.V., Zwevegem, Belgium) with a volumetric porosity of 86%, density of 600 g/m^2 and fiber diameter of 40 μm were used.

The prepared implants were disc-shaped with an outer diameter of 8.0 mm, thickness of 0.8 mm and weight of approximately 33.5 mg. All implants were ultrasonically cleaned with isopropanol and 70% ethanol for 15 minutes, and then sterilized by gamma sterilization. A total of 60 implants were prepared.

Subsequently, 30 of the titanium discs were coated with 100 μM cyclic RGD-peptide (provided by Biomet Deutschland GmbH, Darmstadt) and first synthesized by the group of Prof.dr.H.Kessler at the TU Munich, Germany) containing a phosphonate anchor, in phosphate buffered saline (PBS, pH 7.4). The RGD was connected with a covalent bond, which creates a connection. The Titatium meshes were soaked in with the coating solution and the peptide was allowed to immobilize overnight. After three washes with PBS the meshes were dried and sterilized by gamma sterilization (≈25 kGy) and ready for implantation. Gamma sterilization was confirmed by the manufacturer (Biomet Deutschland) and was shown not to affect the activity of the peptide coating.

Experimental study design

Thirty adult female New Zealand white rabbits (2.5-3.5 kg) were used. National guidelines for the care and use of laboratory animals were observed. In each rabbit three cranial defects with an outer diameter of 8.0 mm were made (Figure 1). The distance between the defects was at least 5 mm. Treatments were titanium fiber mesh (Ti), titanium fiber mesh loaded with RGD peptide sequence (RGD-Ti) and an open control defect to follow the regular healing process of the non-critical sized cranial defects.

The rabbits were sacrificed at different time-intervals of two, four and eight weeks (respectively, group I, II and III; Table 1), and in each case the skull with the implants was retrieved so that histologic evaluation could be performed.

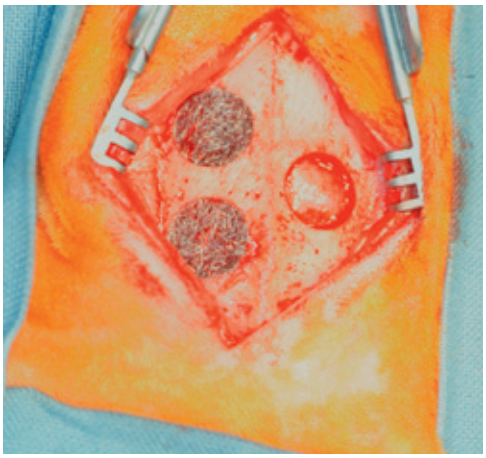

FIGURE 1:
The three cranial full-thickness bone defects with an outer diameter of 8 mm (RGD-Ti, Ti, and open).

Group	Defect size	Number of defects (RGD-Ti, Ti, open)	Implantation time
I n=10	8.0 mm	3	2 weeks
II n=10	8.0 mm	3	4 weeks
III n=10	8.0 mm	3	8 weeks

TABLE 1: *Number of animals, defect size and implantation time.*

Surgical procedure

Surgery was performed under general inhalation anesthesia. The anesthesia was induced by an intravenous injection of Hypnorm® (0.315 mg/ml fentanyl citrate and 10 mg/ml fluanisone) and atropine, and maintained by a mixture of nitrous oxide, isoflurane and oxygen through a constant volume ventilator. To reduce the perioperative infection risk, antibiotic prophylaxis (Baytril 2.5%) was given to the rabbits.

After anaesthetization, the animals were immobilized on their abdomen. Hair from the cranium was shaved and the skin was disinfected with povodine-iodine.

From the nasal bone to the occipital protuberance, a longitudinal incision was made. Thereafter, a midline incision was created in the periosteum. Subsequently, the periosteum was removed gently and lifted from the parietal skull with a blunt instrument. Three cranial full-thickness bone defects with an outer diameter of 8 mm were prepared with a dental-trephine bur at low rotation speed (1000-1500 rpm) in both sides of the parietal bone. The drill depth was limited to 1.5 mm and the cranial bone disks were carefully removed. During the drilling procedure, saline was supplied as a coolant. After this procedure, the RGD-Ti implant was inserted according to a randomized implantation schedule in one of the three defects in the skull (Table 2). The titanium fiber mesh without RGD was placed in the second defect (Ti). The third defect was left open as a control in order to follow the regular healing capacity of this non-critical sized cranial defect in rabbits (Figure 1). The periosteum and skin were closed (tensionless) using Prolene 4.0 sutures.

Rabbit no and location skull	RGD-Ti location	Ti location	Control defect location	No defect
1, 5, 9, 13, 17, 21, 25, 29	1	2	3	4
2, 6, 10, 14, 18, 22, 26, 30	2	3	4	1
3, 7, 11, 15, 19, 23, 27	3	4	1	2
4, 8, 12, 16, 20, 24, 28	4	1	2	3

TABLE 2: *Randomized implantation schedule.*

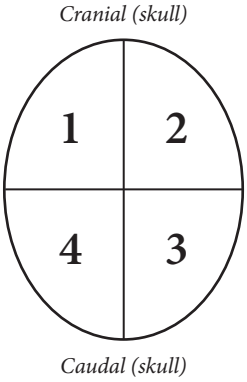

Histological and histomorphometrical evaluation

Skull bones containing the implants were retrieved for histological examination at the various time cited above. Directly after retrieval, skulls were fixed in 4% buffered formalin solution and dehydrated in a graded series of ethanol. Before embedding in methylmethacrylate (MMA), the skulls were divided with a sawing machine into three separate specimens containing one implant each. Finally, thin sections (10 μm) were prepared by a sawing microtome technique after polymerization.[16] All sections were made in the frontal-caudal direction. The slides were stained with methylene blue-basic fuchsin and observed with a light microscope for histological examination (Leica Microsystems BV, Rijswijk, the Netherlands). At least three sections from the central part of each implant were evaluated.

Histological evaluation consisted of a concise description of the observed specimens and a histomorphometrical analysis of the tissue response.

Histomorphometrical evaluation was carried out using computer- based image analysis (Leica® Qwin Pro-image analysis system). From each implant, the data were pooled and the mean used for statistical analysis.

The following histomorphometrical parameters were assessed for the Ti and RGD-Ti cranial implants (Figure 2):

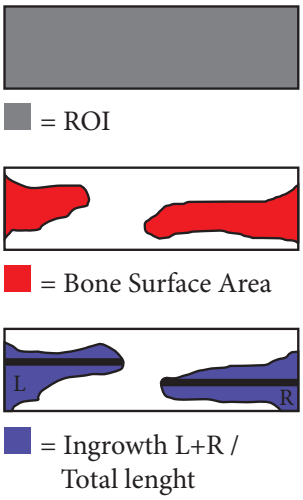

FIGURE 2:
Histomorphometric parameters of Ti and RGD-Ti cranial implants (region of interest (ROI), bone surface area, and bone ingrowth in length).

The surface area where the titanium implant was inserted (the so-called Region of Interest, ROI). The bone surface area in the ROI (expressed as a percentage of the ROI).

The distance of bone ingrowth into the titanium fibre mesh. This was calculated as the sum of ingrowths at the right and left side of the implants divided by the total length of the implant.

For the open control defects only the maximum gap as left at the end of the respective implantation times was measured.

Statistical analysis

All measurements were statistically evaluated with GraphPad® Instat 3.05 software (GraphPad Software Inc, San Diego, CA, USA) using an unpaired Student t test with Welch correction to compare untreated Ti with RGD-treated Ti specimens for each implantation time. All data were tested for normality. Differences were considered significant at p-values less then 0.05.

RESULTS

Macroscopical evaluation

All 30 animals survived the implantation period and remained in good health. At retrieval no macroscopic signs of inflammation or adverse tissue reaction were seen around any of the 90 defects. All implant sites and empty control defects could be easily located. Each implant remained seated at the original site and they were all covered by periosteum. Bone formation could be seen macroscopically in most of the specimens. The newly formed bone appeared normal. No gross macroscopical differences could be observed between the RGD-Ti and the Ti group.

Histological and histomorphometrical evaluation

Two weeks

All of the control defects (10) were open after two weeks. New bone formation started mainly at the edges of the defect (Figure 3). The morphological appearance and thickness of the newly formed bone differed from the original bone. Histomorphometry revealed that the bone had covered 52±8% of the length of the original control defect size.

Also, none of the titanium defects were closed (covered with bone over the whole defect). In all Ti and RGD-Ti implants, blood vessel ingrowth and fibrous tissue formation were present. Blood vessel ingrowth in the RGD-Ti group appeared to be more prominent than in the Ti group. No inflammatory cells or fibrous tissue were present in or around the surface of both types of implant.

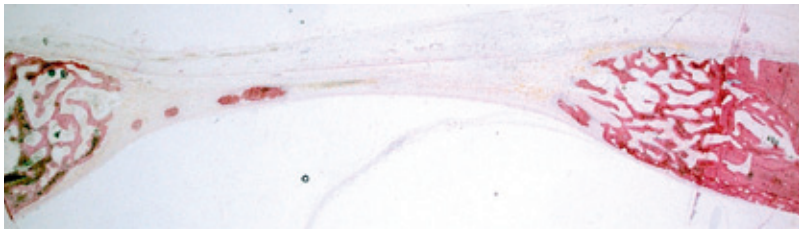

A

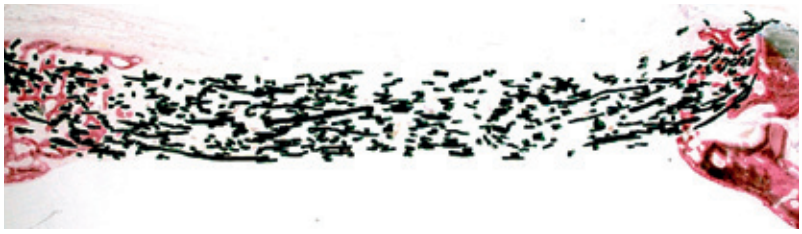

B

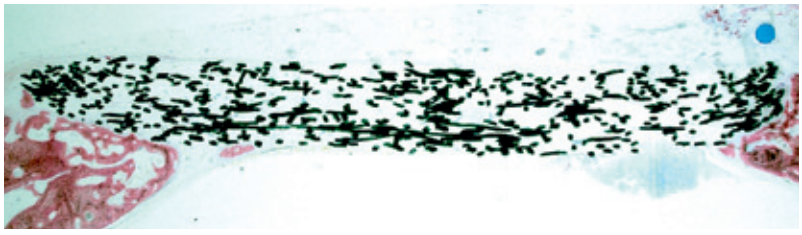

C

FIGURE 3:

Light microscopical overview of A: control defect, B: RGD-Ti scaffold, and C: Ti scaffold, 2 weeks postimplantion (original magnification 1.6x).

After two weeks, 12 ± 5% of the RGD-Ti fiber mesh was covered with bone with a trabecular structure starting at the edges, and 8 ± 6% of the Ti fiber mesh without RGD was covered (no significant difference, Table 3). There was also no significant difference between the total ingrowth (percent ingrowth of the total length of the implant) of the RGD-Ti group (58 ± 24%) and the Ti group (44 ± 26%, Table 4).

Area of bone / ROI (%)	**RGD-Ti**	**Ti**
2 weeks	12 ± 5%	8 ± 6%
4 weeks	12 ± 4%	6 ± 5%
8 weeks	18 ± 10%	10 ± 7%

TABLE 3: *Bone surface area in RGD-Ti and Ti scaffolds 2, 4 and 8 weeks postimplantation.*

Bone-ingrowth right + left / Total lenght of implant (%)	**RGD-Ti**	**Ti**
2 weeks	58 ± 24%	44 ± 26%
4 weeks	71 ± 17%	50 ± 20%
8 weeks	71 ± 21%	52 ± 16%

TABLE 4: *Bone ingrowth (right +left) in RGD-Ti and Ti scaffolds 2, 4 and 8 weeks postimplantation.*

Representative examples of light microscopical sections of control, RGD-Ti and Ti implants 2 weeks postimplantation are depicted in Figure 3.

Four weeks

All of the empty control defects were still open after four weeks (n=10). The newly formed bone covered 52±12% of the total length of the original control defect size (Figure 4). The contour, i.e. thickness, of the ingrown bone differed from the original bone. Inside the empty defect space, fibrous tissue was present and blood vessel invasion had occurred. Always, a fibrous tissue capsule could be observed at the periphery of the bone defect.

The Ti and RGD-Ti mesh implants were also surrounded with a fibrous tissue capsule. No inflammatory cells were seen in or around the surfaces of the implants. There was no observable increase in thickness of the capsule from week 2 to week 4.

After four weeks there was significantly more bone surface area in the RGD-Ti group (12 ± 4%) compared with the Ti group (6 ± 5%, Table 3). Further, the total bone ingrowth in the RGD-Ti group was 71 ± 17% and in the Ti group 50 ± 20%, which is significantly different as well (Table 4).

Figure 4 shows typical histological slides of the control, RGD-Ti and Ti implants.

A

B1

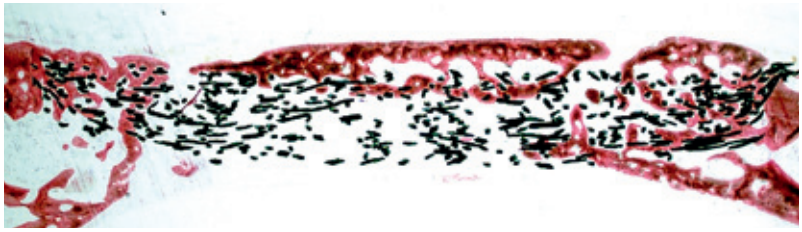

B2

C1

C2

FIGURE 4:
Light microscopical overview of A: control defect, B: RGD-Ti scaffold (B1 shows limited bone ingrowth; B2 shows bone overgrowth of mesh structure), and C: Ti scaffold (C1 shows limited bone growth; C2 shows deep bone penetration in mesh porosity) 4 weeks postimplantion (original magnification 1.6x).

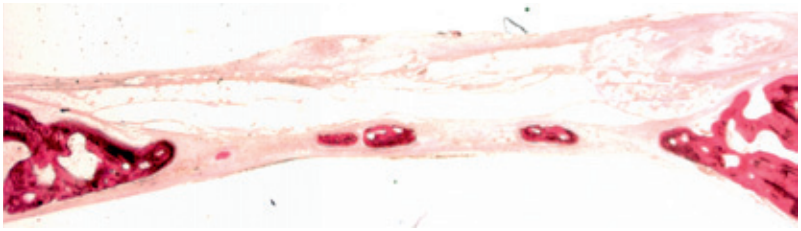

A

B1

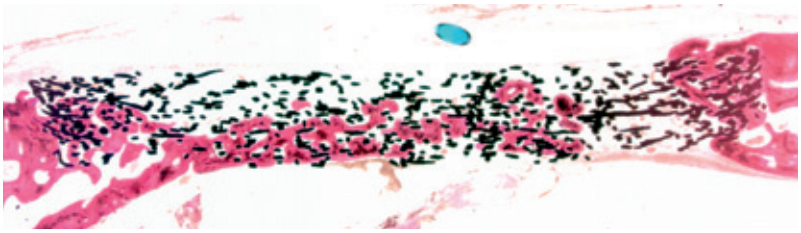

B2

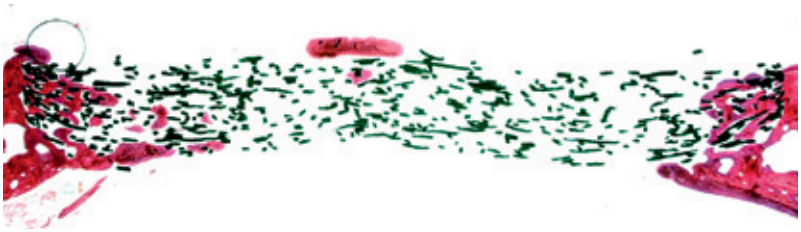

C1

C2

FIGURE 5:
Light microscopical overview of A: control defect, B: RGD-Ti scaffold (B1 showth bone overgrowth; B2 shows bone ingrowth in mesh structure), and C: Ti scaffold (C1 shows no bone ingrowth; C2 shows limited bone ingrowth in mesh porosity) 8 weeks postimplantion (original magnification 1.6x).

Eight weeks

All of the empty defects were still open after 8 weeks. New bone formation covered 64±12% of the total length of the control defect (Figure 5). The newly formed bone still differed in thickness compared with the original bone. A fibrous tissue capsule was maintained at the outside of the gap. One of the RGD-Ti implant was completely covered with bone over its total length. Further, blood vessel ingrowth and fibrous tissue encapsulation was very comparable with the 2- and 4-week specimens. After eight weeks, 18 ±10% of the RGD-Ti fiber mesh surface area was occupied by bone compared to 10 ±7% of the titanium fiber mesh without RGD (Table 3). This difference was not significant (p=0.057). However, the total bone ingrowth percentage in the RGD-Ti group (71 ± 21%) was significantly greater than in the Ti group (52 ± 16%) (Table 4). Figure 5 shows the light microscopical appearance of control, RGD-Ti and Ti implants 8 weeks postimplantation.

DISCUSSION

In this study, we investigated the effect of RGD coated titanium fiber mesh on bone formation in vivo at three different time periods. Histomorphometric analysis determined that 18 ±10% of the RGD-Ti fiber mesh was occupied with bone after 8 weeks compared with 10 ±7% of the titanium fiber mesh without RGD (not significant; p=0.057). Nevertheless, after 4 weeks there was significantly more bone surface area in the RGD-Ti group (12 ±4%) compared with the Ti group (6 ± 5%, Table 3). A significant increase in the ingrowth (length) after 4 and 8 weeks occurred as well, when compared to the reference material (uncoated titanium fiber mesh). We must also note that all control defects stayed open until 8 weeks postimplantation. This emphasizes the relevance of our model. Evidently, the Ti scaffolds also did not hamper or interfere in a negative way with the bone-healing process.

Bone cell adhesion and migration is known to play an important role during the biological processes underlying bone healing and bone regeneration. Cell adhesion peptides, like RGD, are supposed to play a role in the control of bone cell proliferation and differentiation. The peptides must be covalently attached to a suitable carrier material in order to be used in implant surgery. The results, as obtained in the current study, confirm the hypothesis that coating cycled RGD-peptide on titanium fiber mesh will enhance the osteoconductive properties of this carrier material. The results corroborate with other studies. For example, Ferris et al[14] demonstrated a significant increase in new bone thickness around RGDC (Arg-Gly-Asp-Cys) modified surfaces at polished titanium rods in a rats femur after 2 and 4 weeks of implantation. They measured a significantly thicker shell of newly formed bone around the implant as soon as 2 weeks postimplantation, but using another animal model and another titanium implant and implantation site.

Elmengaard et al,[17] showed that cyclic RGD coating on unloaded press-fit titanium implants has an osteoconductive effect only directly at the interface after 4 weeks postimplantation (implanted in the tibia of a dog model). Also, Schliephake et al found an increase in bone-implant contact from 1 to 3 months postoperatively in a group of RGD-coated implants, using a combination of collagen and RGD on dental implants in the mandibles of 10 beagle dogs.[18] However, similar to our study, Schliephake et al showed a large degree of variation in bone contact rates within the various experimental groups, resulting in a decreased level of significance. The experimental model can be an important variable for this phenomenon. Tripeptide RGD has been shown to enhance in vitro the adhesion and spreading of fibroblasts, endothelial cells, smooth muscle cells and osteoblasts when this biomolecule was grafted on different surfaces.[19-22] Concerning the effect of RGD peptides on osteoblast cell differentiation, integrin-mediated cell binding seems to be the

essential parameter. In particular, αvβ3- and αvβ5 integrin selective RGD peptide ligands are responsible for mediating the initial adhesion and increased synthesis of mineralized matrix.[23] Bernhardt et al also indicated that RGD peptides were capable of generating signals for the specific microenvironment around titanium implants in the femur of a goat and thus accelerated the bone formation process.[15] Nevertheless, a decisive factor in the cell attachment-promoting activity of surface bound RGD peptide is, of course, the availability of a sufficient amount of free bone-forming cells. This may have been the major problem in our in vivo study. Periosteal osteo- and chondrogenesis is important for bone defect healing. In our study design, the periosteum was first lifted from the skull bone and at the end of the procedure was sutured back over the mesh implant to its original position. The periosteum consists of two layers: a fibrous outer layer and bordering to the bone a cambium layer, which contains specific osteogenic and chondrogenic precursor cells.[24] Therefore, maintenance of this cambium layer is essential for bone healing to occur in the mesh implant after closure of the periosteum at the end of the implant installation. However, in rabbits this layer is difficult to retain during surgery resulting in delayed healing.[25] Besides preservation of the cambium layer, skull bone is composed mainly of cortical bone with a minimal portion of marrow-rich cancellous bone. In addition, the amount of contact between the mesh scaffold and bone defect wall was limited to a few 40 μm thick titanium fibers due to the specific morphological structure of the mesh material. Apparently, this also did not promote the migration of bone cells into the mesh porosity.

Besides the experimental model, another critical issue dealing with the modification of implant surfaces by peptides is the final selectivity of the peptides used. Besides bone cells, the adhesion of other cell types can be promoted. Also, multiple ligands may be required for a full cell adhesion response.[26] In view of this, two relevant parameters for the final biological effect of grafted RGD peptides are the competitive adsorption of a second protein from the surrounding body fluid and the RGD peptide surface concentration.[27] The second adsorbed protein can result in inefficient cell adhesion, and an increase in RGD peptide surface concentration has been shown to result in increased cell proliferation with, at the same time, reduced matrix production.[27] Unfortunately, we do not know whether optimum surface conditions existed for early differentiation and phenotypic expression on our RGD-coated titanium fiber meshes.[28] In view of the above, it must also be noted that other implant materials are available with perhaps better osteoconductive properties as compared with Ti mesh. Most of these materials belong to the class of calcium phosphate (Ca-P) ceramics. Unfortunately, these materials lack the advantageous mechanical properties of titanium, the result being that titanium, with its improvement in osteoconductive behavior, is still attractive from the final clinical application perspective.[29]

CONCLUSION

In conclusion, cyclic RGD peptide in combination with titanium fiber mesh has a positive effect, compared with titanium fiber mesh alone, on bone formation in vivo after 4 and 8 weeks when implanted in the skull of New Zealand white rabbits. Nevertheless, the amount of bone formation inside the mesh pores was still limited and further studies are required to optimize the bone biological effect of cyclic RGD peptide grafted on titanium fiber mesh scaffold.

Acknowledgement: Biomet Deutschland GmbH provided the cyclic RGD-peptides. This study has been supported by the NWO-AGIKO foundation.

REFERENCES

1) Yang S, Leong KF, Du Z, Chua CK. The design of scaffolds for use in tissue engineering. Part I. Traditional factors. Tissue Engineering 7, 679, 2001.
2) Pohler OE. Unalloyed titanium for implants in bone surgery. Injury 31, 7, 2000.
3) Jansen JA, von Recum AF, van der Waerden JP, de Groot K. Soft tissue response to different types of sintered metal fibre-web materials. Biomaterials 13, 959, 1992.
4) Chang YS, Oka M, Kobayashi M, Gu HO, Li ZL, Nakamura T, Ikada Y. Significance of interstitial bone ingrowth underload-bearing conditions: a comparison between solid and porous implant materials. Biomaterials 17, 1141, 1996.
5) van den Dolder J, Farber E, Spauwen PHM, Jansen JA. Bone tissue reconstruction using titanium fiber mesh combined with rat bone marrow stromal cells. Biomaterials; 24, 1745, 2003.
6) Vehof JW, de Ruijter AE, Spauwen PHM, Jansen JA. Influence of rhBMP-2 on rat bone marrow stromal cells cultured on titanium fiber mesh. Tissue Eng. 7, 373, 2001.
7) Vehof JW, Haus MT, de Ruijter AE, Spauwen PHM, Jansen JA. Bone formation in transforming growth factor _-I-loaded titanium fiber mesh implants. Clin. Oral Implants Res. 13, 94, 2002.
8) Vehof JW, Madmood J, Tikita H, van't Hof MA,Kuboki Y, Spauwen PHM, Jansen JA. Ectopic bone formation in titanium mesh loaded with bone morphogenetic protein and coated with calcium phosphate. Plast. Reconstr. Surg. 108, 434, 2001.
9) Massia, S.P., Hubbell, J.A. Covalent surface immobilization of Arg-Gly-Asp- and Tyr-Ile-Gly-Ser-Arg- containing peptides to obtain well-defined cell-adhesive substrates. Anal Biochem. 187, 292, 1990.
10) Puleo DA, Bizios R. RGDS tetrapeptide binds to osteoblasts and inhibits fibronectin-mediated adhesion. Bone, 12, 271, 1991.
11) Rezania A, Thomas CH, Branger AB, Waters CM, Healy KE. The detachment strength and morphology of bone cells contacting materials modified with a peptide sequence found within bone sialoprotein. J. Biomed. Mat. Res., 37, 9, 1997.
12) Pierschbacher MD, Ruoslahti E. Cell attachment activity of fibronectin can be duplicated by small synthetic fragments of the molecule. Nature, 309, 30, 1984.
13) Pierschbacher MD, Ruoslahti E. Variants of the cell recognation site of fibronectin that retain attachment-promoting activity. Proc. Natl. Acad. Sci. USA, 81, 5985, 1984.
14) Ferris DM, Moodie GD, Dimond PM, Giorani CWD, Ehrlich MG, Valentini RF. RGD-coated titanium implants stimulate increased bone formation in vivo. Biomaterials, 20, 2323, 1999.
15) Bernhardt R, van den Dolder J, Bierbaum S, Beutner R, Scharnweber D, Jansen JA, Beckmann F, Worch H. Osteoconductive modifications of Ti-implants in a goat defect model: Characterization of bone growth with SR _CT and histology. Biomaterials 26, 3009, 2005.
16) van der Lubbe HB, Klein CP, de Groot K. A simple method for preparing thin (10 microM) histological sections of undecalcified plastic embedded bone with implants. Stain Technol., 63, 171, 1988.
17) Elmengaard B, Bechtold JE, Soballe K. Cyclic RGD coated on unloaded press-fit titanium implants increases bone ingrowth in vivo. Presented at the Society for Biomaterials, 29th Annual Meeting Transactions, 2003.
18) Schliephake H, Scharnweber D, Dard M, Rößler S, Sewing A, Meyer J, Hoogestraat D. Effects of RGD peptide coating of titanium implants on periimplant bone formation in the alveolar crest. An experimental pilot study in dogs. Clin. Oral Implants Res., 13, 312, 2002.
19) Fittkau MH, Zilla P, Bezuidenhout D, Lutolf MP, Human P, Hubbell JA, Davies N. The selective modulation of endothelial cell mobility on RGD peptide containing surfaces by YIGSR peptides. Biomaterials, 26, 167, 2005.

20) El-Ghannam AR, Ducheyne P, Risbud M, Adama CS, Saphiro IM, Castner D, Colledge S, Composto RJ. Model surfaces engineerd with nanoscale roughness and RGD tripetides promote osteoblast activity. J. Biomed. Mater Res., 68, 615, 2004.
21) Massia SP, Stark J. Immobilized RGD peptides on surface-grafted dextran promote biospecific cell attachment. J. Biomed. Mater Res., 56, 390, 2001.
22) Massia SP, Hubbell JA. An RGD spacing of 440 nm is sufficient for integrin alpha V beta 3-mediated fibroblast spreading and 140 nm for focal contact and stress fiber formation. J. Cell. Biol., 114, 1089, 1991.
23) Pallu S, Bareille R, Dard M, Kessler H, Jonczyk A, Vernizeau M, Amedee-Vilamitjana J. A cyclo peptide activates signaling events and promotes growth and the production of the bone matrix. Peptides. 24, 1349, 2003.
24) O'Driscoll SW, Fitzsimmons JS. The role of periosteum in cartilage repair. Clin. Orthop. 39, 190, 2001.
25) O'Driscoll SW. Technical considerations in periosteal grafting for osteochondral injuries. Clin. Sports Med., 20, 379, 2001.
26) Drumheller PD, Herbert CB, Hubbell JA. Bioactive peptide and surface design. In: Brash JL and Wojciechowski PW (eds.) Interfacial Phenomena and Bioproducts, Marcel Dekker Inc, New York, 1996, 273-310.
27) Xiao SJ, Kenausis G, Textor M. Biochemical modification of titanium surfaces. In: Brunette DM, Tengvall P, Textor M, Thomsen P, eds. Titanium in Medicine Springer Verlag, Berlin, 2001, 418-455.
28) Tosatti S, Schwartz Z, Campbell C, Cochran DL, van deVondele S, Hubbell JA, Denzer A, Simpson J, Wieland M, Lohmann CH, Textor M, Boyan BD. RGD-containing peptide GCRGYGRGDSPG reduces enhancement of osteoblast differentiation by poly(L-lysine)-graft-poly(ethylene glycol)-coated titanium surfaces. J. Biomed. Mater Res., 68, 458, 2004.
29) Barber TA, Golledge SL, Castner DG, Healy KE. Peptide-modified p(AAm-co-EG/AAc) IPNs grafted to bulk titanium modulate osteoblast behavior in vitro. J. Biomed. Mater Res., 64, 38, 2003.

7

ORTHOTOPIC BONE FORMATION IN PLATELET RICH PLASMA (PRP) LOADED TITANIUM FIBER MESH PLACED IN SEGMENTAL DEFECTS

H.C. Kroese-Deutman, Vehof J.W.M., P.H.M. Spauwen, P.J.W. Stoelinga and J.A. Jansen

Int J Oral Maxillofac Surg. 2008;37(6):542-9.

ORTHOTOPIC BONE FORMATION IN PLATELET RICH PLASMA (PRP) LOADED TITANIUM FIBER MESH PLACED IN SEGMENTAL DEFECTS

INTRODUCTION

The treatment of large bone defects is challenging to orthopedic and reconstructive surgeons. Treatment of bone defects in weight-bearing situations (e.g. limbs) demands the use of a stable construct. Various techniques can be used to bridge defects or regenerate lost bone in these circumstances: Autogenous bone grafts, either vascularized (for example the free fibula flap) or non-vascularized, bridging T2-pens (intramedullairy nailing system for fixation of long bone fractures) and plates. More recently, tissue engineering strategies are being used to create Bone Graft Substitutes. This involves the use of natural or synthetic materials as a scaffold or matrix for cells and/or growth factors. Although these scaffolds improve the migration, proliferation and differentiation of the bone repair process, they do not possess bone-inductive activity. Growth factors can induce the formation of new bone. Among osteoinductive growth factors the use of Bone Morphogenic Proteins (BMPs) has been most extensively studied in animal and clinical models.[23] Drawbacks to the clinical use of BMPs are the high costs and unphysiological high dose needed (milligram range).[15]

An attractive alternative is the use of autologous "Platelet Rich Plasma" (PRP). Multiple growth factors exist in platelets: Platelet Derived Growth Factor (PDGF), Transforming Growth Factor beta 1 (TGFβ1) and beta 2 (TGFβ2), vascular endothelial growth factor (VEGF), Insuline Growth Factor (IGF) and epidermal growth factors (EGF).[2,17,26]

PRP is a volume of autologous plasma that has a platelet (thrombocytes) concentration above baseline (1 ×109 pl / ml). These proteins act on target cells, resulting in the specific stimulation or inhibition of these cells. PRP can be obtained from whole blood by centrifugation and separation of thrombocytes with the use of a cell separator. Depending on the production process, the concentration of thrombocytes in PRP is 3- to 20-fold greater than in whole blood.[17]

The positive effect of PRP can be mainly attributed to the effect of TGF-β and PDGF on cell proliferation, differentiation and angiogenesis. PRP stimulates the proliferation and differentiation of osteoblasts and proliferation of capillaries.[18,21] The clinical use of platelet concentrates in PRP with autologous bone grafts, has been shown to nearly double the rate of bone formation and to enhance bone density by 20 % in some studies.[17]

Recently, the efficacy of PRP combined with a polylactide scaffold and autologous bone graft, in goat mandibular defect model, has been demonstrated.[6] The use of such scaffolds can further limit donor-site morbidity.

Another scaffold material for loaded applications is titanium (Ti) fiber mesh.[24,25] This titanium mesh has excellent mechanical properties, is bone biocompatible and easy to handle during surgery. The porosity of the fiber mesh can influence the amount of bone ingrowth into the material and allows a more normal restoration of the bone unlike nonporous implant materials.[10] Since the application of PRP in the treatment of bone defects demands the presence of autologous bone graft, the titanium mesh scaffold will be filled with autologous bone.

The objective of the present study is to evaluate the bone stimulative effect of PRP on autologous bone graft and the influence of a titanium fiber mesh scaffold in a weight-baring bone defect model in rabbits. It was hypothesized that PRP would have a beneficial effect on bone formation in autologous bone grafts placed in a titanium fiber mesh scaffold.

MATERIALS AND METHODS

Preparation of porous Titanium fiber mesh scaffold

Bekaert N.V. (Zwevegem, Belgium) provided the titanium (Ti) fiber mesh implants. The mesh implants were fabricated by interengaging and intertwining a multiplicity of commercially available pure titanium fibers with a fiber diameter of 45 μm. After compression against a solid Al_2O_3 rod the fiber structures were sintered to bond the fibers at their points of contact. In this way a hollow cylindrical shaped tube was created. The volumetric porosity of the titanium mesh was more than 86% and the weight was 120 grams/m^2. The hollow tubes had a length of 15 mm and an outer diameter of 4 mm with an inner diameter of 2.7 mm. Prior to the experiment, measurements were taken in an anatomical rabbit model of the same age to ensure the implants were sized appropriately.

Preparation of the PRP solution

The definition of PRP is at least $1.\times10^6$ platelets/μl in 5 ml plasma.[18] 10 ml autologous venous blood of the rabbit was taken in the morning before surgery. This was centrifuged in a 50 ml tube (2010 RPM) in a Hettich Rotixa/ AP centrifuge (Gemini BV, Apeldoorn, Netherlands) for five minutes. The plasma and buffy coat were removed and placed in a new tube. The platelets were counted in a Coulter counter (Onyx/ Bürker) The PRP was centrifuged for another five minutes (3170 RPM) in a Hettich Rotixa/ AP centrifuge (Gemini BV, Apeldoorn, Netherlands). In total, a mixture of 1 ml PRP was created, which contained 1000-1500 $\times$ 10^9 trombocytes /l. (1.0-1.5 $\times$ 10^{12}). Also, a substance of 10% calcium chloride and 300 E bovine thrombin (Fibriquick, Organon Teknika, Boxtel, The Netherlands) was made; 0.167 ml of this mixture was taken under sterile circumstances during surgery and then mixed with 1 ml PRP for 10 seconds. The clot initiator (bovine trombin) with an air bubble formed the PRP into a gel to optimize growth factor release. The PRP-gel was added to the bone chips to create a fibrin network. This substance was placed inside the titanium scaffold before implantation (Figure 1).

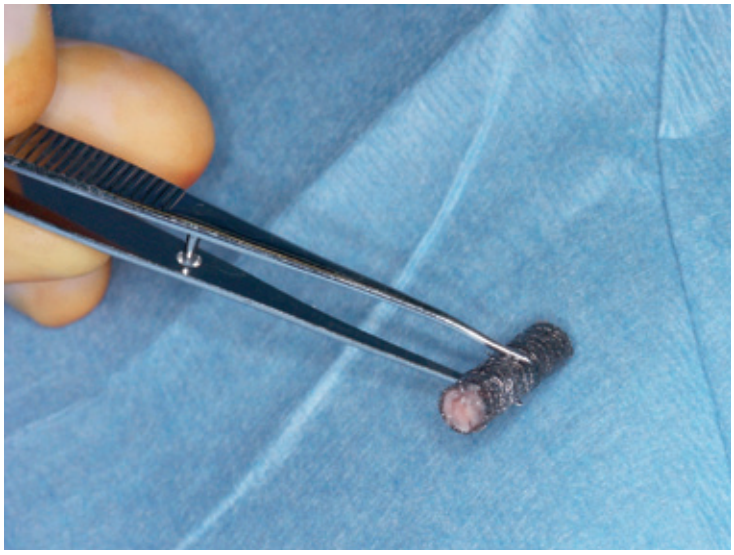

FIGURE 1:
Titanium scaffold filled with bone chips and PRP gel.

Surgical procedure

A total of 18 adult female New Zealand white rabbits (age: three months, mean weight: 2794 g) were used in this study. National guidelines for the care and use of laboratory animals were observed. Surgery was performed under general inhalation anesthesia. The anesthesia was induced by an intravenous injection of Hypnorm® (0.315 mg/ml fentanyl citrate and 10 mg/ml fluanisone) (Abbeyvet Export Ltd, Leeds, UK) and atropine, while maintained by a mixture of nitrous oxide, isoflurane, and oxygen through a constant volume ventilator. To reduce the peri-operative infection risk, antibiotic prophylaxis (Baytril® 2.5% (KPV Pharma, Kiel, Germany) was given to the rabbits. Preoperatively, all the rabbits got Finadyne® (Schering-Plough, Segre, France) 0.02 mg/kg twice a day during two days for pain treatment. We also administered 40 ml extra fluid before surgery to prevent dehydration.

After induction of anesthesia, the animals were immobilized in a prone position. In each animal the front legs were shaved and disinfected with povodine-iodine. A 4.5 cm longitudinal skin incision was made at the dorsal part along the radius. After dissecting the muscles, the radius was exposed. The periosteum was partially pushed off and a 15 mm segmental defect was created in the middle of the radius using a dental drill with a diamant blade with continuous saline cooling. Excess bone obtained from the creation of the segmental defects was grinded (mean weight 0.22 g) in a bone mill (Leibinger®) to form bone chips. In this way, particulate autologous corticocancellous bone grafts were obtained. The amount of bone chips produced by the bone mill was exactly enough to fill all of the titanium scaffolds.

Bilateral segmental radial defects were made in all 18 animals. Three experimental groups were created as described in Table 1. One of each of the three implant types was inserted in the segmental defect of the radius (press fit) (Figure 2). A total of 36 implants were placed: 9 titanium fiber meshes filled with bone chips and PRP-gel (PRP-Ti-Bone) (Figure 1), 9 titanium fiber meshes filled with bone chips (Ti-Bone) and 18 titanium fiber mesh scaffolds alone (Ti) were used as controls. Implants were placed according to

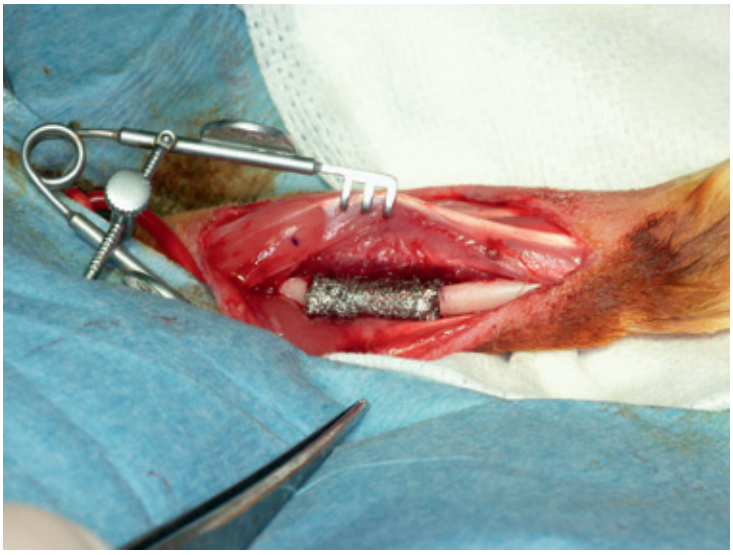

FIGURE 2:
Insertion of the titanium scaffold in the 15 mm segmental radial defect.

a randomization scheme (Table 1). All rabbits received a control implant (Ti) and a PRP-Ti-Bone or Ti-Bone implant.

After placement of the implants the remaining periost and the muscle layers and the skin were closed in separate layers with a Vicryl 4.0 suture. The rabbits were sacrificed 12 weeks postoperatively for histological, histomorphometrical and radiological evaluation.

	Implant	**Number of rabbits**	**Implantation time (weeks)**	**Animal number and side (Right/Left)**
Group I	PRP + Ti + bone chips	n=9	12	1L, 2R, 6R, 7L, 9L, 10R, 13L, 14R, 17L
Group II	Ti + bone chips	n=9	12	3L, 4R, 5L, 8R, 11L, 12R, 15L, 16R, 18R
Group III	Ti (control)	n=18	12	1R, 2L, 3R, 4L, 5R, 6L, 7R, 8L, 9R, 10L, 11R, 12L, 13R, 14L, 15R, 16L, 17R, 18L

TABLE 1: *Design of the experiment: number of animals, defect size, implantation time and implantation scheme.*

Evaluation

Histological and histomorphometrical evaluation

The entire ulna-radius complex was retrieved for histological examination at 12 weeks. The samples were fixed in 4% phosphate-buffered formalin solution, dehydrated in a graded series of ethanol and embedded in methylmethacrylate (MMA). Thin longitudinal sections (10 μm) were prepared (at least three per implant) with a sawing microtome technique after polymerization.[16] These sections were stained with methylene blue/ basic fuchsin and examined with a light microscope for histological evaluation (Leica BV, Rijswijk, the Netherlands) and using a concise description of the observed specimens.

This histomorphometrical analysis was performed using computer based image analysis techniques (Leica® Qwin Pro-image analysis system). Measurements were taken from three sections per implant, and the results pooled to obtain an average for each implant, which was then used in the statistical evaluation.

The following parameters were assessed for digital analysis in the segmental defects (Figure 3):

- The surface of the area where the implant is inserted, which is called the Region of Interest (ROI in mm^2). (Light blue; Figure 3B).
- The amount of bone growth into the implants of the three different groups (mm^2) (Green; Figure 3C).
- The percentage bone in the ROI (%).
- The amount of bone growth outside the implant (mm^2) (Blue; Figure 3D).

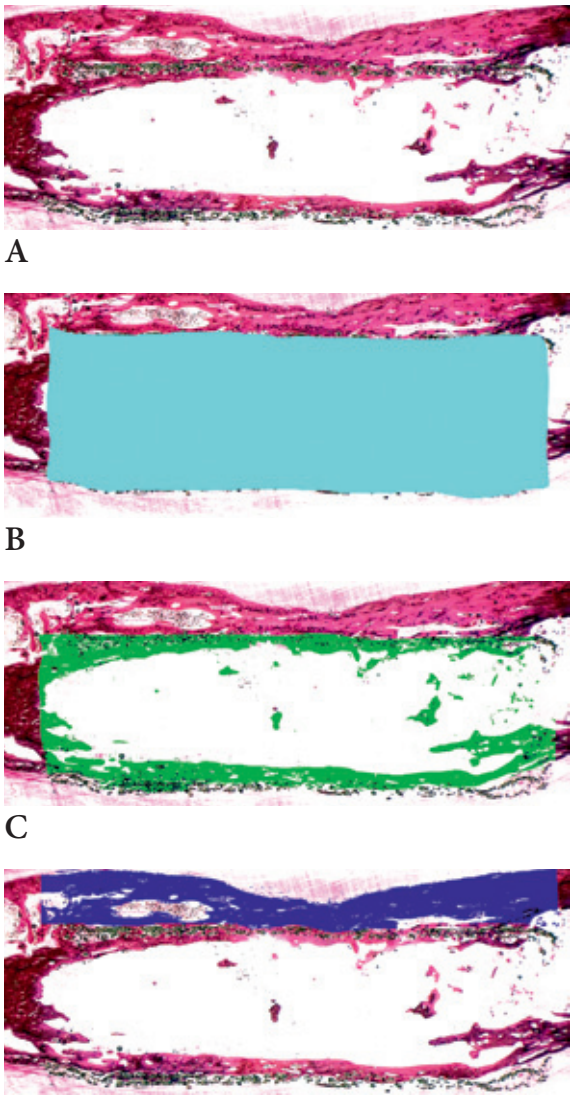

FIGURE 3:
The steps of the histomorphometrical analysis. A: Histology of the Ti implant; B: Region of Interest (Light blue); C: Bone growth (Green); D: Bone outside the implant (Blue).

Radiographic analysis

A medio-lateral X-ray of the ulna-radius complex was made immediately after surgery (day 0) and 12 weeks postoperatively. The radiographs were made with a Siemens Mobilett X-ray machine. Bone healing parameters such as callus formation, quality of union and bone remodelling were compared for the three experimental groups.

Statistical analysis

All data are reported as means and standard deviations. Measurements from the histomorphometrical analysis were statistically evaluated using a One-Way Analysis of Variance (ANOVA) test using GraphPad® Instat 3.05 software (GraphPad Software Inc., San Diego, CA, USA). Differences were considered statistically significant at p-values less than 0.05.

RESULTS

All of the 18 animals survived the surgical procedure and were able to walk within three hours after surgery. All rabbits remained in good health, did not loose weight and and did not show any wound complications. At the end of the 12 week study, all 36 implants could be retrieved: 9 PRP-Ti-Bone, 9 Ti-Bone and 18 Ti implants. Peroperatively, the diameter of the scaffold was larger than the diameter of the bone. At the time of sacrifice the diameter of the implant resembled the bone diameter.

At retrieval, only one of the animals showed an adverse tissue reaction with signs of inflammation. An abcess was visible around the radius and titanium implant. Further, all titanium implants were maintained in place and clearly visible in the radius of the rabbit. The total ulna-radius complex could be taken out for further investigation.

Histology

No inflammatory cells or foreign body reaction was seen in all specimens, except for the specimens retrieved from the rabbit with the infection. A thin fibrous capsule surrounded all implants. Overviews of the sections of each group are shown in Figure 4.

Group I (PRP-Ti-Bone)

After 12 weeks all of the implants showed bone bridging in the titanium implant (Figure 4A). There were no visible remnants of the bone chips. Blood vessel ingrowth was present throughout the implants. All implants showed trabecular bone formation. Bone ingrowth was observed from the defect edges. In the newly formed bone osteoblasts and osteocytes were clearly present. Along the original defect, the newly formed bone was in direct contact with the titanium surface without the presence of an intervening soft tissue layer. Histological analysis could not be performed in one animal (#H6R); the titanium scaffold could not be observed in 2 of the 3 slides due to poor quality of the thin sections. These implants were excluded from the histomorphometrical analysis. Macroscopically, bone bridging was visible outside the titanium scaffold in the majority of these implants.

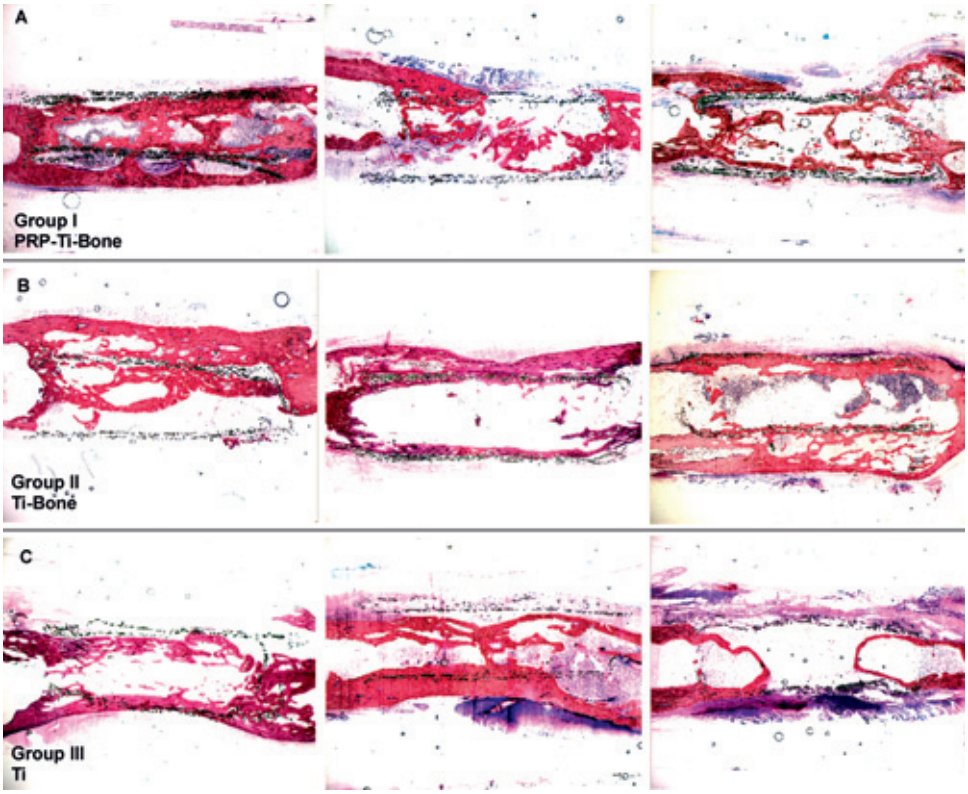

FIGURE 4:

Stained histological sections. (original magnification 1.6). Direct apposition of bone on the rabbits radius is observed. A: Group 1 implant (PRP-Ti-Bone); B: Group 2 implant (Ti-Bone); C: Group 3 implant (Ti / Control).

Group II (Ti-Bone)

In all Ti-Bone specimens, bone formation was present over the total length of the implant as well as inside the implants (Figure 4B). Bone bridging was seen similar to the PRP-Ti-Bone implants. Bone formation was characterized by the presence of osteoblasts and osteocytes. Blood vessel ingrowth was present as well. In contrast to the PRP-Ti-Bone implants an infection was observed in one of the Ti-Bone implants, as characterized by an incorporated abscess. In this scaffold, little bone formation could be seen and the bone chips were still present. This scaffold was excluded for histomorphometrical analysis (#H5L).

Group III (Ti) (control group)

In total 7 of the 18 Ti-implants were excluded for further evaluation because of staining (n=4) and sectioning difficulties, In addition, 3 titanium implants were deformed (n=3; Figure 5). A total of eleven controls remained. In eight of these Ti-implants bone bridging was present at the surface of the entire implant similar to the image of the PRP-Ti-Bone and Ti-Bone implants (Figure 4C). Again, trabecular bone with the presence of osteocytes, osteoblasts and blood vessel ingrowth was observed in these implants. Consequently, three of the control defects did not show bone bridging/ did not heal after 12 weeks.

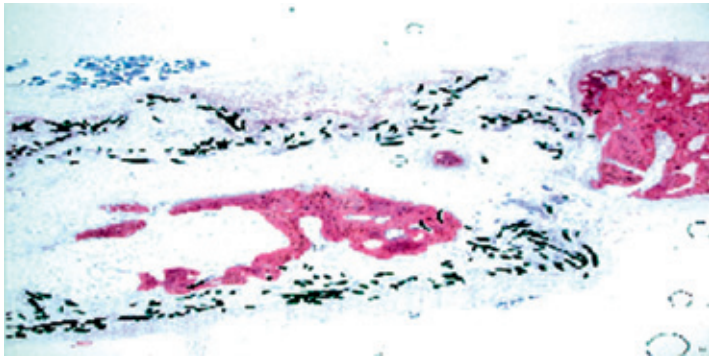

FIGURE 5:
Deformity of a titanium scaffold in the control group.

Histomorphometrical analysis

Histomorphometrical analysis of bone ingrowth was carried out on 8 (of the 9) PRP-Ti-Bone and Ti-Bone implants and 11 (of the 18) control (Ti) implants. The results of the histomorphometrical analysis of the three groups are listed in Table 2.

Statistical analysis of the measurements showed difference in bone surface area between the three different implant groups. A statistical significant difference ($p<0.05$) was seen in between the PRP-Ti-Bone group (group I) vs the Ti-Bone group (group II) (37 ± 8% vs 25 ±6%) and PRP-Ti-Bone group (group I) vs control group (Ti) (group III) (37 ± 8% vs 25 ±5%) after 12 weeks of implantation. Bone/ROI percentage was similar for the Ti-bone and Ti (control) implants.

Groups	**n**	**ROI (mm^2)**	**Bone surface area inside ROI (mm^2)**	**Bone/ ROI (%)**	**Bone formation outside the implant (mm^2)**
I (Ti+PRP+bone)	8	60 (±4)	23 (±5)	37 (±8)	9 (±2)
II (Ti+bone)	8	61 (±5)	15 (±4)	25 (±6)	13 (±2)
III (Ti empty)	11	59 (±4)	15 (±3)	25 (±5)	10 (±2)

TABLE 2: *Histomorphometrical results of ROI, bone surface area inside the ROI (mm2), bone/ROI (%), bone formation outside the implant (mm2), after 12 weeks implantation time.*

Radiographic analysis

At 12 weeks, the X-rays showed bone healing in all defects (9 out of 9) of group I and II (PRP-Ti-Bone and Ti-Bone). In contrast, three of the eleven defects in group III (Ti, control) (H12L, H13R, H18L) appeared to be still open. (Figure 6). The titanium implants also maintained in place on the X-rays and were clearly visible in the radius of the rabbit.

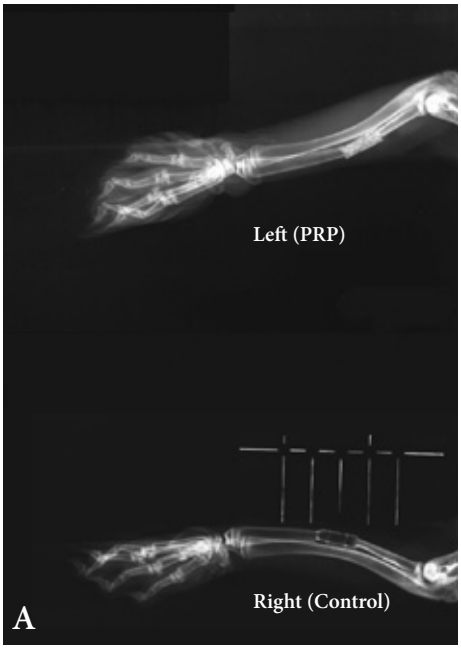

FIGURE 6A:
Radiographic analysis; group 1 (PRP-Ti-Bone) vs group 3 (Ti/control). Post surgery (day 1).

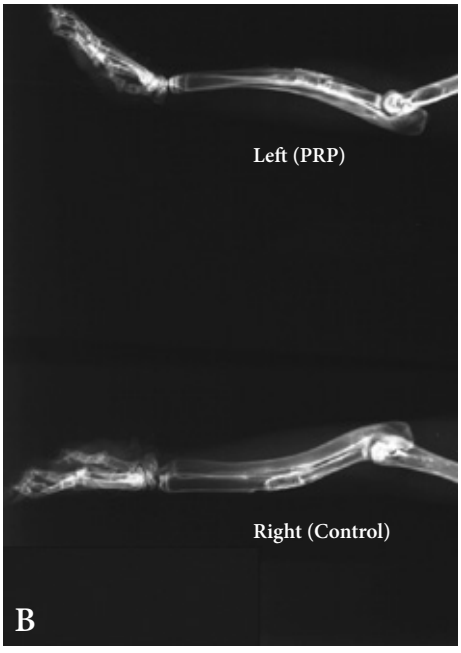

FIGURE 6B:
Radiographic analysis; group 1 (PRP-Ti-Bone) vs group 3 (Ti/control). 12 weeks after surgery.

DISCUSSION

Our histological findings corroborate with the findings in earlier studies and confirm the high compatibility of titanium mesh with bone as demonstrated by the bone ingrowth and absence of an intervening fibrous layer and inflammatory cells.[24,25] The findings also confirm our earlier observations that the titanium fiber mesh has good osteoconductive properties as demonstrated by the bone bridging en bone ingrowth in the Ti-Bone and Ti implants.

Concerning the study design, it is of clinical relevance to use a critical size defect.[4] One of the definitions of a critical size defect is the smallest defect that will not heal spontaneously within a certain time period. Another definition is that a CSD is a defect that has less than 10% healing, or will not heal, within the lifetime of the animal. Other factors like age of the animal will influence the healing of the defect. For rabbits earlier studies defined a 15 mm defect of the radius to be a CSD. Nevertheless, in our experiment in eight of the eleven Ti- implants bone bridging was observed. The bone bridging in the Ti-only implants can be attributed to the excellent osteoconductive properties of the titanium fiber mesh as shown before.[24] Further, it cannot be excluded that the model used is not a CSD. Recently, in our laboratory the healing of similar 15 mm radial defects, which were left untreated, was evaluated by micro-CT scanning. The results showed spontaneous healing of the defects at 12 weeks. However, irrespective the critical-sized nature of our defects, a clear difference in bone healing response was seen for the Ti-bone-PRP implants compared with the other specimens.

In the control group three titanium scaffolds were deformed. This indicates that the Ti-scaffold needs appropriate bone ingrowth or bone grafting in order to remain stable. The other implants were not deformed and all the animals were able to mobilize on the day of surgery without a splint.

As mentioned, a beneficial effect of the PRP on bone formation was observed. This effect of PRP on bone formation by autologous bone transplants in bone defects is in agreement with previous human and animal studies.[3,8,13,14,19,20,27] Marx et al showed a beneficial effect of PRP on bone density (74%±11% with PRP vs 55%±8% without PRP) and radiographic maturation rate (1,6-2,1 times higher) in bone grafts at 6-months in human mandibular defects.[17] Fennis et al showed that the addition of PRP improved bone healing considerably when using cortical scaffolds filled with a particulate cancellous anterior iliac crest bone graft in combination in mandibular defects in goats.[6,7] On the other hand, it has to be noticed that other studies could not confirm the positive effect of PRP preparations on bone formation in bone grafts. Raghoebar at al evaluated the effect of PRP on remodeling of autologous bone grafts for augmentation of the floor of the maxillary sinus and did not observe a beneficial effect of PRP on wound healing and bone remodeling after three months after implantation.[22] However, in this study they used a small sample size and bone from the iliac crest. Jung et al found no beneficial of autologous PRP on the healing of non-critical sized cranial defects in rabbits after four weeks of implantation.[12] In spite of mixing the PRP with autologous bone grafts, they left the PRP in the non-critical size defect.

PRP has also been applied without autologous bone grafts. For example, PRP together with a biodegradable gelatin hydrogel alone showed successful bone generation in an ulnar rabbit model.[9] Dallari et al showed a beneficial effect on bone healing and remodeling when PRP was used in combination with freeze-dried bone allografts (FDBA) with the use of bone marrow stromal cells (BMSC).[5] Still, other studies showed no beneficial effect in which PRP was combined with freeze-dried mineralized bone (FMB) and freeze-dried

demineralized bone (FDDB) in the rabbit cranium1, or frozen or processed bone allograft around non-cemented titanium implants in the femoral condyles of dogs.[11]

PRP is a proven source of growth factors. These growth factors act on the osteoblasts, osteocytes and preosteoblasts and increase the mitosis rate and stimulate the angiogenesis.[18] Due to the presence of multiple growth factors the exact contribution of each of the growth factors to the stimulation of bone formation remains unclear. The variation in the beneficial effect of PRP in different studies might be attributed to variations in composition of the various PRP formulations. In addition, the positive effect of PRP seems to be related to the survival of osteoblasts, osteocytes and preosteoblasts, which are present in the autologous bone grafts.[12] Alternatively, these cells can be added for instance by the addition of bone marrow stromal cells.[5]

In the present study we did not observe any adverse effects of the PRP. One of the advantages of the PRP is that it is autologous. However, there has been some concern about a possible carcinogenic effect of PRP related to the stimulation of cellular proliferation and its local presence in high concentrations. For PRP to be carcinogenic is very unlikely, since the growth factors are merely differentiation factors and not mutagens. These growth factors are known to act on cell membranes in order to activate internal cytoplasmic signal proteins, which promote normal gene expression.[18]

Another consideration is the use of bovine trombine and the risk of transmitting Bovine Spongiform Encephalopathy (BSE) or mad cow disease. Using recombinant human trombine can eliminate this risk.

Possible clinical applications include the treatment of segmental bone defects in long bones or the mandible, bone augmentation, e.g. sinus lifting or treatment of sternal defects, and the fixation of dental implants. More research is needed to eliminate the conflicting results with different PRP preparations.

CONCLUSION

In conclusion, we have shown that titanium fiber mesh is an excellent scaffold material for the application of autologous bone grafts in this present study. Moreover, we confirmed a beneficial effect of PRP on bone formation of autologous bone grafts in titanium fiber mesh scaffolds in radial defects in rabbits.

Acknowledgement: We like to thank dr. J.P.M. Fennis and prof. dr. P.J.W. Stoelinga for sharing their research experience concerning the PRP- subject with us. Also, we would like to thank M. Bakker, S.Lujinovic and M. Boumans of the department of C. Verhagen and C.van Buul (Sanquin Bloedbank, regio Zuid-Oost, Netherlands) for preparing the PRP. At last we like to thank E. Bronkhorst for his statistical support and Vincent Cuypers for his histomorphometrical advises.

This study has been supported by the NWO-AGIKO foundation.

REFERENCES

1) Aghaloo TL, Moy PK, Freymiller EG. Evaluation of platelet-rich plasma in combination with freeze-dried bone in the rabbit cranium. A pilot study. Clin Oral Implants Res. 2005;16(2):250-7.
2) Banks RE, Forbes MA, Kinsey SE et al. Release of the angiogenic cytokine VEGF from platelets: Significance for VEGF measurements and cancer biology. Br. J. of Cancer. 1998; 77: 956.
3) Camargo PM, Lekovic V, Weinlaender M. Vasilic N, Madzarevic N, Kenney M. Platelet-rich plasma and bovine porous bone mineral combined with guided tissue regeneration in the treatment of intrabony defects in humans. Journal of Periodontal Research. 2002; 37: 300–306.
4) Clokie CM, Moghadam H, Jackson MT, Sandor GK. Closure of critical sized defects with allogenic and alloplastic bone substitutes. J Craniofac Surg. 2002; 13(1):111-21; discussion 122-3.
5) Dallari D, Fini M, Stagni C, Torricelli P, Nicoli Aldini N, Giavaresi G, Cenni E, Baldini N, Cenacchi A, Bassi A, Giardino R, Fornasari P.M, Giunti A. In vivo study on the healing of bone defects treated with bone marrow stromal cells, platelet-rich plasma, and freeze-dried bone allografts, alone and in combination. J Orthop Res. 2006; 24(5):877-88.
6) Fennis JPM, Stoelinga PJW, Jansen JA. Mandibular reconstruction: a clinical and radiographic animal-study on the use of autogenous scaffolds and PRP. Int J Oral Maxillofac Surg. 2002;31(3): 281-6.
7) Fennis JPM, Stoelinga PJW, Jansen JA. Mandibular reconstruction: a histological and histomorphometric study on the use of autogenous scaffolds, particulate cortico-cancellous bone grafts and platelet rich plasma in goats. Int J Oral Maxillofac Surg. 2004; 33(1):48-55.
8) Hanna R, Trejo PM, Weltman RL. Treatment of intrabony defects with bovine derived xenograft alone and in combination with platelet-rich plasma: a randomized clinical trial. Journal of Periodontology. 2004; 75: 1668-77.
9) Hokugo A, Ozeki M, Kawakami O, Sugimoto K, Mushimoto K, Morita S, Tabata Y. Augmented bone regeneration activity of platelet-rich plasma by biodegradable gelatin hydrogel. Tissue Eng. 2005;11(7-8):1224-33.
10) Jansen JA, von Recum AF, van der Waerden JP, de Groot K. Soft tissue response to different types of sintered metal fibre-web materials. Biomaterials.1992;13: 959.
11) Jensen TB, Rahbek O, Overgaard S, Soballe K. No effect of platelet-rich plasma with frozen or processed bone allograft around noncemented implants. Int Orthop. 2005; 29(2):67-72.
12) Jung RE, Schmoekel HG, Zwahlen R, Kokovic V, Hammerle CHF, Weber FE. Platelet-rich plasma and fibrin as delivery systems for recombinant human bone morfogenetic protein-2. Clin.Oral Impl. Res. 2005 ;16: 676-682.
13) Kassolis JD, Rosen PS, Reynolds MA. Alveolar ridge and sinus augmentation utilizing platelet-rich plasma in combination with freeze-dried bone allograft: case series. Journal of Periodontolology. 2000; 71: 1654-61.
14) Lekovic V, Camargo PM, Weinlaender M, Vasilic N, Aleksic Z, Kenney EB. Effectiveness of a combination of platelet-rich plasma, bovine porous bone mineral and guide tissue regeneration in the treatment of mandibular grade II molar furcations in humans. Journal of Clinical Periodontology . 2003; 30: 746-751.
15) Li RH, Wozney JM. Delivering on the promise of bone morfogenetic proteins. Trends Biotechnol. 2001; 19: 255-265.

16) van der Lubbe HB, Klein CP, de Groot K. A simple method for preparing thin (10 microM) histological sections of undecalcified plastic embedded bone with implants. Stain Technol 1988: 63: 171-6.
17) Marx RE, Carlson ER, Eichstadt RM, Schimmele SR, Strauss JE, Georgeft RN. Platelet Rich Plasma. Growth factor enhancement for bone grafts. Oral Surg. 1998: 85: 635-46.
18) Marx RE. Platelet-Rich Plasma (PRP): What Is PRP and What is not PRP? Implant Dentistry, volume 2001: 10; 4: 225-228.
19) Nikolidakis D, van den Dolder J, Wolke JG, Stoelinga PJ, Jansen JA. The effect of platelet-rich plasma on the bone healing around calcium phosphate-coated and noncoated oral implants in trabecular bone. Tissue Engineering. 2006; 12: 2555-63.
20) Okuda K, Tai H, Tanabe K, Suzuki H, Sato T, Kawase T, Saito Y, Wolff LF, Yoshiex H. Platelet-rich plasma combined with a porous hydroxyapatite graft for the treatment of intrabony periodontal defects in humans: a comparative controlled clinical study. Journal of Periodontology. 2005; 76: 890-8.
21) Pierce GF, Tarpley J, Yanagihara D, Deuel TF. PDGF-BB, TGK-b1 and basic FGF in dermal wound healing: Neovessel and matrix formation and cessation of repair. Am. J. Pathol. 1992: 140: 1375-88.
22) Raghoebar GM, Liem RS, Bos RR, van der Wal JE, Vissink A. Does platelet-rich plasma promote remodeling of autologous bone grafts used for augmentation of the maxillary sinus floor? Clin Oral Implants Res. 2005; 16(3):349-56.
23) Urist MR. The search for and discovery of bone morphogenic protein (BMP). Bone Grafts, Derivates and Substitute, Butterworth Heinemann, London, 1994.
24) Vehof JW, Haus MT, de Ruijter AE, Spauwen PHM, Jansen JA. Bone formation in transforming growth factor beta-I-loaded titanium fiber mesh implants. Clin. Oral Implants Res. 2002 ; 13(1) : 94-102.
25) Vehof JW, Mahmood J, Takita MA, van 't Hof MA, Kuboki Y, Spauwen PHM, Jansen JA. Ectopic bone formation in titanium mesh loaded with bone morphogenetic protein and coated with calcium phosphate. Plast. Reconstr. Surg 2001 ; 108 : 434.
26) Weibrich G, Kleis WKG, Hafner G. Growth factor levels in the platelet-rich plasma produced by two different methods: Curasan-type PRP kit versud PCCS PRP system. Int. J. Oral Maxillofac. Implants. 2002 ; 17: 184-190.
27) Whitman DH, Berry RL, Green DM. Platelet gel: an autologous alternative to fibrin glue with applications in oral and maxillofacial surgery. Journal of Oral Maxillofacial Surgery. 1997; 55:1: 294-9.

8

GENERAL CONCLUSIONS

SUMMARY AND CONCLUSIONS
SAMENVATTING EN CONCLUSIES

DANKWOORD
CURRICULUM VITAE
LIST OF PUBLICATIONS

GENERAL CONCLUSIONS

SUMMARY AND CONCLUSIONS

Closing capacity of bone defects: scaffolds, porosity and growth factors updated.

In this thesis we described the high need for bone graft substitutes. The main objective of this research was to investigate the feasibility of porous Calcium Phosphate cement (p Ca-P) and titanium (Ti) as a carrier material for growth factors, e.g. Bone Morphogenetic Protein 2 (BMP-2), in the creation of bone graft substitutes (BGS) in cranial or radial defects (critical and non critical sized) or at ectopical site, as created in New Zealand white rabbits. Besides the porosity, we hypothesized that the osteoconductive properties of these carrier materials could be further enhanced by Platelet Rich Plasma (PRP) substitution or surface treatment with the adhesion peptide Arg-Gly-Asp (RGD-peptide).

1 In the first chapter, a general introduction to the current knowledge on bone formation as well as the use of bone engineering methods is presented. Successful and productive teamwork of the osteoconductive scaffold, the bone cells and the osteoinductive growth factors is required for bone formation. Depending on the location and the bone defect size, different scaffolds can be created with or without porosity, to enhance bone formation. A review of the literature is presented.

2 In chapter two, porous Calcium Phosphate (Ca-P) cement is evaluated. Calcium Phosphate (Ca-P) is a well established material for bone repair. It is injectable, can be moulded into the required shape and is bone biocompatible. The bone biological properties of Ca-P cement can even be further improved by creating porosity in the material. The current study was aimed on the evaluation of the osteoconductive behavior of porous Ca-P cement in a critical sized bone defect. Therefore, circular defects with increasing sizes (6, 9, and 15 mm in diameter) were created in the cranium of three months old rabbits and filled with porous Ca-P cement implants. The total porosity of the 6, 9 and 15 mm implants was calculated to be 71%, 74% and 74% respectively and the average pore diameter was 150 μm. In addition, empty control defects were prepared. After 12 weeks implantation time the animals were sacrificed and radiographic, histological and histomorphometrical evaluation was performed. The Critical Size Defect (CSD) of this species at this location for an implantation time of 12 weeks was confirmed to be 15 mm. Bone was observed to be present over and through almost all porous Ca-P cement implants. Only, in one out of eight animals with a 15 mm implant, complete bone bridging of the defect did not occur. The size of the defect was found not to affect the total percentage of bone formation in the cement; (17 ± 7)%, (18 ± 6)% and (17 ± 3)% for respectively 6, 9, and 15 mm diameter implants. In this chapter, it is concluded that porous Ca-P cement is an excellent osteoconductive material in non weight bearing situations and complete bridging of a critical sized skull defect occurs in this rabbit model after 12 weeks of implantation.

3 In chapter three, porous Ca-P cement implant was used as an osteoconductive scaffold in segmental defects. The study was performed to evaluate the osteoconductive behavior of porous Ca-P cement in a supposed Critical Sized Defect (CSD) in a weight-bearing rabbit radius model. Furthermore, evaluation of the torque test measurement was carried out. In this study, increasing defect sizes of a segmental radius (5, 10 and 15 mm), were created bilaterally and filled with either porous Ca-P cement or left open as a control. After 12 weeks of implantation, torque test measurements as well as histological and radiographic

evaluation were performed. In two of the open 15 mm control defects, bone bridging was visible at the radiographic and histological evaluation. Bone was observed to be present in all porous Ca-P cement implants (5, 10 and 15 mm defects) after 12 weeks. No significant differences in torque measurements were observed between the 5 and 10 mm filled and open control defects using the T-test. In addition the mechanical strength of all operated specimens was similar compared to non-operated bone samples. The torsion data for the 15 mm open defect appeared to be lower compared to the filled 15 mm defect as well as the non-operated specimens. However, a significant difference could only be proven for the non-operated samples. Within the limitation of the study design, porous Ca-P cement implants demonstrated osteoconductive properties and confirmed to be a suitable scaffold material in a weight bearing situation. Also, this study confirmed again that a 15 mm radius defect is not a CSD in female New Zealand white rabbits of six month of age.

4 In chapter four, the osteoinductive properties of porous calcium phosphate (Ca-P) cement loaded with Bone Morphogenetic Protein 2 (rhBMP-2) were evaluated and compared with rhBMP-2 loaded Absorbable Collagen Sponge (ACS) in a rabbit cranial model after 2 and 10 weeks of implantation. Recombinant human Bone Morphogenetic Protein- 2 (rhBMP-2) is known for its osteoinductive potential in bone tissue engineering. Discs with a diameter of 8 mm were loaded with a buffer solution with or without 10 µg rhBMP-2 and inserted in 8 mm full thickness cranial defects in rabbits for two and ten weeks of implantation. Histological analysis revealed excellent osteoconductive properties of the porous Ca-P material. It maintained its shape and stability during the implantation time better than the ACS but showed no degradation like the ACS. Quantification of the porous Ca-P cement implants showed that bone formation was increased significantly by administration of rhBMP-2 (ten weeks pore fill: 53.0 ±5.4%), but also reached a reasonable amount without rhBMP-2 (43.1 ±10.4%). In this chapter the conclusion is that: 1. Porous Ca-P cement is an appropriate candidate scaffold material for bone engineering, 2. Bone formation can be enhanced by lyophilization of rhBMP-2 on the cement, 3. Degradation of porous Ca-P cement is species-, implantation site- and implant dimension-specific.

5 In chapter five, the osteoinductive capability of rhBMP-2 loaded porous Ca-P cement at ectopical site was evaluated. Porous Ca-P cement discs were made and loaded with rhBMP-2 in vitro and implanted subcutaneously in the back of New Zealand White rabbits. The implantation period was either two or ten weeks. Histological analysis of retrieved specimens revealed evident bone formation in the rhBMP-2 loaded Ca-P cement discs (pore fill: 18±6%) after ten weeks of implantation. Bone formation occurred only in rhBMP-2 loaded porous Ca-P cement discs. Degradation of the Ca-P cement could not be confirmed after ten weeks of implantation. The scaffold maintained its shape and stability during this time period. We conclude that porous Ca-P cement is a suitable carrier material for ectopic bone engineering.

6 In chapter six, investigation of bone formation in a porous titanium (Ti) fiber mesh implant, which was coated with RGD-peptide, was performed. In vitro research showed that the peptide sequence Arg-Gly-Asp (RGD-peptide) plays an important role in osteoblast adhesion. Integrins, which bind specifically short peptide sequences, are responsible for these cell responses. In this way, information can be transmitted to the nucleus through several cytoplasmic signaling pathways. On the contrary, little is known about the ability of peptide-coated surfaces to influence cell responses in vivo. The RGD-Ti implants were inserted in the cranium of the rabbit and were compared with porous titanium fiber mesh disks without RGD-sequence (Ti) and with an open control defect. Histological and histomorphometrical examinations were performed two, four and eight weeks

postoperatively. A significant increase in bone formation or bone ingrowth was seen in the RGD-Ti group compared to the Ti group after four and eight weeks. All control defects stayed open in all three periods. It was concluded that the use of cyclic RGD-peptide in combination with titanium fiber mesh has a positive contribution on bone formation in vivo in a rabbit animal model.

In the last chapter we evaluated the effect of Platelet Rich Plasma (PRP) on bone formation in a rabbit segmental weight bearing radial defect model. The positive effect of PRP can be mainly attributed to the effect of Transforming Growth Factor (TGF-) and Platelet Derived Growth Factor (PDGF) on cell proliferation, differentiation and angiogenesis. Purpose of the study was to evaluate the bone inductive properties of PRP with titanium fiber mesh and autologous bone chips in a 15 mm rabbit radial defect model. 18 New Zealand white rabbits were divided in three groups: I: PRP with autologous bone (PRP-Ti-Bone), II: autologous bone (Ti-Bone), III: control group (Ti). The implants were placed in the radial defect for 12 weeks. After sacrifice, all specimens were harvested for histological, histomorphometrical and radiographic analysis. Histomorphometrical analysis showed that bone formation was higher in the implants with PRP (PRP-Ti-Bone: 37 ± 8%) than in the implants without PRP (Ti-bone: 25 ± 6% and Ti: 25 ± 5%) after 12 weeks of implantation. On the basis of our observations we conclude that PRP has a stimulatory effect on bone formation in titanium fiber mesh filled with autologous bone graft in segmental bone defects. Furthermore, we have shown titanium fiber mesh to be an excellent scaffold material for the application of autologous bone grafts with or without PRP.

Closing remarks and future perspectives

Several scaffolds can be used to analyze the influence of the growth factors used in an animal study. In this thesis we were focused on porous Ca-P and titanium fiber mesh as a carrier material and installed in rabbits. The results showed that in this rabbit model both are suitable carrier materials. This was proven in weight bearing (radius), in non-weight bearing (cranium) as at ectopical (subcutaneous) location. On the other hand, these porous scaffolds materials can be improved, resulting in an enhanced stability. For example, the functionality of porous Ca-P can be advanced by making use of nanotechnology and biomimetic approaches. Also, with the use of mesenchymal cell seeding and coating technique, earlier research proved that the amount of bone formation can be improved as well. The combination of the different growth factors showed positive results in bone generation. Bone Morphogenetic Protein (BMP-2) substitution showed significantly more bone formation at orthotopical and ectopical sites. Furthermore, we found an increase in bone formation in the experiment with the RGD-peptide sequence and the Platelet Rich Plasma (PRP). More knowledge about the release of these growth factors and the specific interaction between the different growth factors will give us important information. In this way, the amount of for example substituted BMP-2 can be precisely titrated, and an overkill of growth factors can be prevented. Besides the positive result of PRP on bone formation, the thrombocytes have a positive contribution at other locations as well, for instance on wound healing in general. It is important to find out which growth factors are responsible for these promising results. Also the role of synergism between the different growth factors should be investigated.

In this thesis we tried to make further steps in bone engineering using a rabbit animal model. Of course the efficacy of bone engineering with these two scaffold materials (porous Ca-P and titanium fiber mesh) in combination with growth factors has to be proven in higher animals and humans as well. The final aim will be the creation of a (prefabricated) vascularised bone transplant which can be used for large (oncological or traumatological) reconstructions.

Genezingscapaciteit van botdefecten: implantaten, porositeit en groeifactoren.

In dit wetenschappelijk onderzoek beschrijven we mogelijkheden om bot te vervangen omdat hieraan grote behoefte bestaat bij reconstructie van botdefecten. Aangezien autologe bottransplantaties beperkingen en nadelen kunnen hebben, bestaat er een grote belangstelling voor botvervangende middelen. In het onderzoek is poreus calcium fosfaat (p Ca-P) en titanium (Ti) als dragermateriaal gebruikt dat al dan niet gecombineerd werd met groeifactoren zoals Bone Morphogenetic Protein-2 (BMP-2). Er werd dierexperimenteel onderzoek bij konijnen uitgevoerd, waarbij de materialen in craniale defecten (onbelaste situatie), segmentale defecten (belaste situatie) en ook op ectopische locatie (subcutaan) geplaatst werden. Behalve naar de porositeit van het dragermateriaal, werd ook onderzoek gedaan naar effecten van de behandeling van deze materialen met het hechtingseiwit Arg-Gly-Asp (RGD-peptide) en trombocyten-aggregaat (Platelet Rich Plasma: PRP).

1 In het eerste hoofdstuk werd als inleiding een overzicht gegeven van de diverse mogelijkheden op het gebied van het vervangen van bot door middel van 'bone engineering'. Er is daarbij een succesvolle en productieve samenwerking nodig tussen dragermateriaal (het implantaat/de matrix), botcellen en groeifactoren. Afhankelijk van het defect en de locatie, kunnen verschillende dragers, al of niet poreus, gecombineerd worden met groeifactoren. In dit overzicht werd gerefereerd aan de bestaande literatuur. In de hoofdstukken hierna werden de studies beschreven die naar aanleiding van dit onderwerp werden uitgevoerd.

2 In het tweede hoofdstuk werden de osteoconductieve eigenschappen van poreus Ca-P onderzocht. De injecteerbaarheid, vervormbaarheid en de biocompatibiliteit zijn de belangrijkste voordelen van dit materiaal. Door het materiaal poreus te maken, kunnen de biologische eigenschappen van het materiaal verder verbeterd worden. In deze studie werden er in diameter oplopende defecten in het schedeldak (6, 9 en 15 mm diameter) van konijnen gemaakt. Deze werden gevuld met poreus Ca-P met een gemiddelde porositeit van 73%. Ter controle werden ook defecten gecreëerd welke open gelaten werden. Twaalf weken na implantatie werden de Ca-P implantaten met omringend botweefsel uitgenomen en werd er radiologisch, histologisch en histomorfometrisch onderzoek gedaan. De kritische defect grootte (CSD), een defect dat spontaan niet dichtgroeit, bleek bij dit diermodel 15 mm te zijn na een implantatietijd van 12 weken. Botvorming in en over het Ca-P implantaat werd in vrijwel alle situaties gezien. Alleen bij één van implantaten uit de 15 mm groep trad volledige sluiting van het defect op. De grootte van het defect beïnvloedde in het geheel niet de mate van botvorming in het Ca-P cement (17 ± 7)%, (18 ± 6)% and (17 ± 3)% voor respectievelijk 6, 9, and 15 mm diameter implantaten. De conclusie van dit hoofdstuk was dat poreus Ca-P een uitstekend osteoconductief materiaal is in een onbelaste situatie en dat het gebruik van dit materiaal tot volledige sluiting leidt van een CSD 12 weken na implantatie.

3 In het derde hoofdstuk werd gekeken naar de osteoconductieve eigenschappen van poreus Ca-P in een belast radiusmodel bij het konijn. Deze studie werd gedaan om de osteoconductieve eigenschappen van poreus Ca-P cement in een te verwachten 'Critical Size Defect '(CSD) te evalueren. Er werden bilaterale, in grootte oplopende segmentale radius defecten (5, 10 en 15 mm) aangebracht, welke aan één kant gevuld werden met poreuze Ca-P implantaten. Als controle werden de contralaterale kanten open gelaten. Na 12 weken implantatie werd een evaluatie van de torquetest gedaan, gecombineerd met radiologische en histologische analyse. Na 12 weken werd er in twee van de open controle

15 mm defecten sluiting van het defect door ingroei van bot waargenomen (zowel radiologisch en histologisch). Botvorming werd aangetoond in alle poreuze Ca-P cement implantaten (5, 10 en15 mm defecten). Een T-test liet zien dat er geen significante verschillen bestonden tussen de poreuze Ca-P groep en de controle groep (5 mm: p=0.13, 10 mm: p=0.71, 15 mm: p=0.11). De mechanische kracht op de radii van alle geopereerde dieren was gelijkwaardig aan de niet-geopereerde botten. De torquetest resultaten van de 15 mm open defecten waren lager dan de 15 mm defecten met poreus Ca-P implantaten en de niet geopereerde radii. Echter, er werd alleen een significant verschil aangetoond met de niet geopereerde radii. Ondanks de beperkingen van deze studie werd bewezen dat poreus Ca-P goede osteoconductieve eigenschappen heeft in een belast radiusmodel. Ook werd er geconstateerd dat 15 mm defecten, in de radius van een vrouwelijke 'New Zealand white rabbit' van 6 maanden oud, geen CSD zijn.

4 In het vierde hoofdstuk werd gekeken naar de botgroei bevorderende eigenschappen van poreus Ca-P cement dat geladen was met een botgroei bevorderende factor, te weten recombinant humaan Bone Morphogenetic Protein 2. Er werden daartoe defecten gecreëerd in het schedeldak van konijnen. Het van rhBMP-2 voorziene Ca-P implantaat werd in dit defect aangebracht. Dit werd vergeleken met defecten die gevuld waren met een collageen spons (ACS) welke ook voorzien was van rhBMP-2. Als controle werden er ook poreuze Ca-P implantaten zonder rhBMP-2 aangebracht. Na een implantatietijd van 2 en 10 weken, werd histologisch onderzoek gedaan. Conclusie van deze studie was dat poreus Ca-P een goed dragermateriaal voor rhBMP-2 is. Tevens werd er een significante toename van de botvorming gezien in de rhBMP-2 groep. Tot slot werd aangetoond dat de degradatie van poreus Ca-P afhankelijk is van het gebruikte proefdier, de implantaat locatie en de implantaat grootte.

5 In het vijfde hoofdstuk werd gekeken naar de osteoinductieve capaciteit van poreus Ca-P voorzien van rhBMP-2 (zoals in hoofdstuk 4 beschreven). De implantaten werden subcutaan in de rug van konijnen geplaatst gedurende 2 en 10 weken. De Ca-P implantaten werden vergeleken met collageen spons (ACS) welke ook voorzien was van rhBMP-2. Ter controle werden ook poreuze Ca-P implantaten zonder rhBMP-2 geïmplanteerd. Lichtmicroscopisch onderzoek liet zien dat na 10 weken bot aanwezig was in de poreuze Ca-P implantaten welke voorzien waren van rhBMP-2. Degradatie van het cement kon niet worden aangetoond. Het implantaat behield zijn vorm en stabiliteit gedurende deze periode. Opnieuw werd geconcludeerd dat poreus Ca-P cement een goed materiaal is voor 'bone engineering' en dit keer ook op een ectopische locatie waar dus normaliter geen bot aanwezig is. Op deze wijze kunnen in de toekomst geprefabriceerde lappen in combinatie met botvervangende middelen worden ontwikkeld voor botreconstructieve doeleinden.

6 In het zesde hoofdstuk werd onderzoek gedaan naar het hechtingseiwit Arg-Gly-Asp (RGD-peptide). Eerder in vitro onderzoek toonde namelijk aan dat deze aminozuursequentie een belangrijke rol speelt in de hechting van botcellen. In deze studie werd poreus titanium(Ti) vezelgaas voorzien van RGD peptide. Deze implantaten werden in schedeldakdefecten (8 mm) bij konijnen geplaatst en vergeleken met titanium vezelgaas zonder RGD-peptide en een open controle defect. Er werd histologisch en histomorfometrisch onderzoek gedaan na 2, 4 en 8 weken. De resultaten toonden een significante toename in botvorming aan in de RGD-Ti groep vergeleken met de ongeladen Ti groep na 4 en 8 weken implantatie. Alle open controle defecten bleven in deze drie termijnen open. Concluderend levert RGD-peptide een positieve bijdrage aan de botvorming, wanneer dit is aangebracht op titanium vezelgaas bij een implantatieduur van 4 en 8 weken in het schedeldak van het konijn.

In het laatste hoofdstuk werd het effect van Platelet Rich Plasma (PRP) op botingroei in een 15 mm segmentaal radiusdefect bij konijnen onderzocht. PRP is een trombocyten-aggregaat dat uit autoloog bloed verkregen wordt. Het is bekend dat hierin veel verschillende groeifactoren zitten die een positief effect op de botgenezing kunnen hebben. De PRP werd geoogst uit het bloed van het te opereren konijn en werd gemengd met autoloog bottransplantaat, waarna dit mengsel werd aangebracht in kokertjes die van titanium vezelgaas vervaardigd waren. Naast deze Ti-PRP-bot groep werden er ook titanium kokers met alleen autoloog bottransplantaat zonder PRP (Ti-bot) en lege Ti kokertjes (Ti) in de defecten geplaatst. Alle drie de groepen werden na 12 weken geanalyseerd middels histologisch, histomorfometrisch en radiologisch onderzoek. Na 12 weken werd er significant meer bot gezien in de Ti-PRP-bot groep (37 ± 8%) in vergelijking met de implantaten zonder PRP (Ti-bot: 25 ± 6% en Ti: 25 ± 5%). Verder bleek titanium vezelgaas een goed dragermateriaal te zijn voor dit belaste radius model in het konijn.

Afsluitende opmerkingen en toekomstperspectieven:

Verschillende dragermaterialen kunnen worden gebruikt om de invloed van groeifactoren op botvorming te analyseren. In dit onderzoek hebben wij ons gericht op de implantaten poreus Ca-P en poreus titanium vezelgaas. De resultaten laten zien dat in een konijnendiermodel beide materialen aan het doel voldoen zowel op belaste locatie (radius), onbelaste locatie (schedeldak), als op ectopische locatie (subcutaan). Verbetering voor met name het poreuze Ca-P zou bereikt kunnen worden door het verstevigen van dit materiaal. Ondanks het feit dat deze fragiele implantaten zich zelfs op gewichtsdragende locaties konden handhaven, is de verwachting dat met behulp van nanotechnologie en een biomimetische benadering de functionaliteit van het dragermateriaal nog verder verbeterd kan worden. Ook is het mogelijk de implantaten in vivo met cellen te laden waardoor er, zoals eerder beschreven, meer botvorming verkregen wordt.

De combinatie met verschillende groeifactoren liet positieve resultaten zien wat betreft de botaanmaak bij de BMP-2 substitutie op zowel orthotopische (schedeldak) als ectopische (subcutaan) locatie. Eveneens zagen we een significante toename van bot bij de experimenten met gebruik van RGD-peptide en trombocyten-aggregaat (PRP).

Verdere analyse van de 'release' van deze groeifactoren en de specifieke werking van de verschillende groeifactoren zou veel extra informatie kunnen geven. Op deze wijze zou de hoeveelheid van toegediende BMP-2 beter gedoceerd kunnen worden. Met name de exacte werking en concentraties van de multipele groeifactoren die aanwezig zijn in PRP, is iets wat verder uitgezocht zal kunnen worden. Op deze manier zou dit na verder onderzoek kunnen leiden tot meer precieze dosering, waardoor overdosering vermeden kan worden. Dat PRP behoudens bij de botgenezing in vivo op velerlei andere locaties (zoals bij wondgenezingsstoornissen) positieve resultaten geeft, laat zien dat dit trombocyten-aggregaat veel potentie heeft. Ook de samenwerking tussen verschillende groeifactoren (synergisme) dient nader geanalyseerd te worden.

In dit onderzoek hebben we ons gericht op het konijn als diermodel. De effectiviteit van botgenezing met behulp van poreus Ca-P en titanium vezelgaas in combinatie met groeifactoren zal onderzocht moeten worden bij hogere diersoorten en mensen. Het uiteindelijke doel zal zijn om een gevasculariseerd bottransplantaat te vervaardigen (al dan niet met het gebruik van prefabricatie) wat bij grote, vaak oncologische of posttraumatische, reconstructies toegepast kan worden.

DANKWOORD

Tijdens de lange periode van onderzoek gecombineerd met de opleiding, tot slot het dankwoord. Allereerst wil ik alle mensen bedanken die mij positief gestimuleerd en geholpen hebben. Anders was het onmogelijk geweest om gezin, onderzoek, examens en opleiding in deze periode te combineren! De volgende mensen in het bijzonder:

Prof. dr. P.H.M. Spauwen, beste Paul. Dank voor alles. Dank je voor de begeleiding tijdens mijn onderzoek en tijdens de opleiding. Je kan de meest ingewikkelde operaties op een simpele logische manier uitvoeren en overbrengen en stelt de patiënt en opleiding altijd centraal. Een groot voorbeeld. Dank voor het vertrouwen en de mogelijkheid dit mee te kunnen maken en het zetje in de goede richting wanneer het even niet liep.

Prof. dr. J.A. Jansen, beste John. Veel dank voor de heldere en eerlijke begeleiding tijdens mijn onderzoeksfase en hierna. Ondanks de drukte kon je altijd een moment vinden voor overleg. Je hebt me geleerd prioriteiten te stellen en ik bewonder het enorm hoe je je afdeling internationaal op de kaart hebt gezet.

Prof. dr. J.H.G. Klinkenbijl, beste Jean, dank je voor de vijf leuke jaren in het Rijnstate. De chirurgische basis werd bij jullie gelegd en ik profiteer nog dagelijks van alles wat ik in die tijd geleerd heb.

Dr. Ruhé, beste Quinten, dank voor je betrokkenheid bij onze gezamenlijke studies en je altijd goede ideeën en eerlijke, scherpe mening. Ik verwacht nog heel veel van je! Ik heb de samenwerking als zeer prettig ervaren. De operatiedagen op het dierenlab onder het genot van je muziek en verhalen vlogen voorbij.

Dr. Wolke, beste Joop, dank voor je hulp tijdens mijn onderzoek, met name bij de torque test studie en het maken van alle implantaten. Je aanstekelijke gevoel voor humor en de pesterijtjes maakten het een fijne tijd op de afdeling biomaterialen.

Dr. van den Dolder, beste Juliette, dank voor je geduldige uitleg, gezelligheid en hulp bij in vitro experimenten en de RGD studie.

Dr. Vehof, beste Johan, dank voor je co-auteurschap bij de PRP studie en je goede adviezen. Jij was de eerste die de samenwerking tussen de afdeling plastische chirurgie en biomaterialen begon en je hebt veel voorwerk voor ons verricht.

Ook wil ik prof. dr. P.J.W. Stoelinga, dr. Jeroen Fennis en Marianne Bakker danken voor de voor de hulp bij het opstarten van de PRP studie.

Anja, je was de spil van het biomaterialen gebeuren. Bij jou kon iedereen tijdens een kopje thee in de pauze stoom afblazen en je regelde alles. Ik heb daar goede herinneringen aan!

Alle andere collega's van de afdeling biomaterialen: Diederik, Edwin, Frank, Jack, Jacky, Marijke, Olga, Chad, Lenie, Petra, Wouter, Bas, Edwin, Elizabeth, Esther (dank voor al je tips!), Jeroen, Sander, Vincent en natuurlijk Corinne. Het was erg plezierig. Corinne, succes met de laatste loodjes!

De biotechnici van het dierenlaboratorium: Jeroen, Fred, Ton en Alex, veel dank ook voor de samenwerking, gratis ECHO en de flexibiliteit, het liep altijd volgens plan en schema.

Alle (voormalig) stafleden en (voormalig) assistenten van de plastische chirurgie waaronder Rita, Pieter, Ed, David, Stijn, Hans, José, Jan, Flip, Hans-Peter, Maarten, Herm, Ghita, Esther, Xander, Michiel, Erwin, Bas, Alex, Bram, Diederik, Ewa en Mirjam wil ik ook noemen. Tijdens mijn onderzoek waren de operaties op woensdag ochtend en de patiëntenbespreking een prima afwisseling. In het bijzonder wil ik Erwin nog bedanken voor zijn collegialiteit en relativerende blik gedurende de laatste vier jaren. Ik hoop dat wij de samenwerking tussen het CWZ en het UMCN op een leuke manier kunnen uitbouwen. Alle secretaresses en polidames van de afdeling Plastische Chirurgie, fantastisch was jullie hulp en betrokkenheid!

Naheeda Portocarero, geweldig dat je me wilde helpen met de correcties. Dat heb ik zeer gewaardeerd.

Afdeling Groningen: Lief oud huis- en clubgenoten. Jullie zijn altijd betrokken en geïnteresseerd. Ik ben trots: Niet alleen omdat onze vriendschap er nog steeds is maar ook op het feit dat iedereen heeft afgemaakt waar hij aan begonnen is!
Jet, Gabriëlle en Em, zonder jullie had ik mijn studie nooit afgemaakt en was dit boekje er dus niet geweest; de anatomie overhoringen en de positieve motivatie in het Soephuis en daarbuiten waren destijds hard nodig!

Afdeling Nijmegen: Lien, Eus, Oele, Marie-Jeanne, Monique en Hanneke. Dank voor de alweer ± 30-jarige vriendschap en steun! Ik verheug me op al het leuks dat nog gaat komen. Het leven schijnt over twee weken pas echt te beginnen!

Onze oppassen Riet, Greetje en natuurlijk mam, zonder jullie kon dit niet! Het is het aller belangrijkste te weten dat je kinderen in goede handen zijn!

Natuurlijk wil ik mijn familie bedanken:

Lieve Carien, jij ook veel dank voor je betrokkenheid en zusterlijk advies, ik waardeer je enorm. Lieve broertjes, Aug en San, leuk dat jullie je pak weer voor me uit de kast willen trekken. Ik ben trots.
Lieve pap en mam, dank voor jullie onvoorwaardelijke steun. Jullie hebben ons een stabiele basis meegegeven en ons gestimuleerd er iets leuks van te maken in het leven.
Hidde en Imke, zelfs op jullie leeftijd waren jullie zó begaan! Hidde dank voor het vouwen van alle brieven! Im, dank voor je knutsel cadeau dat je me gaf toen ik bevestigend antwoord gaf op je vraag: ”Mam, is dat boekje nu eindelijk af?”.

Tot slot lieve Lars, jij hebt het niet altijd even makkelijk gehad met zo’n drukke, eigenwijze vrouw in het medische wereldje dat je niet kende. Ik ben je heel dankbaar voor je steun, advies en geduld! Of het ooit echt rustig wordt kan ik niet garanderen!

CURRICULUM VITAE

Henriette Kroese-Deutman werd op 2 juni 1969 geboren te Rotterdam. De middelbare schoolperiode in Nijmegen werd afgerond met een HAVO- en een VWO-diploma. In 1989 werd ze nageplaatst voor de studie Geneeskunde aan de Rijksuniversiteit Groningen. Na een wetenschappelijke stage aan de University of Washington te Seattle, USA, onder begeleiding van dr. Marie-Jeanne Baas-Vrancken Peeters, werd in 1995 het doctoraalexamen behaald.

De co-schappen volgden in het Medisch Spectrum Twente in Enschede, welke werden afgesloten met een afsluitend co-schap op de afdeling Plastische en Reconstructieve Chirurgie aldaar. Na het behalen van het artsexamen in 1998 werkte ze als arts op de afdeling Plastische en Reconstructieve Chirurgie in het Universitair Medisch Centrum St. Radboud te Nijmegen (hoofd prof. dr. P.H.M. Spauwen) en op de afdeling Heelkunde in het Rijnstate Ziekenhuis te Arnhem (hoofd prof. dr. J.H.G. Klinkenbijl).

In 2000 werd gestart met de toegekende AGIKO-constructie (assistent geneeskundige in opleiding tot klinisch onderzoeker). De vooropleiding Heelkunde werd in het Rijnstate ziekenhuis in Arnhem gevolgd, die tussen 2001 en 2003 onderbroken werd met het promotieonderzoek op de afdeling Parodontologie en Biomaterialen (hoofd prof. dr. J.A. Jansen) in samenwerking met de afdeling Plastische en Reconstructieve Chirurgie in het Universitair Medisch Centrum St. Radboud te Nijmegen (hoofd prof. dr. P.H.M. Spauwen). Van juni 2005 tot juni 2008 werd de specialisatie tot plastisch chirurg afgerond in het Universitair Medisch Centrum St Radboud. Hier werkt ze sindsdien als staflid.

Henriette is in 2000 getrouwd met Lars Kroese en samen hebben ze twee kinderen, Hidde (2001) en Imke (2003).

LIST OF PUBLICATIONS

1) Bone inductive properties of porous calcium phosphate cement implants loaded with rhBMP-2 and inserted in rabbits.
P.Q. Ruhé, H.C. Kroese-Deutman, P.H.M. Spauwen and J.A. Jansen.
Biomaterials. 2004 May;25(11):2123-32.

2) Bone inductive properties of Rh-BMP-2 porous calcium-phosphate cement implants and inserted at ectopical site in rabbits.
H.C. Kroese-Deutman, P.Q. Ruhé, P.H.M. Spauwen and J.A. Jansen.
Biomaterials. 2005 Apr;26(10):1131-8.

3) The influence of RGD-loaded titanium implants on bone formation in vivo.
H.C. Kroese-Deutman, J. van den Dolder, P.H.M. Spauwen and J.A. Jansen.
Tissue Eng. 2005 Nov-Dec;11(11-12):1867-75.

4) In vivo degradation of porous poly (propylenefumarate)/ poly (DL-lactic-co-glycolic acid) composite scaffolds.
E.L. Hedberg, H.C. Kroese-Deutman, C.K. Shih, R.S. Crowther, D.H. Carney, A.G. Mikos and J.A. Jansen.
Biomaterials. 2005 Aug;26(22):4616-23.

5) Effect of varied release kinetics of the osteogenic thrombin peptide TP508 from biodegradable, polymeric scaffolds on bone formation in vivo.
E.L. Hedberg, H.C. Kroese-Deutman, C.K. Shih, R.S. Crowther, D.H. Carney, A.G. Mikos and J.A. Jansen.
J Biomed Mater Res A. 2005 Mar 15;72A(4):343-53.

6) Methods: a comparative analysis of radiography, microcomputed tomography, and histology for bone tissue engineering.
E. L. Hedberg, H.C. Kroese-Deutman, C.K. Shih, J.J. Lemoine, M.A. Liebschner, M.J. Miller, A.W. Yasko, R.S. Crowther, D.H. Carney, A.G. Mikos, and J.A. Jansen.
Tissue Eng. 2005 Sep-Oct;11(9-10):1356-67.

7) Growth factor-loaded scaffolds for bone engineering.
J.A. Jansen, J.W. Vehof, P.Q. Ruhé, H.C. Kroese-Deutman, Y. Kuboki, H.Takita, E.L.Hedberg, A.G. Mikos.
J Control Release. 2005 Jan 3;101(1-3):127-36.

8) Closing capacity of cranial bone defects using porous Ca-P cement implants in a rabbit animal model.
H.C. Kroese-Deutman, J.G.C.Wolke, P.H.M. Spauwen and J.A. Jansen.
J. Biomedical Materials Research Part A. 2006; 503-511.

9) Orthotopic bone formation in platelet rich plasma (PRP) loaded titanium fiber mesh placed in segmental defects.
H.C. Kroese-Deutman, Vehof J.W.M., P.H.M. Spauwen, P.J.W. Stoelinga and J.A. Jansen.
Int J Oral Maxillofac Surg. 2008 Jun;37(6):542-9.

10) Torque testing as a method to determine the regeneration of segmental bone defects in rabbits provided with porous calcium phosphate cement.
H.C. Kroese-Deutman, J.G.C.Wolke, P.H.M. Spauwen and J.A. Jansen.
In submission Tissue Engineering part C: Methods (2009).

11) CO_2 laser treatment of benign juvenile acanthosis nigricans.
D.S. Wijnberg, H.C. Deutman, P.M. Steijlen.
European Journal of Plastic Surgery 2000; volume 23, Number 4, 238 – 240.

12) The area of transposition of the pedicled deep inferior epigastric perforator flap: an anatomical study.
P.H.M. Spauwen, H.C. Deutman, J.M.G. Kauer.
European Journal of Plastic Surgery. 2000; volume 22, number 5-6, 234-236.

13) A buried reversed radial forearm flap in pharyngeal reconstruction: refinements and monitoring.
H.C. Deutman, E.H.M. Hartman, H.A.M. Marres.
European Journal of Plastic Surgery. 2000; volume 23, Number 4, 204– 207.